Synthesis and Reactivity of ^{Me4}PCP and ^{Me4}POCOP Iridium Complexes

Travis T. Lekich

A dissertation

submitted in partial fulfillment of the

requirements of the degree of

Doctor of Philosophy

University of Washington

2018

Reading Committee:

D. Michael Heinekey, Chair

Brandi M. Cossairt

Gojko Lalic

Program Authorized to Offer Degree:

Chemistry

University of Washington

Abstract

Synthesis and Reactivity of ^{Me4}PCP and ^{Me4}POCOP Iridium Complexes

Travis T. Lekich

Chair of the Supervisory Committee:

Prof. D. Michael Heinekey

Department of Chemistry

This thesis describes new syntheses of ^{Me4}PCP and ^{Me4}POCOP pincer ligands (^{R4}PCP = 1,3-bis(dialkylphosphinomethyl)-benzene; ^{R4}POCOP = 1,3-bis(dialkylphosphinito)-benzene), and the coordination chemistry of the corresponding iridium complexes. Bis(dimethyl)phosphine ligands have been difficult to synthesize because their precursors are expensive or dangerous to obtain. As such, they have not been as extensively studied as the larger ^{R4}PCP (R = ^{t}Bu, ^{i}Pr) derivatives. Chapter 2 shows that aminophosphines, which can be safely synthesized on large scales, are excellent precursors to bis(dimethyl)phosphine ligands: ^{Me4}PCP, ^{Me4}POCOP, and DMPE. Iridium complexes of ^{Me4}PCP and ^{Me4}POCOP show similar and novel reactivity compared to that of larger analogs (R = ^{t}Bu, ^{i}Pr). Chapter 3 illustrates the steric environment of (^{Me4}PCP)Ir(CO) through structure and reactivity comparisons. Chapter 4 describes the facile nature of H_2 addition to (^{Me4}PCP)Ir(CO) and subsequent isomerization. The nature of this reaction allowed us to investigate the isomerization mechanism and revealed that the isomerization likely proceeds through a CO insertion pathway. Chapter 4 also reports the surprising reactivity of DCM and silver acetate with (^{Me4}PCP)Ir(CO), which likely is facilitated by the ligand's reduced steric profile.

Acknowledgments

Thank you, Mike for being an excellent advisor throughout graduate school. You gave me the freedom to explore some of my many ideas but provided direction so that I could finish graduate school.

Thank you to my committee members past and present: Brandi M. Cossairt, Gjoko Lalic, Andrew J. Boydston, Ronald Stenkamp, and Karen I. Goldberg. You all have given me fantastic suggestions on my work.

Thank you, Polly L. Arnold and Jason Love, for allowing me to come work for you in Scotland for a summer and being excellent advisors. This was a fantastic experience that I would not hesitate to do again.

Thank you Walter W. Weare, my undergraduate advisor, for getting me interested in chemical research and providing me the freedom to explore my own ideas even as an undergraduate. Also, thank you, David A. Shultz, for being a fantastic teacher in both organic and inorganic chemistry, sparking my interest in chemistry.

Thank you to my friends and coworkers for the support both in the lab and out. I am certain I would not have completed graduate school without the great and friendly working environment. As well, I would not have been able to stay engaged on my research without the occasional adventures in the pacific northwest with my friends, most of whom are also coworkers.

Thank you to my family for your support throughout my time in graduate school and in life. I certainly would not be here without you. I moved across the country from most of you to attend graduate school, but we still find time to spend together and make the most of it.

Thank you Karena for all your support through the ups and downs of graduate school, for all the adventures we have been on both domestic and abroad, and for being a fantastic partner. You undoubtably helped me push past the mental difficulties of graduate school. I cannot wait to see where our future journey takes us.

Table of Contents

List of Figures

List of Schemes

List of Tables

Chapter 1. Introduction

1.1 Introduction

Numerous research groups have studied tridentate pincer ligands for a variety of chemical transformations. Many of the reported pincer ligands feature two coordinating phosphine "arms" linked with a central aromatic ring through benzylic or oxygen linkers (Figure 1.1).[1]

Figure 1.1 Depiction of ^{R4}POCOP and ^{R4}PCP ligands.

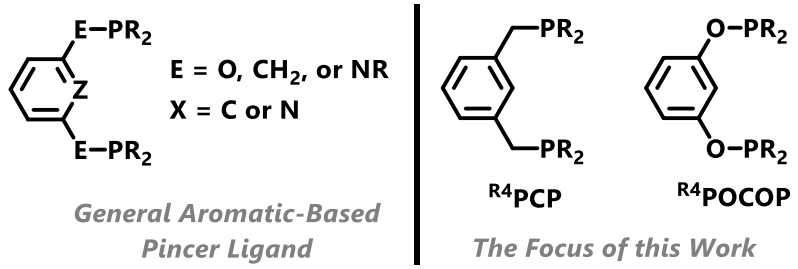

This ligand motif allows for an energetically favorable 5-membered chelate, which provides a thermally and chemically stable metal complex.[1] Moreover, pincer ligands can be modified both sterically through the substituents on phosphorus, and electronically through the substituents on the aryl ring and on phosphorus.[1] These favorable attributes make ^{R4}POCOP and ^{R4}PCP pincer ligands (^{R4}PCP = 1,3-bis(dialkylphosphinomethyl)-benzene; ^{R4}POCOP = 1,3-bis(dialkylphosphinito)-benzene) attractive for use in many transformations, most notably dehydrogenation and hydrogenation chemistry.[2] These application-based studies have also been accompanied by extensive experimental and computational investigations of the electronic and steric effects of the commonly-used pincer ligand derivatives. Despite the rich chemical knowledge of these pincer ligands, many of the possible ligand derivatives are underexplored particularly with respect to the substituents on the phosphorus arms. The lack of straightforward

and safe synthetic methods for installing substituents prevent the study of some potentially interesting derivatives.

1.2 Synthesis of Pincer (PCP and POCOP) Complexes: Challenges

1.2.1 Benzyl-Derived Pincer Ligands (^{R4}PCP)

In 1976, Moulton and Shaw reported the first synthesis of a ^{R4}PCP ligand (^{tBu4}PCP); this synthesis proceeds with an S_N2 displacement of the halides from 1,3-bis(bromomethyl)benzene by two equivalents of $HP(^tBu)_2$, followed by deprotonation of the resulting bis-phosphonium HBr salt.[3] Others have used this method with the secondary phosphine, HPR_2, or phosphide, MPR_2 (M = Na, K), to synthesize other ^{R4}PCP ligands (R = Me,[4] Ph,[5] ^{i}Pr,[6,7] Cy,[8,9] ^{t}Bu,[5] Ad[10]) (Scheme 1.1).

Scheme 1.1 Synthesis of ^{R4}PCP ligands through nucleophilic displacement.

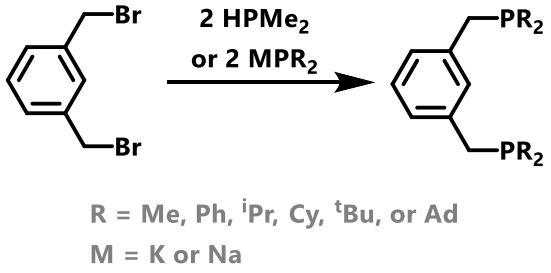

This method is adequate for synthesizing a variety of ^{R4}PCP derivatives as well as unsymmetrical species[11], however it relies on the electronic character of the phosphine precursor; the secondary phosphine or phosphide must be nucleophilic enough to react with 1,3-bis(bromomethyl)benzene. This requirement excludes the use of electron-poor phosphines. Moreover, the reported yield of the methyl-substituted derivative, ^{Me4}PCP, was reported as "trace".[4] Thus, research groups developed other methods to synthesize electron-poor and sterically-undemanding ^{R4}PCP ligands.

Scheme 1.2 Synthesis of ^{R4}PCP ligands via a di-Grignard intermediate.

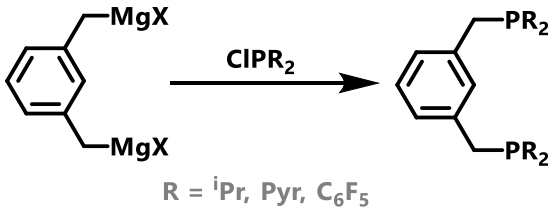

In 2005, Milstein and van Koten reported the synthesis of ^{Py}PCP and $^{(C6F5)4}$PCP via a di-Grignard intermediate (Scheme 1.2).[12–14] In this preparation, a di-Grignard reagent is formed *in situ*, then it nucleophilically attacks two equivalents of $ClPR_2$ to afford ^{R4}PCP. This method relies on the availability of XPR_2, which is easily prepared or commercially available for large R groups (see Chapter 2 for more details), however this is not the case when R is small (e.g. Me CF_3, OR').

Scheme 1.3 Synthesis of ^{R4}PCP ligands via ^{Cl4}PCP.

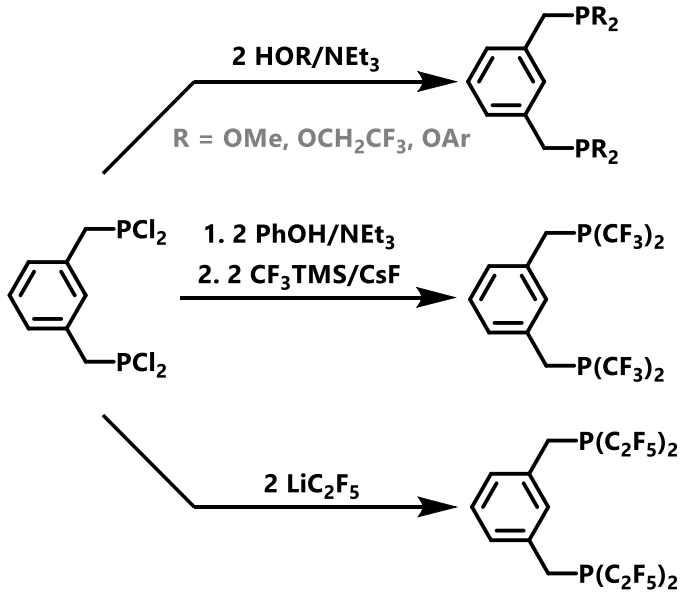

To access smaller and electron-deficient ^{R4}PCP ligands, the Roddick group developed a synthesis for ^{Cl4}PCP which they used as a precursor for ^{R4}PCP (R = CF_3, C_2F_5, OMe, OCH_2CF_3, and OAr; Scheme 1.03).[15] ^{Cl4}PCP is a versatile precursor, but its synthesis is tedious and involves

phosgene.[15] These syntheses allow one to obtain a variety of ^{R4}PCP ligands, however there is still opportunity for a more direct and safer solution.

1.2.2 Resorcinol-Derived Pincer Ligands (^{R4}POCOP)

Scheme 1.4 Generalized, commonly-used synthesis for ^{R4}POCOP ligands.

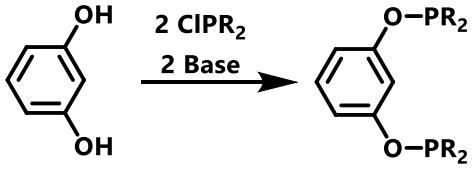

R = Me, Ph, ^{i}Pr, ^{t}Bu, Various OR'
Base = NaH, NEt_3, DMAP

In 2000, Jensen and coworkers reported the first use of ^{R4}POCOP as a ligand.[16] They reported that two equivalents of $ClP^{i}Pr_2$ react with resorcinol (1,3-benzenediol) in the presence of a base, DMAP (4-Dimethylaminopyridine) to afford ^{iPr4}POCOP. This synthesis has been further modified by using other functional groups on phosphorus and the aryl backbone.[17,18] This general synthesis of ^{R4}POCOP is more straightforward than the methods for the ^{R4}PCP analogs (Scheme 1.4). However, this method relies on $ClPR_2$ which is difficult to obtain for small R groups (see Chapter 2 for more details). Unlike Jensen and coworkers' procedure, the method described in Maier's initial report in 1968 of POCOP compounds has not been widely used. Maier described the synthesis of a variety of ^{R4}POCOP compounds by the reaction of resorcinol and two equivalents of an aminophosphine (R'_2NPR_2) at elevated temperatures.[19] Aminophosphines (R'_2NPR_2), where R is small, are more facile to synthesize than the $ClPR_2$ analogs.[20]

Chapter 2 further explores the more recent and new methods for the synthesis of ^{R4}PCP and ^{R4}POCOP, with a focus on the methyl-substituted derivatives, ^{Me4}PCP and ^{Me4}POCOP, and other heteroleptic bis-dimethylphosphine ligands.

1.3 Pincer Ligands in Practice: (De)hydrogenation Chemistry

An important application of metal PCP and POCOP complexes is alkane dehydrogenation. The Goldman group found that iridium PCP and POCOP complexes are effective catalysts and they reported multiple experimental and theoretic studies on acceptorless alkane dehydrogenation, transfer alkane dehydrogenation, and hydrogen addition/elimination.[2,11] The commonly-accepted catalytic cycle for alkane dehydrogenation is shown in Scheme 1.5.

Scheme 1.5 Catalytic cycle for alkane dehydrogenation by (^{R4}PCP)Ir.[11]

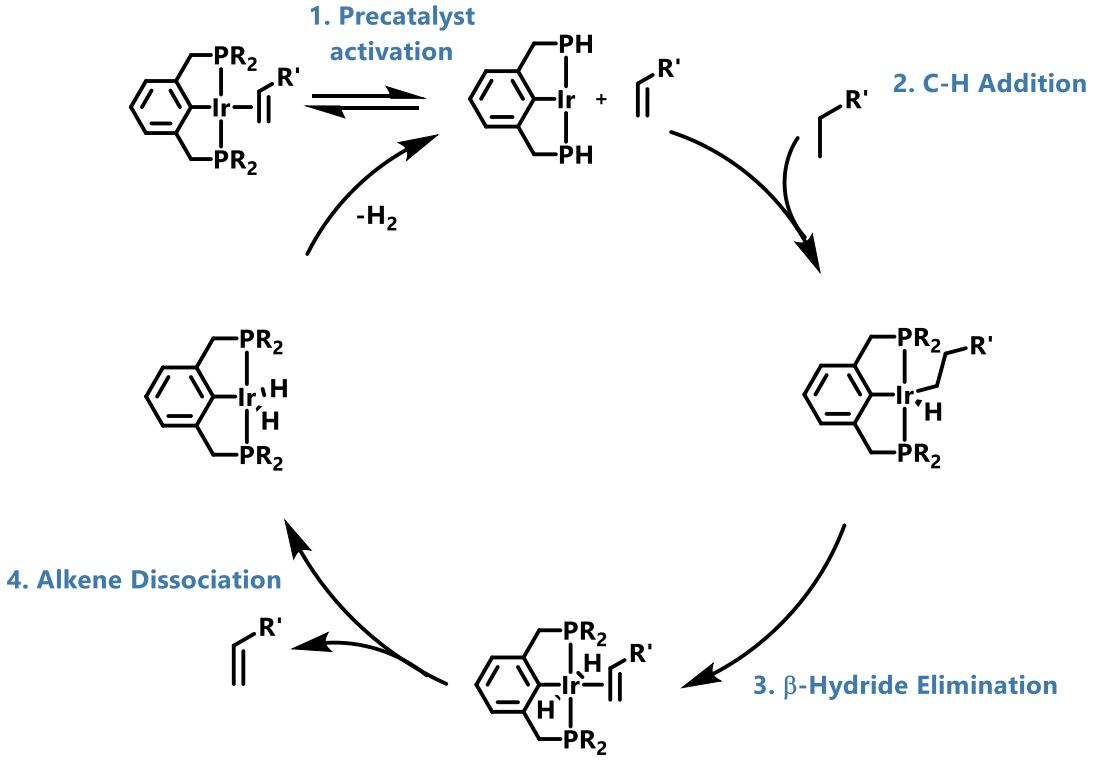

Initially, the 14-electron iridium(I) 3-coordinate species forms from dissociation of the alkene (1). Then, this reactive iridium species C-H activates an alkane to form a hydrido-alkyl species (2). The alkyl ligand undergoes β-hydride elimination to afford a dihydride alkene complex (3). Finally, the alkene dissociates from the iridium dihydride species (4). The resulting iridium dihydride species then can hydrogenate a sacrificial olefin or eliminate hydrogen at elevated

temperature to regenerate the reactive 3-coordinate iridium species. Goldman, Krogh-Jespersen and coworkers calculated that the highest energy transition state in this cycle for (^{tBu4}PCP)Ir, (^{iPr4}PCP)Ir, and (^{Me4}PCP)Ir complexes are 32.7, 32.2, and 25.9 kcal/mol respectively.[11] The (^{tBu4}PCP)Ir and (^{iPr4}PCP)Ir catalysts are already highly active for alkane dehydrogenation, thus barring any undesirable reactivity, (^{Me4}PCP)Ir derived catalysts are predicted to be more active for alkane dehydrogenation.

Table 1.1 Table 1 Select values for the activity of (^{R4}PCP)Ir complexes for transfer-dehydrogenation. [a]Average of the meso and trans isomers. [b]Conditions: 1 mM [catalyst], 0.2 M [NBE], 150 °C.[11]

Pre-Catalyst	Calc Highest Energy TS	Octanes Equiv. After 20 Minutes
(^{tBu4}PCP)IrH_4	32.7 (kcal/mol)	27
(^{iPr4}PCP)IrH_4	32.2 (kcal/mol)	110
(^{tBu3Me}PCP)IrH_4	28.3 (kcal/mol)	190
(^{tBu2Me2}PCP)IrH_4	27.1[a] (kcal/mol)	128

Goldman and coworkers experimented with sequentially replacing the phosphine groups on (^{tBu4}PCP)IrH_4 with Me groups to give ($^{(tBu)x(Me)4-x}$PCP)IrH_4 (X = 2 or 3).[11] Table 1.1 summarizes the results that they found when using these complexes for alkane dehydrogenation, and the corresponding highest energy calculated transition state. Surprisingly, (^{tBu3Me}PCP)IrH_4 was the best catalyst as measured by total octenes produced at 20 minutes, but it was not calculated to have the lowest energy transition state.[11] Goldman and coworkers found the sterically-smaller (^{tBu2Me2}PCP)IrH_4 species is less active for alkane dehydrogenation because it forms dimeric species during the course of the catalytic reaction (Scheme 1.6).[11]

Scheme 1.6 Proposed mechanism for C-H activated dimer formation observed by Goldman and coworkers.[11]

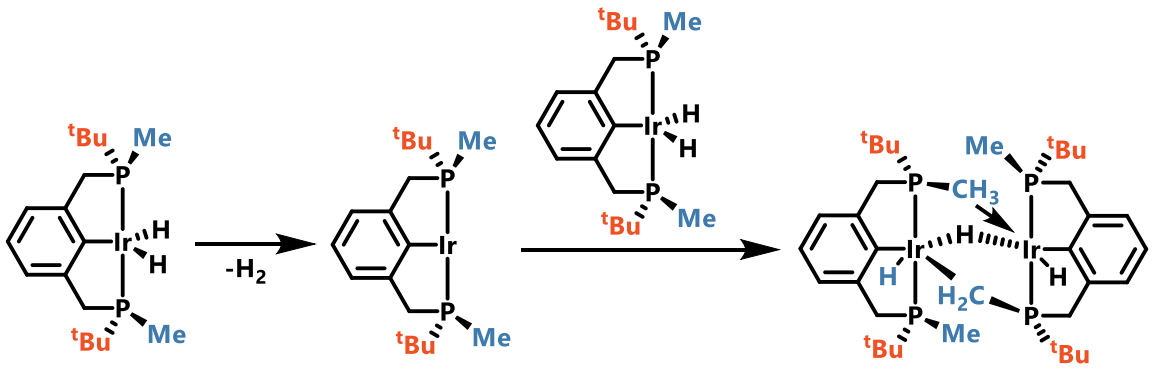

This dimer formation is likely the result of the reduced steric profile of the ^{tBu2Me2}PCP ligand and the activation of C-H bonds on the phosphorus R groups. Thus, (^{Me4}PCP)Ir may not be ideal for alkane dehydrogenation even though the calculated energetics suggests that (^{Me4}PCP)Ir should be the most active species out of the series.

The Roddick group investigated their ($^{(CF3)4}$PCP)Ir(COD) complex for alkane dehydrogenation.[21] They found that the ($^{(CF3)4}$PCP)Ir(COD) species was less active than previously reported (^{tBu4}POCOP)Ir catalysts, and attributed this observation to the competition of substrates with the COD ligand, and the complex's reduced thermal stability.[21] They did not observe catalyst deactivation via a dimer formation like the Goldman group observed with (^{tBu2Me2}PCP)Ir.[11] Through calculations, Roddick and coworkers showed that $^{(CF3)4}$PCP and ^{Me4}PCP iridium complexes energetically prefer more saturated species than the ^{t}Bu or ^{i}Pr PCP and POCOP analogs; thus a 3-coordinate species with a sterically-small PCP ligand is unlikely to form or persist long enough to complete in alkane dehydrogenation with ^{R4}PCP or ^{R4}POCOP (R = ^{t}Bu or ^{i}Pr) iridium complexes.[21]

Scheme 1.7 Reaction pathway for alkane dehydrogenation with (Phebox)Ir(OAc)2(OH2).[22]

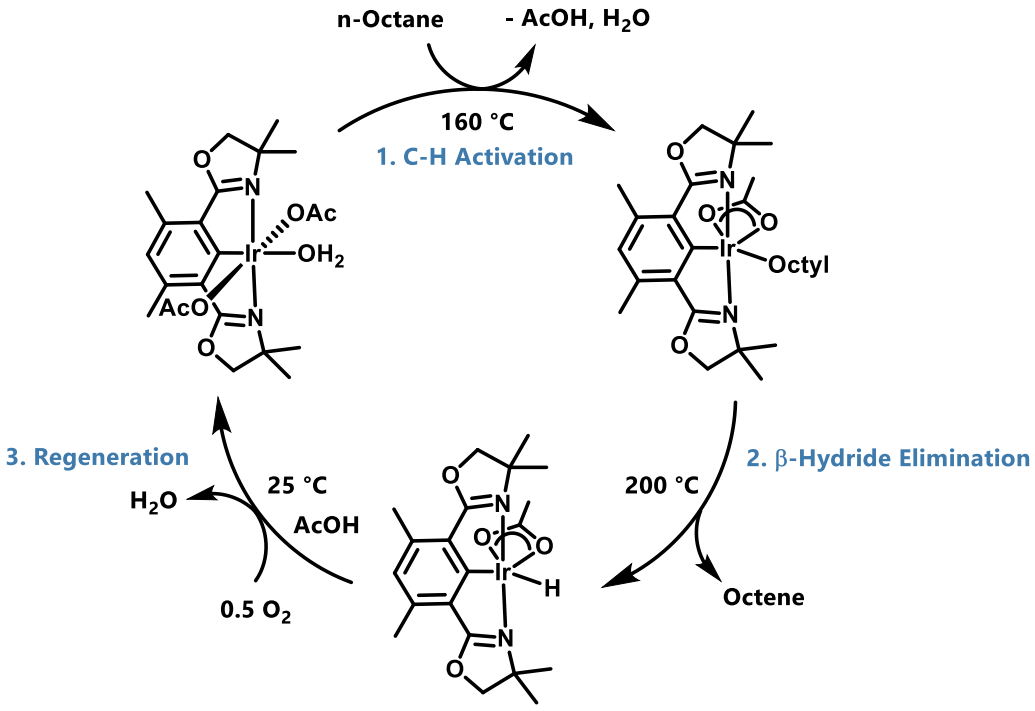

Although reducing the steric bulk of PCP and POCOP ligands is unlikely to yield a more active 3-coordinate iridium(I) catalyst, our group, the Goldman, Goldberg, and Jones groups have recently shown that coordinatively saturated iridium(III) bis acetate species with a different pincer ligand, Phebox (2,6-bis(4,4-dimethyloxazolinyl)-3,5-dimethylphenyl), is active for each step of the aerobic alkane dehydrogenation pathway (Scheme 1.7).[22–24] This stoichiometric dehydrogenation cycle proceeds with the activation of octane by a bis acetate species at 160 °C to afford an alkyl acetate complex. Then the alkyl complex undergoes β-hydride elimination at 200 °C to afford a hydrido acetate complex. This hydrido acetate complex reacts with oxygen in the presence of acetic acid at room temperature regenerate the bis-acetate complex. Though this reactivity has only been observed for Phebox derived iridium complexes, no one has attempted to synthesize similar complexes with PCP and POCOP derivatives. Phebox is sterically-

undemanding, and most likely, the steric bulk of the commonly-used PCP and POCOP derivatives would prohibit similar reactivity.

Furthermore, our group and others have shown that a 4-coordinate iridium carbonyl species (^{R4}PCP)Ir(carbonyl) or (^{R4}POCOP)Ir(carbonyl) (R = ^{t}Bu or ^{i}Pr, carbonyl = CO or acetone) can facilitate (de)hydrogenation chemistry with alcohols, ketones, and aldehydes.[25–29] Previous work from our group showed that (^{tBu4}POCOP)Ir(CO) complexes are active for glycerol hydrogenation.[25,26] Glycerol is a waste product of biodiesel synthesis, but some of the potential hydrogenation products, 1-propanol, 1,2-propane diol, and 1,3-propane diol, are more valuable chemicals. The proposed mechanisms for this transformation is shown in Scheme 1.8.

Scheme 1.8 Proposed Catalytic Cycle for Alcohol Hydrogenation by [(^{tBu4}POCOP)Ir(H)(CO)]$^{+}$.[25]

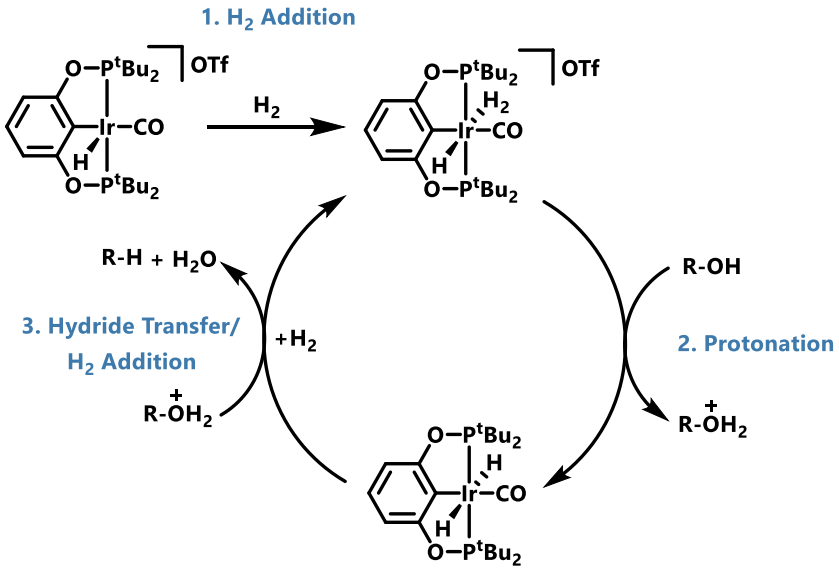

(^{tBu4}POCOP)Ir(CO) is a competent catalyst for the hydrogenation of glycerol, however it is not highly active or selective. To further understand this reaction, our group has investigated the fundamental reactivity for each of the steps in the proposed mechanism and compared this reactivity with both ^{t}Bu and ^{i}Pr groups on phosphorus and between PCP and POCOP ligands.[17,30]

As expected, the (^{iPr4}PCP)Ir(CO) and (^{iPr4}POCOP)Ir(CO) derived complexes generally form more stable higher-coordinate species and are more reactive than the (^{tBu4}PCP)Ir(CO) and (^{tBu4}POCOP)Ir(CO) analogs.[17,30] We hypothesize that the methyl-substituted analogs will be even more reactive than the *iso*-propyl and *tert*-butyl substituted complexes.

1.4 Summary

Previous dehydrogenation chemistry with PCP and POCOP iridium complexes shows that the smaller pincer iridium complexes decompose under the harsh reaction conditions, however the analogous chemistry facilitated by an Ir(III) catalyst and the C-O (de)hydrogenation chemistry involving Ir(CO) species shows that higher-coordinate pincer iridium complexes display interesting reactivity. Thus, research is needed to explore the coordination environment and reactivity of smaller, electron-rich PCP and POCOP ligands. The ^{Me4}PCP and ^{Me4}POCOP ligands are likely understudied because of their difficult syntheses. This work describes the synthesis of ^{Me4}PCP and ^{Me4}POCOP (see Chapter 2), investigates the coordination chemistry of ^{Me4}PCP and ^{Me4}POCOP iridium complexes (see Chapter 3), and compares the reactivity of these ^{Me4}PCP and ^{Me4}POCOP systems to that of the larger ^{R4}PCP and ^{R4}POCOP (R = ^{i}Pr or ^{t}Bu), and electron-poor ^{R4}PCP (R = CF_3) complexes (see Chapter 4).

1.5 References

1 D. M. Roddick, in *Organometallic Pincer Chemistry*, Springer, 2012, pp. 49–88.

2 A. Kumar, T. M. Bhatti and A. S. Goldman, *Chem. Rev.*, 2017, **117**, 12357–12384.

3 B. C. J. Moulton and B. L. Shaw, *J.C.S. Dalt.*, 1975, **0**, 1020–1024.

4 C. S. Creaser and W. C. Kaska, *Inorg. Chim. Acta.*, 1978, **30**, 325–326.

5 M. A. Bennett, H. Jin and A. C. Willis, *J. Organomet. Chem.*, 1993, **451**, 249–256.

6 B. Rybtchinski, Y. Ben-David and D. Milstein, *Organometallics*, 1997, **16**, 3786–3793.

7 C. M. Frech, Y. Ben-David, L. Weiner and D. Milstein, *J. Am. Chem. Soc.*, 2006, **128**, 7128–7129.

8 E. Hollink, J. C. Stewart, P. Wei and D. W. Stephan, *J. Chem. Soc. Dalt. Trans.*, 2003, **20**, 3968–3974.

9 A. R, R. J. Cross and K. W. Muir, *Inorg. Chim. Acta.*, 1995, **231**, 195–200.

10 B. Punji, T. J. Emge and A. S. Goldman, *Organometallics*, 2010, **29**, 2702–2709.

11 S. Kundu, Y. Choliy, G. Zhuo, R. Ahuja, T. J. Emge, R. Warmuth, M. Brookhart, K. Krogh-Jespersen and A. S. Goldman, *Organometallics*, 2009, **28**, 5432–5444.

12 E. Kossoy, M. A. Iron, B. Rybtchinski, Y. Ben-David, L. J. W. Shimon, L. Konstantinovski, J. M. L. Martin and D. Milstein, *Chem. Eur. J.*, 2005, **11**, 2319–2326.

13 P. A. Chase, M. Gagliardo, M. Lutz, A. L. Spek, G. P. M. Van Klink and G. Van Koten, *Organometallics*, 2005, **24**, 2016–2019.

14 M. Gagliardo, P. A. Chase, S. Brouwer, G. P. M. Van Klink and G. Van Koten, *Organometallics*, 2007, **26**, 2219–2227.

15 J. J. Adams, A. Lau, N. Arulsamy and D. M. Roddick, *Inorg. Chem.*, 2007, **46**, 11328–11334.

16 D. Morales-Morales, C. Grause, K. Kasaoka, R. Redón, R. E. Cramer and C. M. Jensen, *Inorganica Chim. Acta*, 2000, **300**, 958–963.

17 J. M. Goldberg, G. W. Wong, K. E. Brastow, W. Kaminsky, K. I. Goldberg and D. M. Heinekey, *Organometallics*, 2015, **34**, 753–762.

18 I. Göttker-Schnetmann, P. White and M. Brookhart, *J. Am. Chem. Soc.*, 2004, **126**, 1804–1811.

19 L. Maier, *Helv. Chim. Acta*, 1968, **51**, 405–413.

20 L. Maier, *Helv. Chim. Acta*, 1964, **47**, 2129–2137.

21 J. J. Adams, N. Arulsamy and D. M. Roddick, *Organometallics*, 2012, **31**, 1439–1447.

22 Y. Gao, C. Guan, M. Zhou, A. Kumar, T. J. Emge, A. M. Wright, K. I. Goldberg, K. Krogh-Jespersen and A. S. Goldman, *J. Am. Chem. Soc.*, 2017, **139**, 6338–6350.

23 K. E. Allen, D. M. Heinekey, A. S. Goldman and K. I. Goldberg, *Organometallics*, 2013, **32**, 1579–1582.

24 H. Yuan, W. W. Brennessel and W. D. Jones, *ACS Catal.*, 2018, **8**, 2326–2329.

25 D. B. Lao, A. C. E. Owens, D. M. Heinekey and K. I. Goldberg, *ACS Catal.*, 2013, **3**,

2391–2396.

26 T. A. Foskey, M. Heinekey and G. I. Goldberg, *ACS Catal.*, 2012, **2**, 1285–1289.

27 S. Park and M. Brookhart, *Organometallics*, 2010, **29**, 6057–6064.

28 S. Park, D. Bézier and M. Brookhart, *J. Am. Chem. Soc.*, 2012, **134**, 11404–11407.

29 L. Monsigny, E. Feghali, J. C. Berthet and T. Cantat, *Green Chem.*, 2018, **20**, 1981–1986.

30 J. M. Goldberg, S. D. T. Cherry, L. M. Guard, W. Kaminsky, K. I. Goldberg and D. M. Heinekey, *Organometallics*, 2016, **35**, 3546–3556.

Chapter 2. Aminophosphines as Precursors to Pincer Ligands

Sections of the following chapter have been previously published.[1]

2.1 Introduction

Ligands featuring dimethylphosphino (Me_2P-) moieties offer an open steric environment but are underexplored because their syntheses involve dangerous reagents and cumbersome methods.[2,2] The methyl derivatives of the commonly-used ^{R4}PCP, ^{R4}PNP, and ^{R4}POCOP ligand families are prime examples (^{R4}PCP = 1,3-bis(dialkylphosphinomethyl)-benzene; ^{R4}PNP = 1,3-bis(dialkylphosphinomethyl)-pyridine; ^{R4}POCOP = 1,3-bis(dialkylphosphinito)-benzene).

Research groups found that (^{R4}PCP)Ir (R = ^{t}Bu or ^{i}Pr) complexes are excellent alkane dehydrogenation catalysts.[4] Yet, they have not studied the (^{Me4}PCP)Ir analogs, even though calculations suggest that reducing the ligand's steric profile decreases energy barriers within the catalytic cycle.[5] This may be because the synthesis of ^{Me4}PCP is low-yielding and requires a pyrophoric gas dimethylphosphine ($HPMe_2$; Scheme 2.1).[6,7] Furthermore, the synthesis of $Me_2P(S)P(S)Me_2$, the precursor to $HPMe_2$, has caused numerous explosions.[8,9]

Scheme 2.1 Previous synthesis of ^{Me4}PCP.

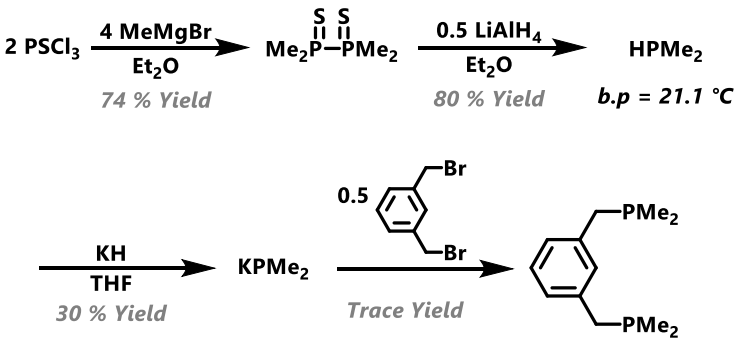

Many groups have also used derivatives of ^{R4}PNP ligated (R = ^{t}Bu, Np, ^{i}Pr) late-transition metal complexes for a variety of transformations.[10] However, the ^{Me4}PNP analogs have never been reported.[2] Previous synthetic methods for ^{R4}PNP proceed through the reaction of a lithium picoline salt and a chlorodialkylphosphine, or an alkyl halide and a secondary phosphine (Scheme 2.2).[11–13] Again, $HPMe_2$ is a pyrophoric gas at room temperature.[7] Additionally, unlike bulkier chlorodialkylphosphines, $ClPMe_2$ is difficult to synthesize because it is volatile and spontaneously flammable.[14–16]

Scheme 2.2 Previous syntheses of ^{R4}PNP ligands.[11–13]

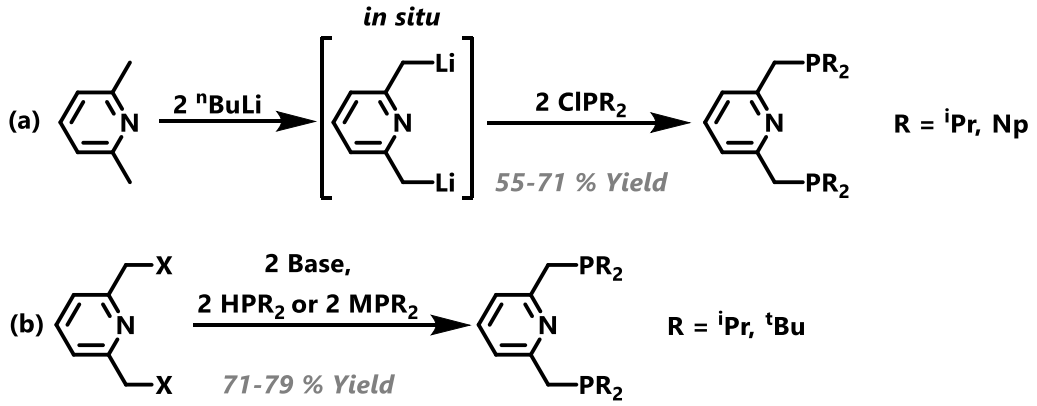

Typically chlorodialkylphosphines are synthetized through the reaction of PCl_3 and two equivalents of MR (R = ^{t}Bu or ^{i}Pr) in a one pot or stepwise procedure.[14,15] However, if R = Me, the distribution of alkylated products spreads to afford Cl_2PMe, $ClPMe_2$ and PMe_3 (Scheme 2.3).[16] Because Cl_2PMe and $ClPMe_2$ have similar boiling points, they are difficult to separate. Therefore, others have reported various methods to synthesize $ClPMe_2$. Slota reported that treating Me_2NPMe_2 with HCl results in impure $ClPMe_2$.[17] A more recent $ClPMe_2$ preparation involves a two-step process: SO_2Cl_2 chlorinates $Me_2P(S)P(S)Me_2$ to afford $Me_2P(S)Cl$, then $^{n}Bu_3P$ abstracts the sulfide from $Me_2P(S)Cl$ to afford $ClPMe_2$ (Scheme 2.4).[16]

Scheme 2.3 Syntheses of chlorodialkylphosphines from PCl_3.[14–16]

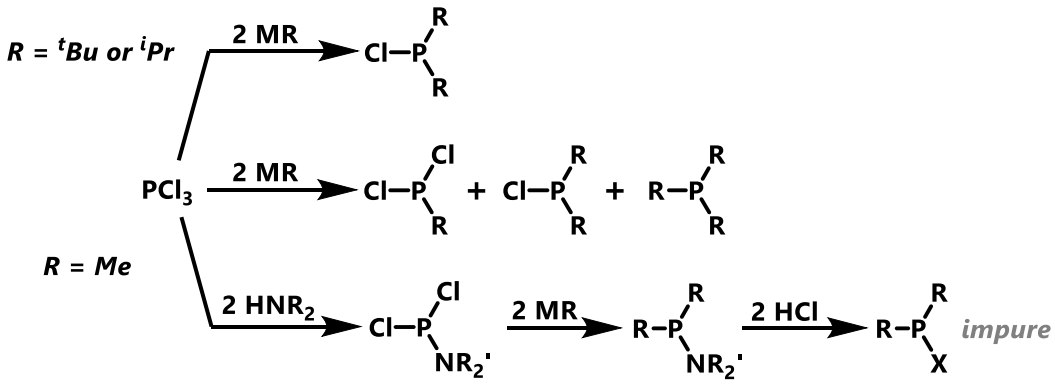

Scheme 2.4 Parshall's synthesis of $ClPMe_2$.

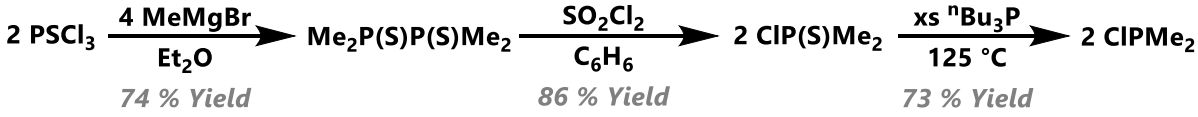

Like the ^{R4}PCP and ^{R4}PNP analogs, ^{R4}POCOP ligated metal complexes see significant use in various catalytic transformations, and the ^{Me4}POCOP derivates are underexplored for similar reasons.[2,18] Commonly-used syntheses of ^{R4}POCOP ligands are straightforward, but require the use of $ClPR_2$ precursors (Table 2.1).[19–22]

Table 2 Select previous syntheses of ^{R4}POCOP.

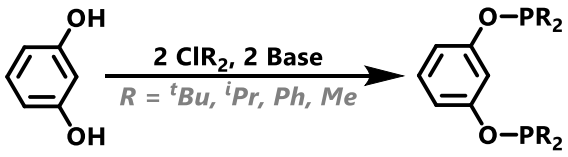

R	Base	Yield	Ref
^{t}Bu	NaH	93 %	19
^{i}Pr	NEt_3	95 %	22, 23
Ph	NEt_3	86 %	20
Me	NaH	*Not Isolated*	21

The precarious nature of preparing $ClPMe_2$ and $HPMe_2$ creates the need for a safer and more convenient -PMe_2 reagent. Newly-developed syntheses of heteroleptic phosphines (R'PR_2) bypass some of these difficult and dangerous-to-obtain synthetic precursors, but introduce other difficulties when R = Me.[24–28]

In 2014, Tyler and coworkers described the synthesis of phosphine oxides and phosphines through the alkylation of a phosphonate (Scheme 2.05).[24] This preparation begins with an Arbuzov reaction between a phosphite and alkyl halide to afford a phosphonate, then a Grignard reagent alkylates the phosphonate to afford a phosphine oxide (Scheme 2.5).[24] Tyler and coworkers provided a wide substrate scope of phosphine oxides, but only reduced a few of these examples to the corresponding phosphines.[24] They noted that the alkylation step is highly sensitive to the temperature and addition rate of the Grignard reagent, which can make this procedure irreproducible and arduous.[24]

Scheme 2.5 Synthesis of R'PR_2 reported by Tyler and coworkers.

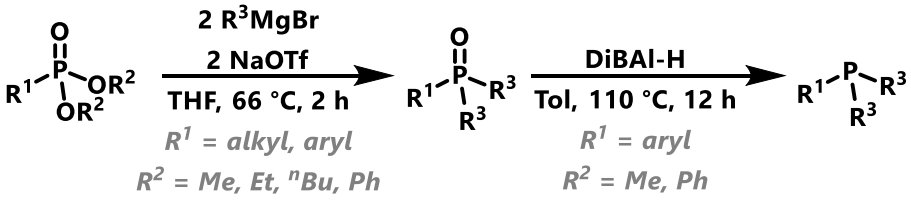

Subsequently, the Tyler and Ashley groups built upon Hays's method originally reported in 1968 (Scheme 2.6).[25–27] This method proceeds with the reaction of a secondary phosphite and three equivalents of MeMgX to form a magnesium-phosphinite intermediate.[26] Then, this nucleophilic intermediate undergoes an S_N2 addition with an alkyl halide to afford a heteroleptic phosphine oxide or undergoes protonation to afford a secondary phosphine oxide.[26]

Scheme 2.6 Synthetic method reported by Hays for $R_2P(O)H$ and $R_2R'P(O)$.

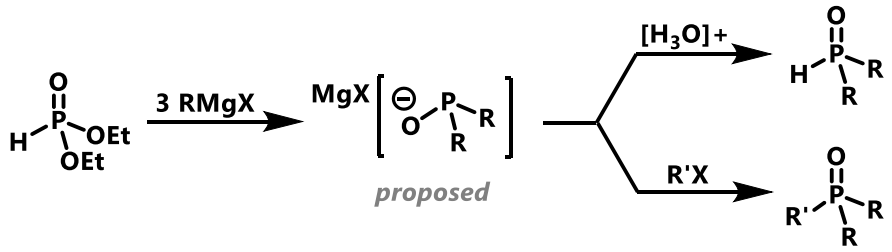

Ashely and coworkers modified Hays's method to synthesize 1,2-bis(dialkylphosphino)-ethane derivatives and ^{tBu}PNP (Scheme 2.7).[27] They found that reducing aliphatic phosphine oxides via reported procedures, which generally use phenyl-substituted phosphine oxides as substrates, was not effective.[27,29] They found that converting the phosphine oxide to a chlorophosphonium chloride was preferable because they could efficiently reduce the chlorophosphonium chlorides with $NaAlH_4$.[27]

Scheme 2.7 Ashley and coworkers' general synthetic method for 1,2-bis(dialkylphosphino)-ethanes.

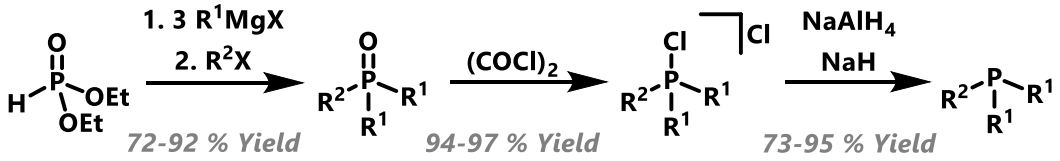

Although convenient and high-yielding, Ashley and coworkers' method is difficult to adapt to other substrates because the purity of the initial phosphine oxide varies significantly depending on the alkyl halide.[25] Tyler and coworkers improved the reproducibility of this reaction by using a sodium phosphinite instead of a magnesium phosphinite (Scheme 2.8).[25]

Scheme 2.8 Tyler and coworkers' synthetic method for heteroleptic phosphine oxides. [a]Reported by Hays.[26]

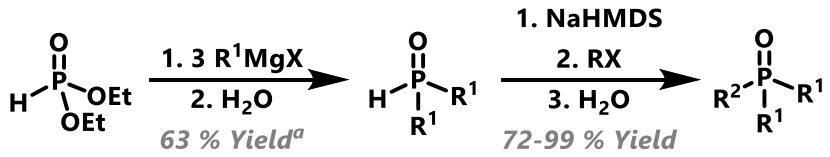

Tyler and coworkers' modification to the preparation of heteroleptic phosphines is effective for a variety of RX substrates, including 1,3-bis(chloromethyl)-benzene (a possible precursor to ^{Me4}PCP). However, this procedure adds an extra step to obtain the desired phosphine and requires the isolation of the dialkylphosphine oxide. Dimethylphosphine oxide needs to be distilled, but readily disproportionates to dimethyl phosphine and dimethylphosphinic acid under distillation conditions.[25,26] Additionally, Tyler and coworkers showed that their method was surprisingly ineffective at synthesizing DMPE oxide (dimethylphosphinoehtane oxide), a precursor to DMPE which is a commonly-used bis(dimethyl)phosphine.[25]

These methods involving a phosphine oxide intermediate are effective for obtaining the desired phosphine oxide or phosphine but involve laborious and hazardous preparations. This is particularly true of synthesizing dimethylphosphine oxide via a magnesium phosphinite. Ozerov and coworkers devised a more convenient method to directly synthesize a halo phosphonium halide.[28] In their method, a dialkylchlorophosphine nucleophilically adds to a benzyl halide to afford the respective halo phosphonium halide (Scheme 2.9).[28] They showed that magnesium or nickel powder can reduce the halo phosphonium halides to the corresponding phosphine or nickel phosphine complex respectively.[28]

Scheme 2.9 Ozerov and coworkers' synthetic method for heteroleptic phosphine oxides.

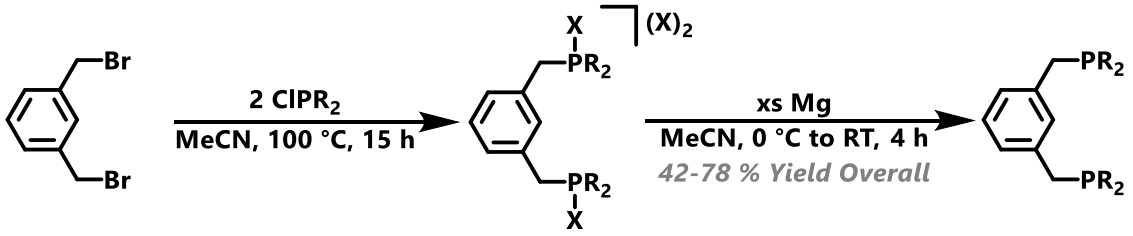

Ozerov and coworkers' method is elegant for synthesizing PCP and PNP ligands with large R groups on phosphorus. However, the use of $ClPR_2$ makes a direct adaptation of this method to synthesize ^{Me4}PCP challenging.[16] Furthermore, this method's scope is confined to electrophilic substrates because chlorodialkylphosphines are insufficiently nucleophilic to react with aliphatic halides or other electron-rich halocarbons. Synthesizing a phosphonium salt then reducing it to a phosphine is an interesting strategy that one could extend to other phosphine precursors.

In 1957, Buckley and Bailey reported the synthesis of phosphines through a phosphonium intermediate (Scheme 2.10).[30] This method is step-wise: $P(Bn)_3$ reacts with MeBr to afford $[P(Bn)_3(Me)]Br$, $LiAlH_4$ reduces $[P(Bn)_3(Me)]Br$ to afford $P(Bn)_2Me$, then this cycle is repeated until the desired $P(Bn)_{3-x}Me_x$ is obtained.[30] This method is not ideal because it requires many steps, but it is encouraging that a phosphonium can be selectively reduced to afford the desired phosphine.

Scheme 2.10 Buckley and Bailey's synthetic method for $P(Bn)_{3-x}Me_x$.

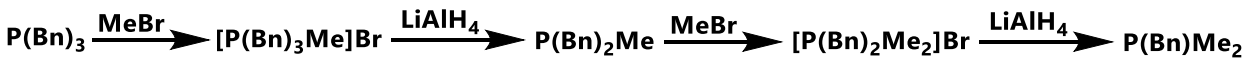

We hypothesized that an aminophosphine could be used in place of $ClPR_2$ in a pathway like that described by Ozerov and coworkers (Scheme 2.09).[17,28,31,32] Aminophosphines and their precursors, aminodichlorophosphines, are oxygen and water sensitive, but can be safely prepared

and stored in large quantities with commercially available reagents PCl_3, HNR_2, and MR' (M = Li, MgX (X = Cl, Br, I); Scheme 2.11a).[17,31,33,34] Furthermore, aminophosphines react with alkyl halides to form the corresponding aminophosphonium salt (Scheme 2.11b).[35]

Scheme 2.11 A generalized synthesis of aminophosphines (a) and aminophosphonium salts (b).

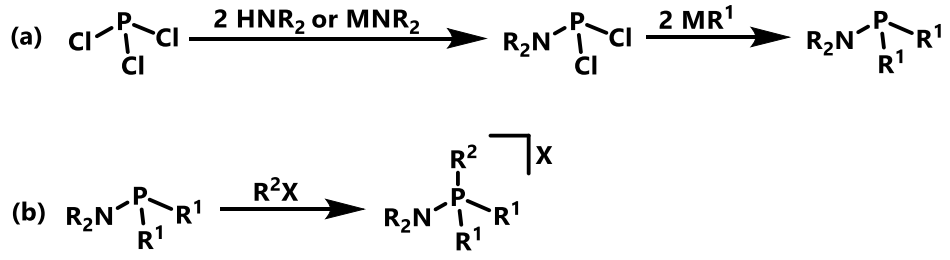

Conveniently, aminophosphines also react with alcohols to afford the corresponding phosphinite. In 1968, Maier reported the synthesis of phenolic phosphinites from the reaction of aminophosphines and phenol derivatives (Scheme 2.12).[36] This precedent shows that one can also use aminophosphines as precursors to ^{R4}POCOP derivatives.

Scheme 2.12 A generalized synthesis of phosphinites from aminophosphines.

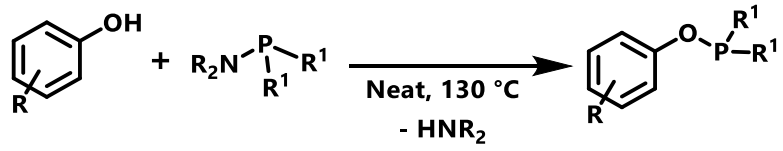

Here, we use an aminophosphine as a starting reagent for bis-phosphine (^{Me4}PCP, DMPE, ^{Me4}PNP) and bis-phosphinite ligands (^{Me4}POCOP, ^{Me}POP), which are representative of commonly used ligand frameworks. we discuss how these methods were optimized through the difficulty in modifying the aforementioned syntheses.

2.2 Results and Discussion

2.2.1 Towards the Synthesis of $^{Me4}PCP_{R2}$

I initially attempted to adapt Tyler and coworkers' phosphonate alkylation method to synthesize ^{Me4}PCP derivatives. Two equivalents of diethylphosphite undergo an Arbuzov reaction with 1,3-bis(bromomethyl)-4,6-dimethylbenzene (**1**^{Br}) to afford 1,3,4,6-$Me_2C_6H_2(CH_2PO_3Et_2)_2$ (**2**^{Et}; Scheme 2.13a). Similarly, two equivalents of dimethylphosphite undergo an Arbuzov reaction with 1,3-bis(chloromethyl)-4,6-dimethylbenzene (**1**^{Cl}) to afford 1,3,4,6-$Me_2C_6H_2(CH_2PO_3Et_2)_2$ (**2**^{Me}; Scheme 2.13b).

Scheme 2.13 Synthesis of **2**^{Et} and **2**^{Me}.

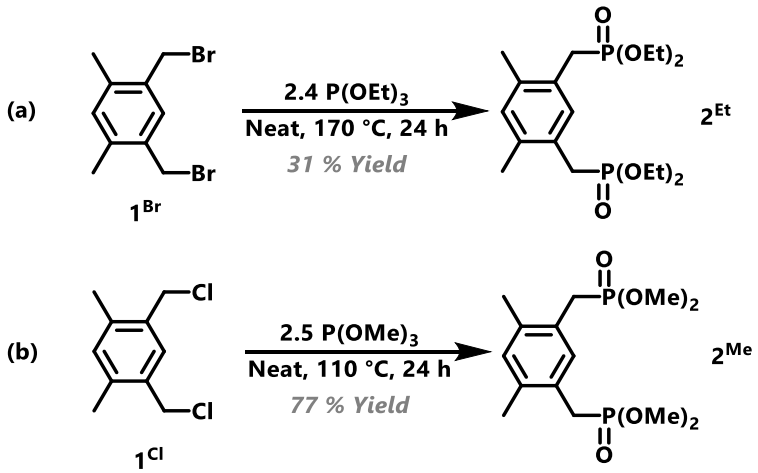

Compounds **2**^{Et} and **2**^{Me} react with two equivalents of methyl magnesium halide under similar conditions to those described by the Tyler group to afford an mixture of intractable products (Scheme 2.14).[24] The literature suggests that this reaction is extraordinarily sensitive to the addition rate of the Grignard reagent to the phosphonate.[24] We initially attempted this Grignard reaction with **2**^{Et} and hypothesized that the ethyl groups were participating in extraneous reactivity with the Grignard reagent. However, we observed similar reactivity with **2**^{Me}. With no obvious route to proceed with this method, we decided to investigate other strategies to synthesize ^{Me4}PCP.

Scheme 2.14 Attempted syntheses of $^{Me4}PCP_{Me2}$ by nucleophilic substitution.

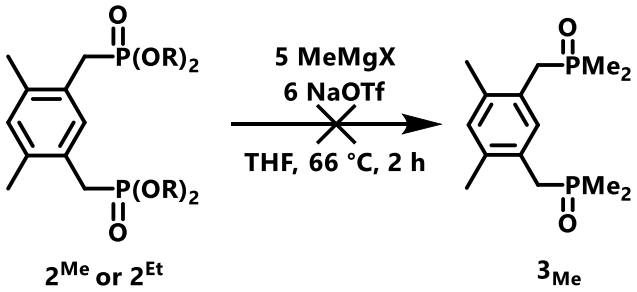

Next, I attempted to adapt Hays and Ashley and coworkers' method to synthesize $^{Me4}PCP_{Me2}$ (Scheme 2.15). Subsequent additions of 3 equiv. MeMgCl and 0.5 equiv. 1,3-bis(chloromethyl)-4,6-dimethylbenzene to diethylphosphite affords $^{Me4}PCP_{Me2}$ oxide (**3Me**). However, consistent with reports by Tyler and coworkers,[25] I was unable to purify **3Me**. At the time of this work, Tyler and coworkers had not published their strategy of using a sodium phosphinite, so I proceeded to reduce **3Me** with the hypothesis that I could purify the final product, $^{Me4}PCP_{Me2}$ (**5Me**).

Scheme 2.15 $^{Me4}PCP_{Me2}$ (**5Me**) and ^{Me4}PCP (**5**) by modification of Ashley and coworkers' method.

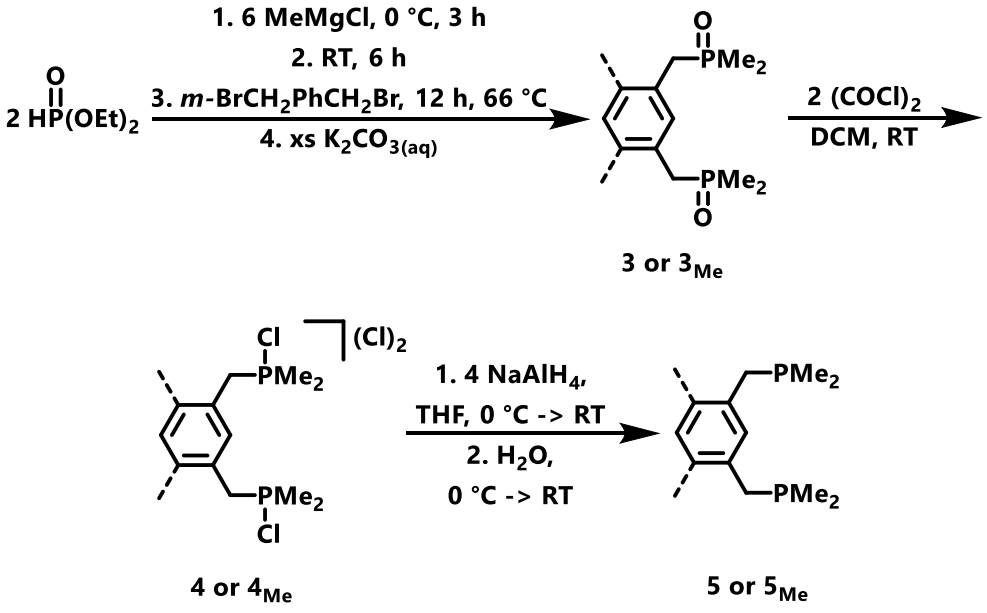

Table 2.2 summarizes attempts to reduce **3$_{Me}$**. Consistent with reports by Ashley and coworkers, I was unable to obtain **5** cleanly and in good yields when using commonly reported reduction procedures for phosphine oxides.[27] I hypothesize that this results from a discrepancy between the electronic character of **3$_{Me}$** versus phenyl-substituted phosphine oxides that are commonly used as substrates in the phosphine-oxide reduction literature.[29] Phenyl-substituted phosphines are electron poor, and thus are less likely to oxidize (easier to reduce).

Table 3 Attempts to reduce **3^{Me}** or **4^{Me}**

Starting Material	Reductant	Result
$^{Me4}PCP_{Me2}$ dioxide (**3$_{Me}$**)	$LiAlH_4$	40 % Crude Yield
	TMDS/Ti(O^iPr)$_4$/BH_3	Intractable
	$P(O)Cl_3$	Intractable
$^{Me4}PCP_{Me2}$ bis(dichloride) (**4$_{Me}$**)	Mg(s) Turnings	No Reaction
	Mg(s) Powder	Intractable
	$NaAlH_4$	91 % Crude Yield
	$NaAlH_4$/NaH	36 % Crude Yield
	Zn(Cu)	Intractable
	Na/Naphthalene	Intractable
	Ni	Intractable
	$[Me_3S][I]$	No Reaction

Ashley and coworkers' method of reducing a phosphine oxide by converting it to a chlorophosphonium chloride, then subsequently reducing the chlorophosphonium halide with $NaAlH_4$/NaH was inadequate to reduce **3$_{Me}$** cleanly and in good yields.[27] This result may be due to a combination of factors including the purity of **3$_{Me}$**, the purity of $NaAlH_4$ or NaH, and the difference in structure between **3$_{Me}$** and the substrates used by Ashley and coworkers. Nevertheless, we attempted to reduce both **3$_{Me}$** and **4$_{Me}$** with a variety of reductants (Table 2.2). Reducing **4$_{Me}$** with four equivalents of $NaAlH_4$ ultimately was the most successful in terms of purity and yield of $^{Me4}PCP_{Me2}$ (**5$_{Me}$**). Unfortunately, the impurities of **3$_{Me}$** were carried through the entire synthetic

route. These impurities made the metallation of $\mathbf{5_{Me}}$ difficult to study because we was unable to discern if the impurities or the ligand's steric profile was the cause of unsuccessful metallation attempts. Thus, we explored other methods to synthesize ^{Me4}PCP.

2.2.2 Synthesis of ^{Me4}PCP and DMPE[1]

Next, we investigated the synthesis of ^{Me4}PCP and other heteroleptic phosphines via a phosphonium intermediate. Table 2.3 summarizes the syntheses of aminophosphonium salts. In general, an aminophosphine equivalent reacts with an alkyl halide equivalent to afford the respective aminophosphonium halide. Aminophosphonium halides (**7-10**) are benchtop-stable but hydrolyze in the presence of alkali aqueous conditions. As expected, benzyl halides are more reactive towards aminophosphines than the alkyl halides.

Table 4 Synthesis of aminophosphonium salts.

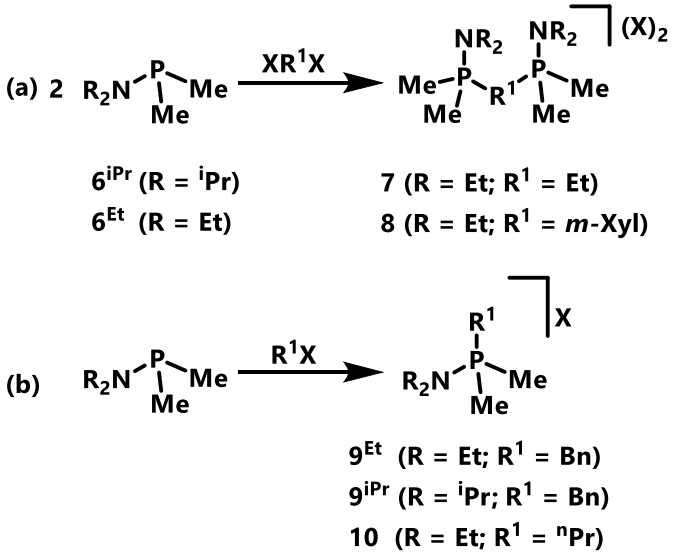

Aminophosphine	R^1X	Result	Yield	Conditions
$\mathbf{6^{Et}}$	*m*-dibromoxylene	**7**	92	RT, 15 h
$\mathbf{6^{Et}}$	1,2-dibromoethane	**8**	75	80 °C, 15 h
$\mathbf{6^{Et}}$	benzylbromide	$\mathbf{9^{Et}}$	89	RT, 15 h
$\mathbf{6^{iPr}}$	benzylbromide	$\mathbf{9^{iPr}}$	90	RT, 15 h
$\mathbf{6^{Et}}$	Iodopropane	**10**	88	60 °C, 15 h

Table 5 Reduction of aminophosphonium salts.

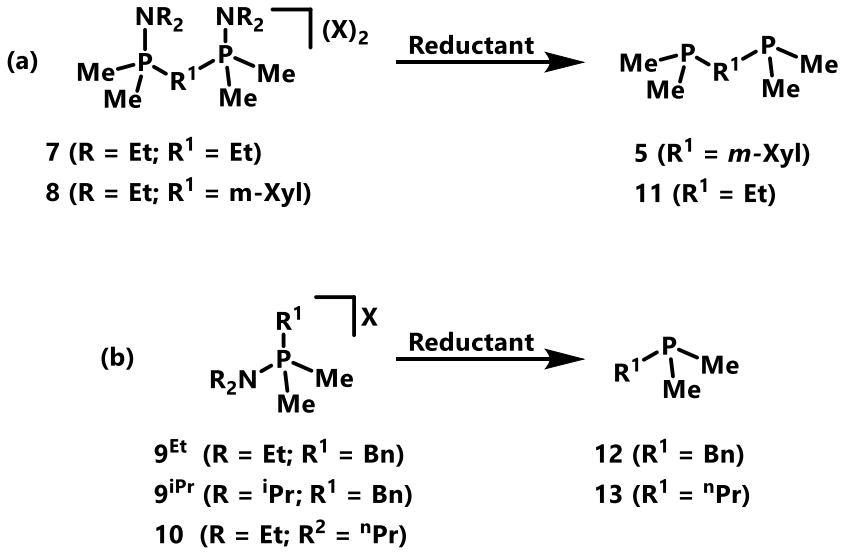

SM[d]	Reductant	Result	Yield (%)[a]	Solvent	Conditions
7	4 $NaAlH_4$	**5**	88	THF	RT, 2 h
7	xs $NaAlH_4$	**5**	Quant.[b]	THF	RT, 2 h
7	1.5 NaAlH4	**5**	63	THF	RT, 2 h
7	xs $LiAlH_4$	**5**[c]	55[b]	THF	RT, 2 h
7	xs Red-Al	Intractable	-	THF/Tol	RT, 2 h
7	xs Mg Powder	Intractable	-	MeOH/Dioxane	RT, 15 h
8	4 $NaAlH_4$	**11**	81, Quant.[b]	THF	RT, 2h
8	xs $LiAlH_4$	**11**	Quant.[b]	THF	RT, 2h
9^{Et}	xs $NaAlH_4$	**12**	Quant.[b]	THF	RT, 3h
9^{Et}	xs Mg Powder	No Reaction	0	THF	RT, 8 h
9^{Et}	xs $LiAlH_4$	**12**[c]	70[b]	THF	RT, 3 h
9^{iPr}	xs $NaAlH_4$	**6^{iPr}**	Quant.[b]	THF	RT, 1 h
10	xs Mg Powder	No Reaction	0	MeCN	80 °C, 15 h
10	xs $LiAlH_4$	**13**	Quant.[b]	THF	RT, 3 h

[a] Isolated yield unless otherwise stated. [b] Measured by $^{31}P\{^1H\}$ NMR. [c] Accompanied by multiple P-containing species.[d] Starting aminophosphonium halide.

Table 2.4 summarizes attempts to reduce aminophosphiniums **7-10**. Using two equivalents of $NaAlH_4$ per phosphonium equivalent was the most effective for reducing **7** and **8** to the desired phosphines ^{Me4}PCP (**5**) and DMPE (**11**). Under similar conditions, using less than two equivalents of $NaAlH_4$ per phosphonium equivalents results in lower yields; this may be due to the weaker

reducing potential of $[AlH_nX_{n-m}]^-$ species. Surprisingly, $LiAlH_4$ cleanly reduces **8** but not **7**. Others observed similar discrepancies between the reactivity of MAH_4 salts and attributed these differences to variations in the solubility of the resulting MX salt.[37–39]

The reductions of the benzyl phosphoniums $\mathbf{9^{Et}}$ and $\mathbf{9^{iPr}}$ show that the small differences between amino groups dictates if the P-N or P-C_{benzyl} bond cleaves during reduction. $NaAlH_4$ reduces $\mathbf{9^{Et}}$ to afford the desired dimethylbenzylphosphine, but $NaAlH_4$ reduces $\mathbf{9^{iPr}}$ to afford the aminophosphine $\mathbf{6^{iPr}}$. Fortunately, $\mathbf{6^{Et}}$ is an excellent precursor in this synthetic pathway for both benzyl and aliphatic-derived $RPMe_2$.

2.2.3 Towards the Synthesis of ^{Me4}PNP

We investigated if this synthetic method for aliphatic and benzylic phosphines could be extended to ^{R4}PNP derivatives. Two equivalents of aminophopshine $\mathbf{6^{Et}}$ react with 2,6-bis(bromomethyl)pyridine to afford $\mathbf{14^{Et}}$ **(**Scheme 2.16a). Aminophosphinum $\mathbf{14^{Et}}$ reacts with 1.5 equivalents of $NaAlH_4$ to afford the phosphorus-containing products **15**, **16**, $\mathbf{6^{Et}}$**,** and $HPMe_2$ (by $^{31}P\{^1H\}$ NMR spectroscopy; Scheme 2.16b).

Scheme 2.16 (a) Synthesis of **14**. (b) Reduction of **14** with $NaAlH_4$.

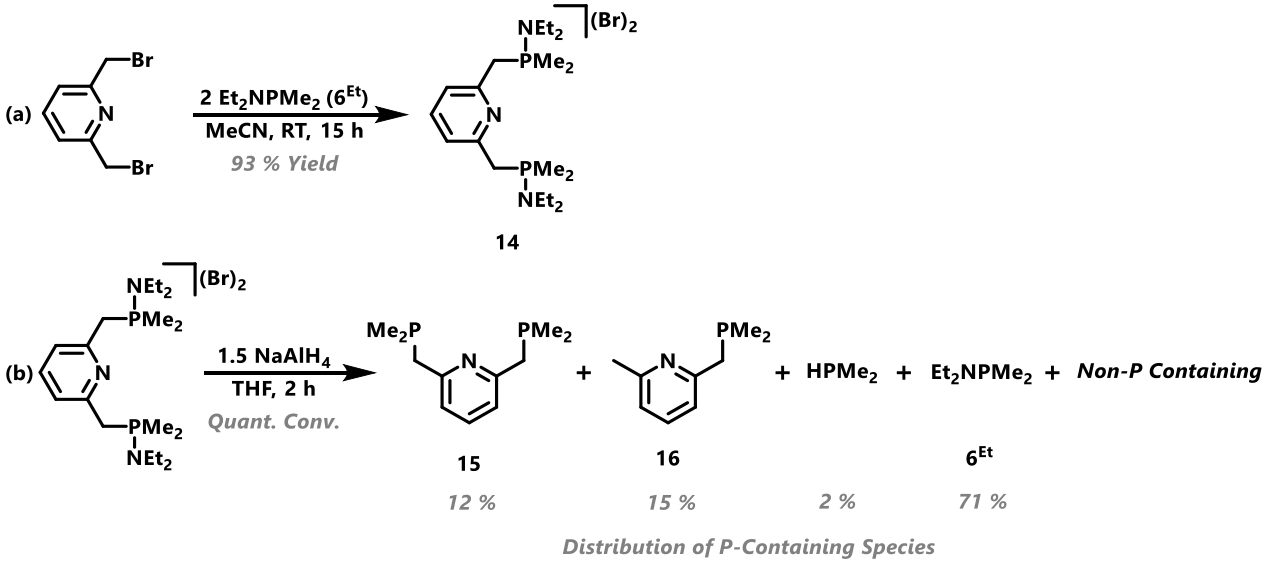

We hypothesized this mixture would shift in the favor of the desired phosphine if we used a more electron-deficient aminophosphine so that the reductant would selectively cleave the aminophosponium P-N bond. We chose to use -NMe(Ph) as the amido moiety because it was one of the most electron deficient amido synthons among reported aminophosphine derivatives that can be synthesized via a R_2NPCl_2 intermediate (Scheme 2.17).[40] Nielson and coworkers reported the synthesis of -$N(SiMe_3)_2$ derived aminophosphines which are similarly electron-deficient; however, they showed that silyl groups migrate when these aminophosphines react with halocarbons.[41–43]

Scheme 2.17 Synthesis of $Me(Ph)NPMe_2$.

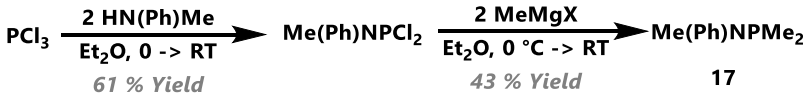

Scheme 2.18 (a) Synthesis of **18**. (b) Reduction of **18** with $NaAlH_4$.

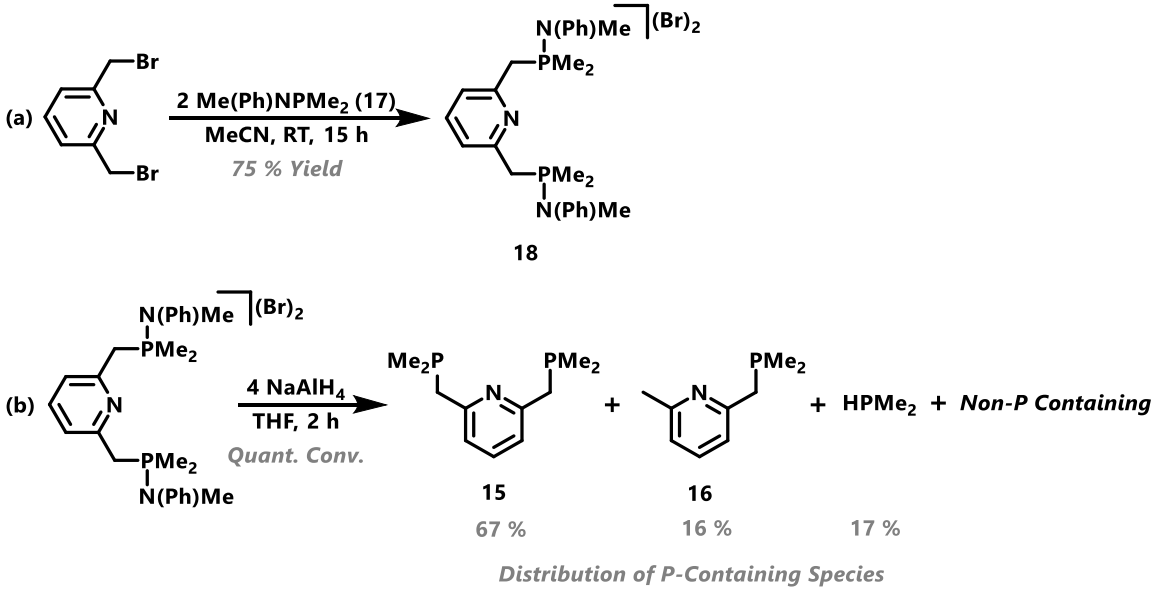

$Me(Ph)NPMe_2$ (**17**) is synthesized in a similar manner to Et_2NPMe_2 (**6**$^{\mathbf{Et}}$), though MeMgX must be used because stronger alkylating reagents such as MeLi will cleave the P-N bond of

$Me(Ph)NPR_2$ to give PR_2Me (Scheme 2.17).[40] Two equivalents of $Me(Ph)NPMe_2$ (**17**) react with 2,6-bis(bromomethyl)pyridine to afford **18** (Scheme 2.18a). Aminophosphonium **18** reacts with 4 equivalents of $NaAlH_4$ to afford the phosphorus-containing products **15**, **16**, and $HPMe_2$ (Scheme 2.18b); this mixture favors the desired phosphine **15**, but a mixture of **15** and **16** is still unideal. Interestingly, I did not observe **17** after the reduction; this may be the result of aminophosphine P-N bond cleavage by the nucleophilic $NaAlH_4$ hydrides. Attempts to separate **15** and **16** were unsuccessful.

2.2.4 Synthesis of $^{Me4}POCOP_{R2}$

Aminophosphines are also competent precursors for phosphinite ligands. Two equivalents of $^{i}Pr_2NPMe_2$ (**6^{iPr}**) or Et_2NPMe_2 (**6^{Et}**) react with resorcinol at 130 °C to afford ^{Me4}POCOP (**19**; Table 2.5). This synthesis is highly sensitive to the purity of resorcinol; commercially-obtained samples need to be recrystallized and dried extensively prior to use. This preparation is convenient, however as discussed further in Chapter 3, ^{Me4}POCOP (**19**) is difficult to metallate because sterically-undemanding phosphinite pincer ligands tend to form oligomers with common metal precursors.[44]

Bulky substituents in the 4 and 6 positions of the aryl ring prevent or reduce the tendency of these ligands to form oligomers during metallation.[22,44] With this design criterium, I targeted two bulky yet electronically different ligands: $^{Me4}POCOP_{tBu2}$ (**20**) and $^{Me4}POCOP_{(COOMe)2}$ (**21**). Two equivalents of $^{i}Pr_2NPMe_2$ (**6^{iPr}**) react with 4,6-ditertbutyl-1,3-benzenediol at 130 °C to afford $^{Me4}POCOP_{tBu2}$ (**20**). In contrast, two equivalents of $^{i}Pr_2NPMe_2$ (**6^{iPr}**) react with 4,6-dimethylester-1,3-dihydroxybenzene to afford a mixture of $^{Me4}POCOP_{(COOMe)2}$ (**21**) and intractable byproducts. In this later case, trace impurities of the resorcinol derivative likely prevented a clean reaction with the aminophosphine.

Table 6 Summary of $^{Me4}POCOP_{R2}$ Synthesis.

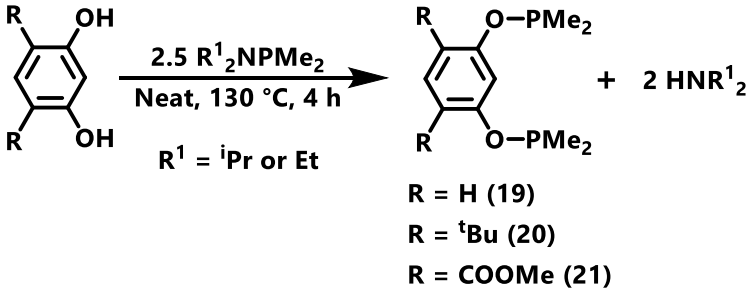

R	R^1	Product	Yield
Resorcinol	^{i}Pr (**6^{iPr}**)	**19**	> 95 %
Resorcinol	Et (**6^{Et}**)	**19**	> 95 %
4,6-ditertbutyl-resorcinol	^{i}Pr (**6^{iPr}**)	**20**	> 95 %
4,6-dimethylester-resorcinol	^{i}Pr (**6^{iPr}**)	**21**	60 % Crude

2.2.5 Synthesis of $Me_2P(O)PMe_2$

Aminophosphines, R_2NPMe_2, also react with other -OH containing functional groups. For example, Et_2NPMe_2 (**6^{Et}**) reacts with one equivalent of H_2O to afford $HP(O)Me_2$ and $HNEt_2$. $HP(O)Me_2$, which is in equilibrium with its tautomer $HOPMe_2$, reacts with one equivalent of Et_2NPMe_2 (**6^{Et}**) to afford $Me_2P(O)$-PMe_2 (**22**). Unsurprisingly, two equivalents of Et_2NPMe_2 (**6^{Et}**) react with one equivalent of H_2O to afford $Me_2P(O)$-PMe_2 (**22**) (Scheme 2.19). Figures 2.1 and 2.2 show the NMR spectra and crystal structure of $Me_2P(O)$-PMe_2 (**22**) respectively. The ^{1}H NMR spectrum of $Me_2P(O)$-PMe_2 shows two doublets for the chemically inequivalent methyl groups coupled to the two chemically inequivalent phosphorus atoms. The $^{31}P\{^{1}H\}$ NMR spectrum of $Me_2P(O)PMe_2$ shows two coupled phosphorus signals for the two chemically inequivalent phosphorus atoms. This synthetic method provides a convenient synthesis of methyl-substituted diphosphane monoxides. Previous syntheses for diphosphine monoxides use $ClPR_2$ reagents.[45] Like secondary phosphine oxides, diphosphane oxides are in equilibrium with their tautomer, a

diphosphoxane (Scheme 2.19).[46] Groups have used diphosphane monoxides as fire retardants and the diphosphoxane tautomers as a phosphinite analog to dialkylphosphinomethane ligands.[45–47]

Table 7 Synthesis of $Me_2P(O)PMe_2$ from Et_2NPMe_2.

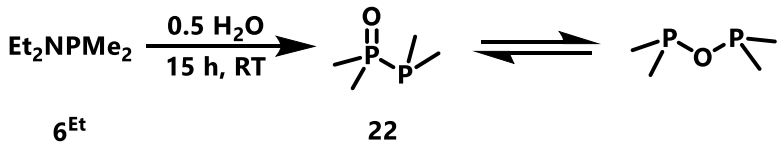

Figure 2.1 NMR Spectra of $Me_2P(O)PMe_2$. ^{1}H (left), $^{31}P\{^{1}H\}$ (middle), $^{13}C\{^{1}H\}$ (right) NMR Spectra of $Me_2P(O)PMe_2$.

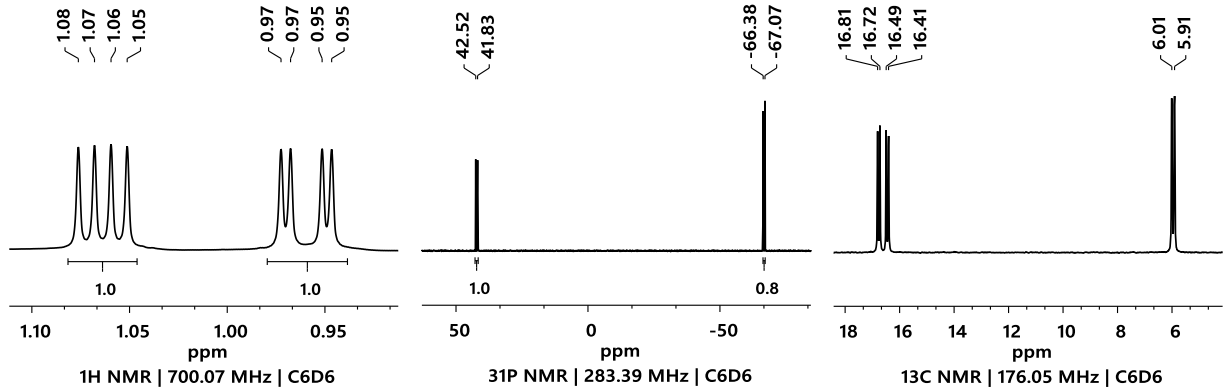

2.3 Conclusions

These presented methods show that aminodimethylphosphines (R_2NPMe_2) are convenient reagents for synthesizing methyl-substituted, heteroleptic phosphines. Synthetic control can be tuned to the alkyl halide substrate by changing the aminophosphine amino group. Since aminophosphines are modular, I hypothesize that these synthetic methods could be modified to use other aminophosphines with varying P-R groups. When possible, the $ClPR_2$ precursors should be used, however, these methods provide an attractive alternative for replacing $ClPR_2$ reagents when they are difficult or dangerous to obtain.

2.4 Experimental

General Considerations

All manipulations and reactions used standard Schlenk techniques under an argon atmosphere unless otherwise stated. Glassware, diatomaceous earth, and sodium sulfate were stored in an oven maintained at 140 °C for at least 24 h prior to use. All protio solvents were passed through activated alumina and activated 3Å molecular sieves prior to use. Deuterated solvents (C_6D_6, THF-d_8, and CD_2Cl_2) were dried over calcium hydride or molecular sieves. CD_3CN was used as received. ^1H, $^{31}P\{^1H\}$, and $^{13}C\{^1H\}$ NMR spectra were recorded on a Bruker AV-500, DRX-499, or AV-300 instrument. ^1H NMR and $^{13}C\{^1H\}$ NMR spectra were referenced to residual solvent signals.[48] $^{31}P\{^1H\}$ NMR spectra were referenced to an 85% H_3PO_4 standard. All NMR spectra were recorded at ambient temperature unless otherwise stated. 1,5-bis(chloromethyl)-2,4-dimethylbenzne (**1**$^{\mathbf{Cl}}$)[49], 1,5-bis(bromomethyl)-2,4-dimethylbenzne (**1**$^{\mathbf{Br}}$)[50], 2,6-bis(bromomethyl)-pyridine,[51] Et_2NPMe_2 (**6**$^{\mathbf{Et}}$),[33,35] $^iPr_2NPMe_2$ (**6**$^{\mathbf{iPr}}$),[33] and Me(Ph)NPMe$_2$ (**17**)[33] were synthesized as previously described. Reagents MeLi (in Et_2O), MeMgX (in THF or Et_2O; X = Cl or Br), PCl_3, $HNEt_2$, 1,2-dibromoethane, α,α'-dibromo-m-xylene, iodopropane, benzyl bromide and reagent grade 90% $NaAlH_4$ were purchased from Sigma Aldrich. MeLi solutions in Et_2O and MeMgX (X = Cl or Br) solutions in THF or Et_2O were titrated with salicylaldehyde phenylhydrazone to determine their concentrations prior to use.[52] 1,2-Dibromoethane and $HNEt_2$ were stored over activated 3Å molecular sieves prior to use. α,α'-dibromo-m-xylene, resorcinol, and di-tertbutyl resorcinol were recrystallized prior to use. Elemental analysis was performed at the CENTC facility at the University of Rochester (funded by NSF CHE-0650456) and at Atlantic Microlab, GA.

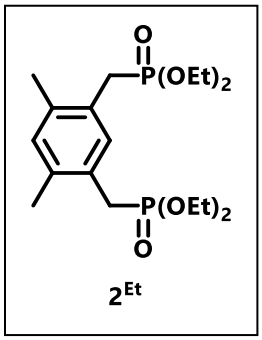

2^{Et}

2^{Et}: 1,5-bis(diethylphosphono)-2,4-diemthylbenzene. A round bottom flask was charged with 1,3-bis(bromomethyl)-4,6-dimethylbenzne (1.00 g, 3.42 mmol) and triethylphosphite (1.35 g, 8.14 mmol). The round bottom flask was equipped with a Dean Stark trap and condenser to remove the generated ethyl bromide. The mixture was heated to 170 °C for 24 h. The volatiles were removed under vacuum and the resulting white solid was eluted through a silica plug with hexane:acetone (2:1). The volatiles were removed under vacuum to afford **2^{Et}** (0.43 g, 1.06 mmol, 31 % yield). ^{1}H NMR (300 MHz, $CDCl_3$): δ 7.14 (t; $^{4}J_{HP}$ = 2.8 Hz; 1H; Ar-*H*), 6.97 (s; 1H; Ar-*H*), 4.00 (dq; 8H; P-(O-C*H*$_2$-CH$_3$)), 3.12 (d; $^{3}J_{HP}$ = 22.1 Hz; 4H; P-(-C*H*$_2$-)), 2.31 (vt; 6H; Ar-(C*H*$_3$)), 1.25 (t; $^{3}J_{HH}$ = 7.1 Hz; 12H; P-(O-CH$_2$-C*H*$_3$)). ^{31}P{^{1}H} NMR (121.5 MHz, $CDCl_3$): δ 27.2 (s).

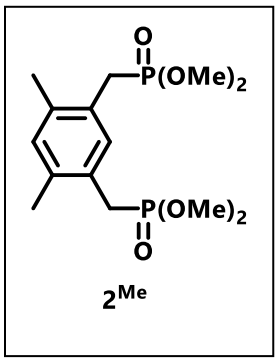

2^{Me}

2^{Me}: 1,5-bis(dimethylphosphono)-2,4-diemthylbenzene. A round bottom flask was charged with 1,3-bis(bromomethyl)-4,6-dimethylbenzne (1.00 g, 3.42 mmol) and triethylphosphite (1.35 g, 8.14 mmol). The round bottom flask was equipped with a Dean Stark trap and condenser to remove the generated ethyl bromide. The mixture was heated to 170 °C for 24 h. The volatiles were removed under vacuum and the resulting white solid was eluted through a silica plug with hexane:acetone (2:1). The volatiles were removed under vacuum to afford **2^{Me}**. (0.43 g, 1.06 mmol, 31 % yield). ^{1}H NMR (300 MHz, CD_2Cl_2): δ 7.09 (t; $^{4}J_{HP}$ = 2.8 Hz; 1H; Ar-*H*), 7.00 (s; 1H; Ar-*H*), 3.64 (d; $^{3}J_{HP}$ = 10.8 Hz; 12H; P-(O-C*H*$_3$)), 3.11 (d; $^{3}J_{HP}$ = 22.0 Hz; 4H; P-(C*H*$_2$)-), 2.30 (vt; 6H; Ar-(C*H*$_3$)). ^{31}P{^{1}H} NMR (121.5 MHz, CD_2Cl_2): δ 30.8 (s).

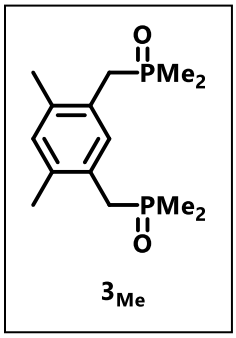

3_{Me}: $^{Me4}PCP_{Me}$ dioxide. ***Method A.*** A solution of MeI (1.90 g, 13.4 mmol) in THF (10 mL) was added dropwise to a mixture of magnesium turnings (0.42 g, 17.4 mmol) in THF (10 mL) at room temperature. A crystal of I_2 was added to the mixture during the addition. The brown solution became cloudy gray after 1 hour of reflux. The concentration of the Grignard reagent was determined by titration. The Grignard reagent was added dropwise (1 drop every 10 seconds, through a chilled (0 °C.) reflux condenser) to a solution of $\mathbf{2^{Et}}$ and NaOTf in THF at 0 °C. After the addition, the mixture was refluxed for 2 hours, resulting in a yellow-green solution. The solution was stirred for an additional 15 h at room temperature. The solution was cooled to 0 °C, then 0.1 M H_2SO_4 (34 mL) was added dropwise. The organics were extracted with DCM (3 x 30 mL) and dried over Na_2SO_4. The volatiles were removed under vacuum to afford a yellow oil. The yellow oil was dried under vacuum at 50 °C for 1 hour. ^1H and $^{31}P\{^1H\}$ NMR spectroscopy showed the presence of multiple intractable species in similar concentrations.

Method B. A solution of MeMgCl in THF (14.4 mL, 43.1 mmol) was added dropwise (1 drop every 10 seconds, through a chilled (0 °C.) reflux condenser) to a solution $\mathbf{2^{Me}}$ (3.41 g, 8.62 mmol) and NaOTf (8.89 g, 51.7 mmol) in THF at 0 °C. After the addition, the mixture was refluxed for 2 hours, resulting in a yellow-green solution. The solution was cooled to 0 °C, then 0.1 M H_2SO_4 (100 mL) was added dropwise. The organics were extracted with DCM (3 x 30 mL) and dried over Na_2SO_4. The volatiles were removed under vacuum to afford a white solid. As determined by ^1H and $^{31}P\{^1H\}$ NMR spectroscopy, the solid contained multiple species. Attempts to isolate a single species by recrystallization in chloroform were unsuccessful.

Method C. *EXPLOSION WARNING*: *Methane is produced upon deprotonation of dimethylphospite with MeMgCl – make sure the reactor has proper ventilation and that the rate of dimethylphospite addition is SLOW*. MeMgCl (3 M, 102 mL) in THF was added to a 500 mL 3-neck round bottom flask. A solution of dimethylphospite (13.0 mL, 0.102 moles) in THF (15 mL) was added dropwise to the Grignard solution at 0 °C. The solution was stirred for 4 h at room temperature, over which time a white precipitate formed. 1,3-bis(dichloromethyl)-4,6-dimethylbenzne (10.28 g, 0.051 mol) was added to the mixture as a solid. The mixture was heated to reflux overnight (ca. 15 hours). The mixture was cooled to room temperature, opened to air, then poured over an aqueous K_2CO_3 solution (42.3 g, 0.306 mol) at 0 °C. The abundant precipitate was removed by filtration and washed with boiling methanol (10 x 20 mL). *Note: The precipitate tends to clog filters.* The volatiles were removed under vacuum to afford a hydroscopic white solid, **3$_{Me}$** (13.2 g; 92 % yield*). *The final product is accompanied by ca. 10 % unidentified impurities that could not be removed by recrystallization in chloroform. ^{1}H NMR (300 MHz, $CDCl_3$): δ 6.81 (t, $^4J_{HP}$ = 2.6 Hz 1H; Ar-*H*), 6.74 (s, 1H; Ar-*H*), 2.85 (d, $^2J_{HP}$ = 14.8 Hz; 4H; -(C*H*$_2$)-), 2.03 (s; 4H; Ar-(C*H*$_3$)), 1.18 (d; $^2J_{HP}$ = 12.8 Hz; 12H; P-(C*H*$_3$)). ^{31}P{^{1}H} NMR (121 MHz, $CDCl_3$): δ 43.5.

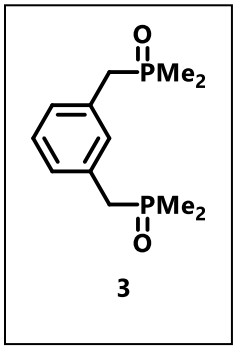

3

3: ^{Me4}PCP dioxide. *EXPLOSION WARNING*: *Methane is produced upon deprotonation of dimethylphospite with MeMgCl – make sure the reactor has proper ventilation and that the rate of dimethylphospite addition is SLOW*. MeMgCl (2.14 M, 84 mL) in THF was added to a 500 mL 3-neck round bottom flask. A solution of dimethylphosphite (7.72 mL, 0.060 moles) in THF (15 mL) was added dropwise to the Grignard solution at 0 °C. The solution was stirred for 4 h at room temperature, over which time a white precipitate formed. 1,3-bis(dibromomethyl)benzne (7.90 g,

0.030 moles) was added to the mixture was a solid. The mixture was heated to reflux overnight (ca. 15 hours). The mixture was cooled to room temperature, opened to air, then poured over an aqueous potassium carbonate solution (24.8 g, 0.180 moles) at 0 °C. The abundant precipitate was removed by filtration and washed with boiling methanol (5 x 20 mL). *Note: The precipitate tends to clog filters.* The volatiles were removed under vacuum to afford a hydroscopic white solid, X (3.30 g; 43 % yield).

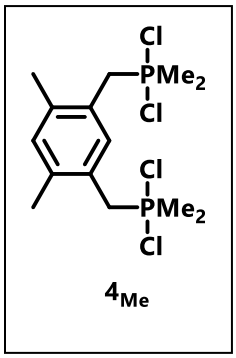

4Me

4Me: Me4PCPMe2 bis(dichloride). In a well ventilated Schlenk flask, oxalyl chloride (6.85 g, 52.9 mmol) was added dropwise to a solution of ^{Me4}PCP dioxide (**X**) (7.39 g, 25.8 mmol) in DCM. The addition was accompanied by vigorous gas evolution. The mixture was stirred for 2 hours at room temperature. The volatiles were removed under vacuum to afford an off-white solid. The solid was washed with Et_2O (2 x 25 mL) to afford $^{Me4}PCP_{Me2}$ bis(dichloride) (**4Me**) (8.43 g, 21.3 mmol, 83 % yield). **4Me** is sparingly soluble in common organic solvents. ^{1}H NMR (300 MHz, CD_2Cl_2): δ 7.24 (s; 1H; Ar-*H*), 7.16 (s; 1H; Ar-*H*), 3.52 (d; $^2J_{HP}$ = 14.2 Hz; 4H; -(C*H*$_2$)-), 2.29 (s; 6H; Ar-(C*H*$_3$)), 1.80 (d; $^2J_{HP}$ = 13.1 Hz; 12H; P-(C*H*$_3$)).

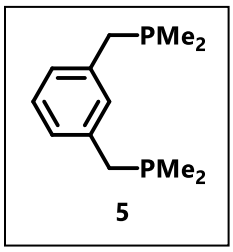

5

5: Me4PCP. [^{Me4}PCP][Br]$_2$ (2.14 g, 4.03 mmol) and $NaAlH_4$ (0.87 g, 16.0 mmol) were stirred together in THF (15 mL) for 2 hours at room temperature. The reaction was cooled to 0 °C, and a 15 % NaOH aqueous solution was added dropwise to quench the reductant and byproducts. The volume of the solution was reduced under vacuum, and pentane (3 x 10 mL) was used to extract from the aqueous layer. The organic layer was dried over anhydrous Na_2SO_4. The drying agent was removed by

filtration, and the volatiles were removed under vacuum to afford ^{Me4}PCP (0.80 g, 88 % yield). The spectroscopic data is consistent with previous reports.[6,53] ^{1}H NMR (300 MHz, C_6D_6): δ 7.11 (t; $^{3}J_{HH}$ = 7.8 Hz 1H; Ar-*H*), 6.90 (d; $^{3}J_{HH}$ = 7.8 Hz, 2H; Ar-*H*), 2.50 (br s; 4H; -(C*H*$_2$)-), 0.79 (d; $^{2}J_{HP}$ = 3.4 Hz; 12H; -P(C*H*$_3$)$_2$). ^{31}P{^{1}H} NMR (121 MHz, C_6D_6): δ -49.0. ^{13}C{^{1}H} NMR (125.8 MHz, C_6D_6): δ 138.4 (s; *C*$_{Ar}$), 130.2 (t; $^{3}J_{CP}$ = 4.0 Hz; *C*$_{Ar}$), 128.5 (s; *C*$_{Ar}$), 126.8 (d; $^{3}J_{CP}$ = 3.6 Hz; *C*$_{Ar}$), 39.09 (d; $^{2}J_{CP}$ = 15.5 Hz; Ar(-*C*H$_2$-)), 13.68 (d; $^{2}J_{CP}$ = 16.5 Hz; -P(*C*H$_3$)$_2$).

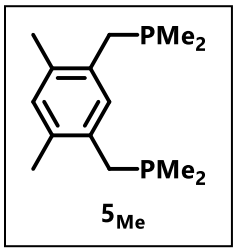

5$_{Me}$: ^{Me4}PCP$_{Me2}$. Solid $NaAlH_4$ (1.02 g, 18.9 mmol) was added portion-wise to a well-ventilated suspension of ^{Me4}PCP$_{Me2}$ bis(dichloride) (**X**) (1.826 g, 4.61 mmol) in THF at 0 °C. The additions were accompanied by effervescence. After the addition, the mixture was warmed to room temperature and stirred for 2.5 hours. The mixture was cooled to 0 °C, and a deoxygenated solution of 15 % NaOH in water (10 mL) was added dropwise. The volume was reduced under vacuum, then the organics were extracted with Et_2O (3 x 25 mL). The organic fraction was filtered through diatomaceous Earth and Na_2SO_4. The volatiles were removed to afford a colorless oil (1.10 g, 4.30 mmol, 47 % yield*). *The final product is accompanied by ca. 10 % unidentified impurities. ^{1}H NMR (300 MHz, CD_2Cl_2): δ 6.91 (s; 1H; Ar-*H*), 6.74 (s; 1H; Ar-*H*), 2.65 (s; 4H; -(C*H*$_2$)-), 2.26 (s; 6H; Ar-(C*H*$_3$)), 1.00 (d; $^{2}J_{HP}$ = 3.0 Hz; 12H; P-(C*H*$_3$)). ^{31}P{^{1}H} NMR (121.5 MHz, CD_2Cl_2): δ -46.6.

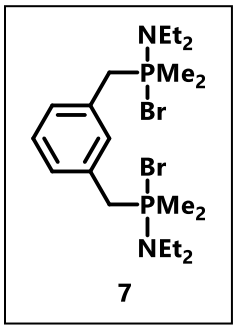

7

7: Bis(diethylamino) ^{Me4}PCP dibromide. 2,6-dibromomethylbenzene (1.53 g, 5.77 mmol) was added to a solution of N,N-diethylamino-P,P-dimethylphosphine (1.69 g, 12.7 mmol) in MeCN (30 mL). The solution was stirred for 15 hours. The resulting white precipitate was collected by vacuum filtration in air, then washed with cold MeCN (0 °C, 3 x 5 mL) and diethyl either (3 x 5 mL) to afford **7** (2.76 g, 5.19 mmol, 90 % yield). Crystals of **7** suitable for X-ray diffraction were grown from a saturated MeCN solution at -30 °C. ^{1}H NMR (300 MHz, CD_3CN): δ 7.52-7.29 (m; 4H; Ar-*H*), 3.83 (d; $^{2}J_{HP}$ = 15.5 Hz; 4H; Ar(-C*H*$_2$-)), 3.10 (m; 8H; -N((C*H*$_2$)CH$_3$)$_2$), 1.96 (d; $^{2}J_{HP}$ = 14.8 Hz; 12H; -P(C*H*$_3$)$_2$), 1.02 (t; $^{3}J_{HH}$ = 7.3 Hz; -N((CH$_2$)C*H*$_3$)$_2$). ^{31}P{^{1}H} NMR (121 MHz, CD_3CN): δ 60.0. ^{13}C{^{1}H} NMR (125.8 MHz, CD_3CN): δ 131.0 (t, $^{2}J_{CP}$ = 2.72 Hz, C_{Ar}), 130.8 (t; $^{2}J_{CP}$ = 3.7 Hz; C_{Ar}), 41.73 (s; -N((*C*H$_2$)CH$_3$)$_2$), 33.89 (d; $^{1}J_{CP}$ = 49.1 Hz; Ar(-*C*H$_2$-)), 14.77(s; -N((CH$_2$)*C*H$_3$)$_2$) 10.03 (d; $^{1}J_{CP}$ = 65.8 Hz; -P(*C*H$_3$)$_2$). Anal. Calcd: C, 45.30; H, 7.60; N, 5.28. Found: C, 45.20; H, 7.53; N, 5.27.

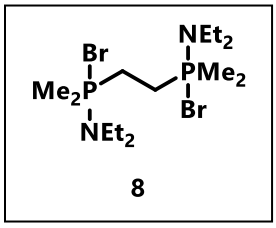

8

8: [(DMPE)(NEt$_2$)$_2$][Br]$_2$. 1,2-dibromoethane (1.76 g, 9.37 mmol) was added to a solution of N,N-diethylamino-P,P-dimethylphosphine (2.74 g, 20.6 mmol) in MeCN (30 mL). The solution was stirred for 15 hours at 80 °C. The volatiles were removed under vacuum, and the resulting white solid was washed with cold MeCN (-45 °C, 3 x 5 mL) and Et_2O (3 x 5 mL) to afford **8** (3.20 g, 7.04 mmol, 75 % yield). ^{1}H NMR (300 MHz, CD_3CN): δ 3.20 (m; 8H; -N(C*H*$_2$CH$_3$)$_2$), 2.81 (d; $^{2}J_{HP}$ = 4.5 Hz; 4H; -C*H*$_2$C*H*$_2$-), 2.18 (vt; 12H; -P(C*H*$_3$)$_2$), 1.16 (t; $^{3}J_{HH}$ = 7.0 Hz; 12H; -N(CH$_2$C*H*$_3$)$_2$). ^{31}P{^{1}H} NMR (121 MHz, CD_3CN): δ 61.4. ^{13}C{^{1}H} NMR (125.8 MHz, CD_3CN):

δ 40.62 (s; -N((*C*H$_2$)CH$_3$)$_2$), 18.75 (vt; -*C*H$_2$*C*H$_2$-), 13.90 (s; -N((CH$_2$)*C*H$_3$)$_2$), 9.55 (vt; -P(*C*H$_3$)$_2$). Anal. Calcd: C, 37.02; H, 7.99; N, 6.17. Found: C, 36.99; H, 8.11; N, 6.05.

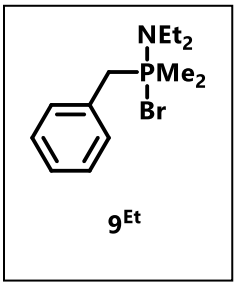

9^{Et}

9^{Et}: [Et$_2$NP(Bn)Me$_2$]Br. A Schlenk flask was charged with Et$_2$NPMe$_2$ (0.209 g, 1.57 mmol), benzyl bromide (0.268 g, 1.57 mmol) and MeCN (5 mL). The mixture was stirred overnight at room temperature. The white precipitate was collected by filtration and washed with cold MeCN and Et$_2$O to afford **9^{Et}** (0.429 g, 1.43 mol, 90 % yield). ^{1}H NMR (300 MHz, CD_2Cl_2): δ 7.48-7.30 (m; 5H; Ar-*H*), 3.72 (d; $^2J_{HP}$ = 14.8 Hz; 2H; Ar(-C*H*$_2$-)), 3.07 (dsp; 4H; N(C*H*(CH$_3$)$_2$)$_2$), 1.94 (d; $^2J_{HP}$ = 13.0 Hz; 3H; -P(C*H*$_3$)$_2$), 1.02 (t; $^3J_{HH}$ = 7.0 Hz; 6H; N(CH(C*H*$_3$)$_2$)$_2$), ^{31}P{^{1}H} NMR (121 MHz, CD_2Cl_2): δ 55.4.

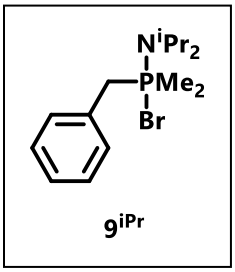

9^{iPr}

9^{iPr}: [^{i}Pr$_2$NP(Bn)Me$_2$]Br. A Schlenk flask was charged with ^{i}Pr$_2$NPMe$_2$ (51.6 mg, 0.32 mmol), benzyl bromide (54.7 mg, 0.32 mmol) and acetonitrile (0.5 mL). The mixture was stirred overnight at room temperature. The white precipitate was collected by filtration and washed with cold MeCN and Et$_2$O to afford **9^{iPr}**. ^{1}H NMR (300 MHz, CD_2Cl_2): δ 7.62-7.28 (m; 5H; Ar-*H*), 4.20 (d; $^2J_{HP}$ = 17.7 Hz; 2H; Ar(-C*H*$_2$-)), 3.77 (dsp; 2H; N(C*H*(CH$_3$)$_2$)$_2$), 2.29 (d; $^2J_{HP}$ = 13.6 Hz; 6H; -P(C*H*$_3$)$_2$), 1.20 (d; $^3J_{HH}$ = 6.8 Hz; 12H; N(CH(C*H*$_3$)$_2$)$_2$), ^{31}P{^{1}H} NMR (121 MHz, CD_2Cl_2): δ 55.4.

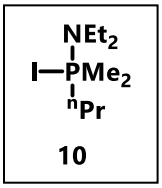

10

10: [Et$_2$NP(^{n}Pr)Me$_2$]I. A Schlenk flask was charged with Et$_2$NPMe$_2$ (0.185 g, 1.38 mmol), iodopropane (0.236 g, 1.38 mmol) and acetonitrile (5 mL). The mixture was stirred overnight at 60 °C. The white precipitate was collected by filtration and washed with pentane to afford **10** (0.367 g, 1.21 mmol, 88 % yield). ^{1}H NMR (300 MHz, CD_3CN):

δ 2.90 (dq; 4H; -N(CH_2CH$_3$)$_2$) 2.00 (m; 2H; -(CH_2)-), 1.70 (d; $^4J_{HP}$ = 13.2 Hz; 6H; -P(CH_3)$_2$) 1.37 (m; 2H; -(CH_2)-), 0.94 (t; $^3J_{HH}$ = 7.20 Hz; 6H; -N(CH$_2$CH_3)$_2$), 0.87 (td; $^3J_{HH}$ = 7.2 Hz; $^4J_{HP}$ = 1.3 Hz ; 3H; -P(CH$_2$CH$_2$CH_3)). ^{31}P{^{1}H} NMR (121 MHz, CD$_3$CN): δ 60.8.

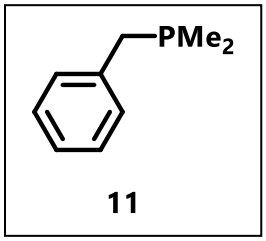

11

11: BnPMe$_2$. A J-Young tube was charged with **9^{Et}** (31.0 mg, 0.10 mmol), NaAlH$_4$ (22.0 mg, 0.58 mmol) and THF-d$_8$ (350 μL). The mixture was periodically agitated for 4 hours, over which time gas evolved. The white precipitate was separated from the solution by centrifugation. The species in solution matched previous spectroscopic reports of BnPMe$_2$.[30,54]

^{n}PrPMe$_2$
12

12: ^{n}PrPMe$_2$. A J-Young tube was charged with **10** (0.32 mg, 0.10 mmol), NaAlH$_4$ (0.08 mg, 0.21 mmol) and THF-d$_8$ (350 μL). The mixture was periodically agitated for 4 hours, over which time gas evolved. The white precipitate was separated from the solution with centrifugation. The species in solution matched previous spectroscopic reports of ^{n}PrPMe$_2$.[55]

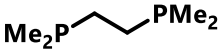

13

13: DMPE. Compound **8** (2.32 g, 4.91 mmol) and NaAlH$_4$ (1.06 g, 19.6 mmol) were stirred together in THF (15 mL) for 2 hours at room temperature. The reaction was cooled to 0 °C, and a 15 % NaOH aqueous solution was added dropwise to quench the reductant and byproducts. The volume of the solution was reduced under vacuum, and pentane (3 x 10 mL) was used to extract from the aqueous layer. The organic layer was dried over anhydrous Na$_2$SO$_4$. The drying agent was removed by filtration, and the volatiles were removed under vacuum to afford **13**(0.60 g, 4.00 mmol, 81 % yield). The spectroscopic data is consistent with previous reports.[27] ^{1}H NMR (300 MHz, C$_6$D$_6$): δ 1.30 (vt; 4H; -CH_2CH_2-), 0.81

(vt; 12H; -P(CH_3)$_2$). ^{31}P{^{1}H} NMR (121 MHz, C_6D_6): δ -47.3. ^{13}C{^{1}H} NMR (125.8 MHz, C_6D_6): δ 28.16 (vt; -CH$_2$$CH_2$-), 14.01 (dd; -P($CH_3$)$_2$).

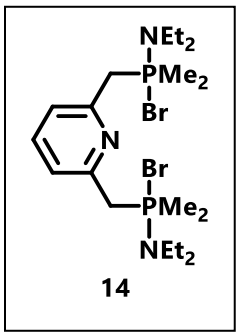

14

14: [(^{Me4}PNP)(NEt$_2$)$_2$][Br]$_2$. A mixture of N,N-diethylamino-P,P-dimethylphosphine (0.274 g, 2.05 mmol) were added to a solution of 2,6-bis(bromomethyl)-pyridine (0.220 g, 0.84 mmol) in MeCN. The solution was stirred overnight (ca. 15 h), over which time an abundant white precipitate formed. The precipitate was collected by filtration and washed with cold MeCN (0 °C) (3 x 10 mL), then Et$_2$O (3 x 10 mL) to afford **14** (0.420 g, 0.79 mmol; 94 % yield). ^{1}H NMR (300 MHz, CD_3CN): δ 7.8 (t; $^3J_{HP}$ = 7.5 Hz 1H; Ar-H), 7.4 (d; $^3J_{HP}$ = 7.5 Hz 2H; Ar-H), 3.92 (d; $^2J_{HP}$ = 15.0 Hz; 4H; -(CH_2)-), 3.05 (dsep; 8H; -N(CH_2CH$_3$)), 2.03 (d; $^2J_{HP}$ = 13.5 Hz; 12H; -P(CH_3)$_2$), 0.97 (t; $^2J_{HP}$ = 7.0 Hz; 2H; -N(CH$_2$$H_3$)). ^{31}P{^{1}H} NMR (121 MHz, CD_3CN): δ 60.0.

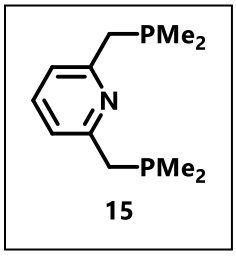

15

15: ^{Me4}PNP. $NaAlH_4$ (0.059 g, 1.1 mmol) was added portion-wise to a solution of **14** (0.506 g, 0.84 mmol) in THF at room temperature. The solution was stirred for 2 h. An argon sparged aqueous solution of NaOH (15 %) was added dropwise to the reaction mixture at 0 °C. The mixture was stirred for 30 minutes at RT. The volume of the mixture was reduced under vacuum, then the organics were extracted with pentane. The volatiles were removed under vacuum to afford a mixture of **15** and the analogous mono-phosphine **16** (0.298 g, 80:20). The following characterization omits signals for **16** unless specified. ^{1}H NMR (500 MHz, CD_2Cl_2): δ 7.48 (t; $^3J_{HH}$ = 7.8 Hz; 1H; Ar-H), 6.90

(d; $^{3}J_{HH}$ = 7.8 Hz; 2H; Ar-*H*), 2.87 (app s; 4H; -(CH_2)-), 1.01 (d; $^{2}J_{HP}$ = 3.2 Hz; 12H; -P(CH_3)$_2$). ^{31}P{^{1}H} NMR (121 MHz, CD_2Cl_2): δ -42.7 (^{Me4}PNP; 80 %). -43.0 (^{Me2}PN; 20 %).

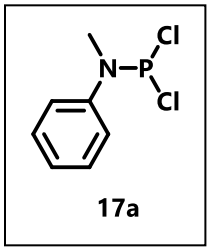

17a

17a: Me(Ph)NPCl$_2$. A solution of methylaniline (18.7 g, 0.17 mol) and triethylamine (17.3 g, 17 mol) in diethyl ether was added dropwise to a solution of PCl_3 (23.5 g, 0.17 mol) in diethyl ether (250 mL) at - 78°C. After the addition, the mixture was warmed to room temperature and stirred overnight (ca. 15 h). The abundant precipitated was removed by filtration and washed with diethyl ether (3x 50 mL). The diethyl either was removed under vacuum, then the remaining yellow oil was distilled under vacuum to afford **17a** (14.0 g, 0.07 mol, 40 % yield). ^{1}H NMR (300 MHz, C_6D_6): δ 7.18-6.9 (m, 5H; Ar-*H*), 3.08 (d; $^{3}J_{HP}$ = 4.6 Hz; 3H; -N(CH_3)). ^{31}P{^{1}H} NMR (121 MHz, C_6D_6): δ 157.5.

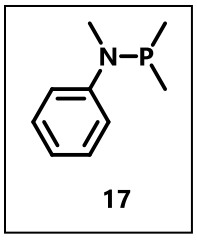

17

17: Me(Ph)NPMe$_2$. *Method A:* A solution of MeMgBr in diethyl either (23.3 mL, 0.070 mol) was added dropwise to a solution of Me(Ph)NPCl$_2$ (7.37 g, 0.035 mol) in diethyl either at 0 °C. After the addition, the mixture was stirred for 2 hours at room temperature. The resulting precipitate was removed by filtration and was washed with diethyl ether (3 x 20 mL). The precipitate was reactive when exposed to moisture and smelled of phosphine. The diethyl either was removed under vacuum and the resulting oil was distilled under vacuum to afford **17** (1.60 g, 0.01 mol, 30 % yield). ^{1}H NMR (300 MHz, C_6D_6): δ 7.4-6.4 (m, 5H; Ar-*H*), 2.64 (d; $^{3}J_{HP}$ = 2.1 Hz; 3H; -N(CH_3)), 1.02 (d; $^{2}J_{HP}$ = 6.7 Hz; 6H; -P(CH_3)$_2$). ^{31}P{^{1}H} NMR (121 MHz, C_6D_6): δ 31.7. *Method B:* A solution of N,N-diethylamino-P,P-dimethylphosphine (**6^{Et}**) (0.100 g, 0.75 mmol) and methyl aniline (0.072 g, 0.68 mmol) was heated

to 100 °C for 15 hours under a flow of argon to afford a mixture of N,N-methylphenlamino-P,P-dimethylphosphine and methyl aniline (62 : 38).

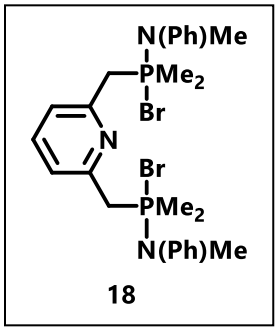

18

18: [(^{Me4}PNP)(N(Ph)Me)$_2$][Br]$_2$. A mixture of N,N-methylphenylamino-P,P-dimethylphosphine (0.588 g, 3.52 mmol) and Me(Ph)NH were added to a solution of 2,6-bis(bromomethyl)pyridine (0.430 g, 1.60 mmol) in MeCN. The solution was stirred overnight (ca. 15 h), over which time an abundant white precipitate formed. The precipitate was collected by filtration and washed with cold MeCN (0 °C) (3 x 10 mL), then diethyl either (3 x 10 mL) to afford **18** (0.73 g, 1.22 mmol; 76 % yield). ^{1}H NMR (300 MHz, CD_3CN): δ 7.9-7.0 (m, 13H; Ar-*H*), 4.04 (d; $^2J_{HP}$ = 15.5 Hz; 4H; -(C*H*$_2$)-), 3.10 (d; $^3J_{HP}$ = 9.5 Hz; 3H; -N(C*H*$_3$)), 2.00 (d; $^2J_{HP}$ = 13.6 Hz; 12H; -P(C*H*$_3$)$_2$). ^{31}P{^{1}H} NMR (121 MHz, CD_3CN): δ 61.6.

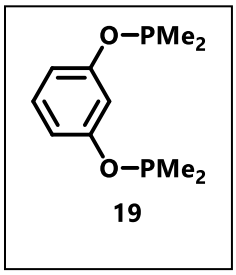

19

19: ^{Me4}POCOP. A J-Young tube was charged with 1,3-benzenediol (0.019 g, 0.17 mmol) and N,N-diisopropylamino-P,P-dimethylphosphine (**6^{iPr}**) (0.075 g, 0.47 mmol). The mixture was heated to 130 °C for 4 h to afford a yellow solution. The volatiles were removed under vacuum to afford **19** (0.040 g, 0.17 mmol; 99 % yield). ^{1}H NMR (300 MHz, Tol-d$_8$): δ 7.17-6.83 (m, overlapping Tol-d$_8$; Ar-*H*), 1.18 (d; $^3J_{HP}$ = 6.3 Hz; 12H; -P(CH$_3$)$_2$). ^{31}P{^{1}H} NMR (121 MHz, Tol-d$_8$): δ 123.5.

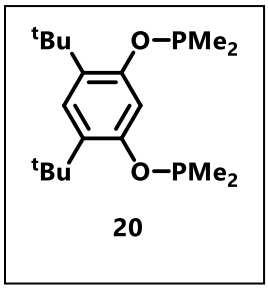

20

20: ^{Me4}POCOP$_{tBu2}$. *Method A:* A J-Young tube was charged with 4,6-ditertbutyl-1,3-benzenediol (0.049 g, 0.22 mmol) and N,N-diisopropylamino-P,P-dimethylphosphine (**6^{iPr}**) (0.96 g, 0.59 mmol). The mixture was heated to 130 °C for 4 hours to afford a light-yellow solution. The volatiles were removed under vacuum to afford a yellow solid, ^{Me4}POCOP$_{tBu2}$ (0.067 g, 0.22 mmol; 98 % yield). ^{1}H NMR (500 MHz, Tol-d$_8$): δ 7.44 (t; $^{4}J_{HP}$ = 4.7 Hz; 1H; Ar-*H*), 7.30 (s; 1H; Ar-*H*), 1.42 (s; 18H; -C(C*H*$_3$)$_3$), 1.24 (d; $^{3}J_{HP}$ = 6.4 Hz; 12H; -P(CH$_3$)$_2$) . ^{31}P{^{1}H} NMR (202 MHz, Tol-d$_8$): δ 117.9.

Method B[56]*:* A Schlenk flask equipped with a Teflon stopper was charged with 4,6-ditertbutyl-1,3-benzenediol (0.202 g, 0.90 mmol). NaH (0.047 g, 2.00 mmol) and THF (3 mL). The mixture was heated at 60 °C for 2 hours. The mixture was degassed, then ClPMe$_2$ (0.184 g, 1.9 mmol) was added. The yellow mixture was stirred overnight at room temperature. The volatiles were removed under vacuum, and the remaining solids were extracted with Et$_2$O (4 x 3 mL). The solvent was removed under vacuum to afford a yellow oil, **20** (0.065 g, 0.21 mmol; 23 % *crude* yield). The spectroscopic characterization shows peaks matching those from method A, and several other unidentified species.

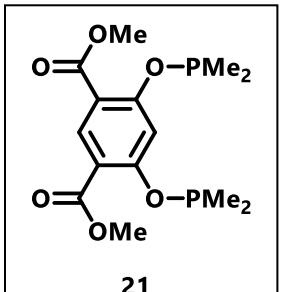

21

21: ^{Me4}POCOP$_{COOMe2}$. *Attempted Synthesis:* A J-Young tube was charged with 4,6-dimethylester-1,3-benzenediol (0.020 g, 0.09 mmol) and N,N-diisopropylamino-P,P-dimethylphosphine (**6^{iPr}**) (0.037 g, 0.23 mmol). The mixture was heated to 130 °C for 4 hours to afford a dark-brown mixture. The volatiles were removed under vacuum to afford a brown oil. The ^{31}P{^{1}H} NMR spectrum showed 6+ phosphorus-containing species.

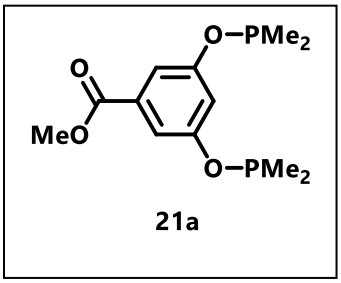

21a

21a: ^{Me4}POCOP$_{COOMe}$: *Method A:* A J-Young tube was charged with 5-methylester-1,3-benzenediol (0.030 g, 0.18 mmol) and N,N-diisopropylamino-P,P-dimethylphosphine (**6^{iPr}**) (0.80 g, 0.49 mmol). The mixture was heated to 130 °C for 4 hours to afford a light-yellow solution. The volatiles were removed under vacuum to afford a yellow solid, **21a** (0.050 g, 0.18 mmol; 97 % yield). ^{1}H NMR (500 MHz, Tol-d$_8$): δ 7.17-6.83 (m, overlapping Tol-d$_8$; Ar-*H*), 3.44 (s; 3H; COO(C*H*$_3$)), 1.09 (d; $^{3}J_{HP}$ = 6.3 Hz; 12H; -P(C*H*$_3$)$_2$). ^{31}P{^{1}H} NMR (202 MHz, Tol-d$_8$): δ 125.5.

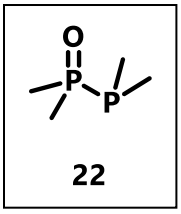

22

22: Me$_2$P(O)-PMe$_2$. Water (3 µl, 0.17 mmol) was added to a solution of Et$_2$NPMe$_2$ (0.05 g, 0.37 mmol) in THF; the solution was stirred for 15 h at RT. The volatiles were removed under vacuum to afford **22** (0.02 g, 0.14 mmol; 85 % yield). Crystals of Me$_2$P(O)-PMe$_2$ were grown from a concentrated solution of Me$_2$P(O)-PMe$_2$ in THF at room temperature.^{1}H NMR (300 MHz, C$_6$D$_6$): δ 1.06 (dd; $^{2}J_{HP}$ = 11.8 Hz, $^{3}J_{HP}$ = 5.8 Hz 3H; P(C*H*$_3$)$_2$), 0.96 (dd; $^{2}J_{HP}$ = 14.8 Hz, $^{3}J_{HP}$ = 3.4 Hz 3H; P(O)(C*H*$_3$)$_2$). ^{31}P{^{1}H} NMR (121.5 MHz, C$_6$D$_6$): δ 42.2 (d; $^{1}J_{PP}$ = 195.4 Hz; *P*(O)(CH$_3$)$_2$), -66.7 (d; $^{1}J_{PP}$ = 195.4 Hz; *P*(CH$_3$)$_2$).

2.5 Crystal Structures

Figure 2.1

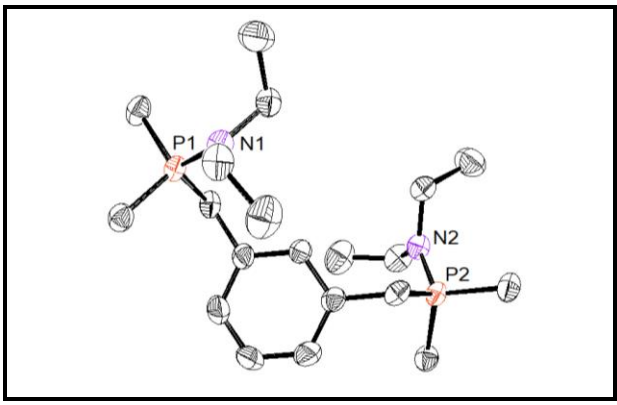

Bond (Å) or Angle (°)	Value
N(1)-P(1)	1.618 (3) Å
N(2)-P(2)	1.618 (3) Å
P(1) to Br(1)	4.5283 (6) Å

(Left) ORTEP of **7** shown with thermal ellipsoids at 50% probability. (Right) A table of selected angles and bond-distances for **7**. The bromide ions are omitted for clarity.

Figure 2.2

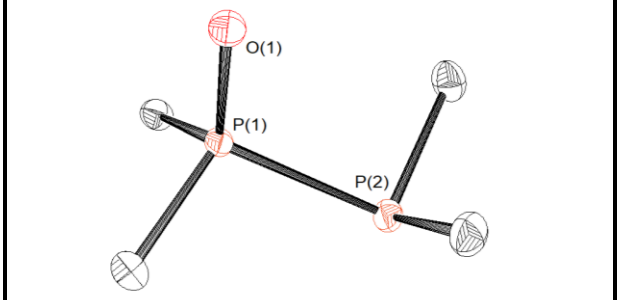

Bond (Å) or Angle (°)	Value
P(1)-P(2)	2.1973 (6) Å
P(1)-O(1)	1.4989 (10) Å
O-P(1)-P(2)	112.99 (4) °

ORTEP of **22** shown with thermal ellipsoids at 50% probability. (Right) A table of selected angles and bond-distances for **22**.

2.6 References

1 T. T. Lekich, P. G. Askelson, R. K. Burdick and D. M. Heinekey, *Organometallics*, 2018, **37**, 211−213.

2 D. M. Roddick, in *Organometallic Pincer Chemistry*, Springer, 2012, pp. 49–88.

3 A. J. Kendall and D. R. Tyler, *Dalt. Trans.*, 2015, **44**, 12473–12483.

4 A. Kumar, T. M. Bhatti and A. S. Goldman, *Chem. Rev.*, 2017, **117**, 12357–12384.

5 S. Kundu, Y. Choliy, G. Zhuo, R. Ahuja, T. J. Emge, R. Warmuth, M. Brookhart, K. Krogh-Jespersen and A. S. Goldman, *Organometallics*, 2009, **28**, 5432–5444.

6 C. S. Creaser and W. C. Kaska, *Inorg. Chim. Acta.*, 1978, **30**, 325–326.

7 H. Vahrenkamp, C. Laboratorium and D. U. Freiburg, *Inorg. Synth.*, 1982, **21**, 180–181.

8 G. W. Parshall, *J. Inorg. Nucl. Chem.*, 1960, **14**, 291–292.

9 J. E. Bercaw and G. W. Parshall, *Inorg. Synth.*, 1985, **23**, 199–200.

10 J. Zhang, E. Balaraman, G. Leitus and D. Milstein, *Organometallics*, 2011, **30**, 5716–5724.

11 M. Kawatsura and J. F. Hartwig, *Organometallics*, 2001, **20**, 1960–1964.

12 T. Yano, Y. Moroe, M. Yamashita and K. Nozaki, *Chem. Lett.*, 2008, **37**, 1300–1301.

13 D. Hermann, M. Gandelman, H. Rozenberg, L. J. W. Shimon and D. Milstein, *Organometallics*, 2002, **21**, 812–818.

14 M. Fild, O. Stelzer, R. Schmutzler and G. O. Doak, *Inorg. Synth.*, 1973, **14**, 4–9.

15 W. Voskuil and J. F. Arens, *Org. Synth.*, 1968, **48**, 47–49.

16 G. W. Parshall, R. C. Stocks and L. D. Quin, in *Inorganic Syntheses*, ed. G. W. Parshall, 1974, vol. 15, pp. 7–9.

17 A. B. Burg and P. J. Slota, *J. Am. Chem. Soc.*, 1958, **80**, 1107–1109.

18 D. Morales-Morales and C. Jensen, Eds., *The Chemistry of Pincer Compounds*, Elsevier, 2007.

19 I. Göttker-Schnetmann, P. White and M. Brookhart, *J. Am. Chem. Soc.*, 2004, **126**, 1804–1811.

20 W. J. Hunks, M. C. Jennings and R. J. Puddephatt, *Inorg. Chem.*, 2000, **39**, 2699–2702.

21 J. Zhang, C. M. Medley, J. A. Krause and H. Guan, *Organometallics*, 2010, **29**, 6393–6401.

22 J. M. Goldberg, G. W. Wong, K. E. Brastow, W. Kaminsky, K. I. Goldberg and D. M.

Heinekey, *Organometallics*, 2015, **34**, 753–762.

23 D. Morales-Morales, C. Grause, K. Kasaoka, R. Redón, R. E. Cramer and C. M. Jensen, *Inorganica Chim. Acta*, 2000, **300**, 958–963.

24 A. J. Kendall, C. A. Salazar, P. F. Martino and D. R. Tyler, *Organometallics*, 2014, **33**, 6171–6178.

25 A. J. Kendall, D. T. Seidenkranz and D. R. Tyler, *Organometallics*, 2017, **36**, 2412–2417.

26 H. R. Hays, *J. Org. Chem.*, 1968, **33**, 3690–3694.

27 L. R. Doyle, A. Heath, C. H. Low and A. E. Ashley, *Adv. Synth. Catal.*, 2014, **356**, 603–608.

28 W. C. Shih and O. V. Ozerov, *Organometallics*, 2015, **34**, 4591–4597.

29 D. Hérault, D. H. Nguyen, D. Nuel and G. Buono, *Chem. Soc. Rev.*, 2015, **44**, 2508–2528.

30 W. J. Bailey and S. A. Buckler, *J. Am. Chem. Soc.*, 1957, **79**, 3567–3569.

31 J. Gopalakrishnan, *Appl. Organomet. Chem.*, 2009, **23**, 291–318.

32 A. J. Kendall and D. R. Tyler, *Dalton Trans.*, 2015, **44**, 12473–12483.

33 L. Maier, *Helv. Chim. Acta*, 1964, **47**, 2129–2137.

34 H. H. Sisler and N. L. Smith, 1962, US Patent 3131204.

35 K. Muraishi, K. Sueto and Y. Gao, 2007, European Patent 1956026A1.

36 L. Maier, *Helv. Chim. Acta*, 1968, **51**, 405–413.

37 E. C. Ashby, J. R. Sanders, P. Claudy and R. D. Schwartz, *Inorg. Chem.*, 1973, **12**, 2860–2868.

38 E. C. Ashby and J. Prather, *J. Am. Chem. Soc.*, 1966, **88**, 729–733.

39 E. C. Ashby and J. R. Boone, *J. Org. Chem.*, 1976, **41**, 2890–2903.

40 S. Singh and K. M. Nicholas, *Chem. Commun.*, 1998, 149–150.

41 R. H. Neilson and P. Wisian-Neilson, *Inorg. Chem.*, 1982, **21**, 3568–3569.

42 D. W. Morton and R. H. Neilson, 1982, 623–627.

43 R. R. Ford, M. A. Goodman, R. H. Neilson, A. K. Roy, U. G. Wettermark and P. Wisian-neilson, *Inorg. Chem.*, 1984, **23**, 2063–2068.

44 R. B. Bedford, Y.-N. Chang, M. F. Haddow and C. L. McMullin, *Dalt. Trans.*, 2011, **40**, 9034.

45 E. L. Evans, T.C., Gavrilovich, E., Mihai, R.C. and Isbasescu, I., 2015, US Patent Appl. 13/384,772.

46 B. Hoge and B. Kurscheid, *Angew. Chemie - Int. Ed.*, 2008, **47**, 6814–6816.

47 A. B. Burg and R. A. Sinclair, *J. Am. Chem. Soc.*, 1966, **88**, 5354–5355.

48 G. R. Fulmer, A. J. M. Miller, N. H. Sherden, H. E. Gottlieb, A. Nudelman, B. M. Stoltz, J. E. Bercaw and K. I. Goldberg, *Organometallics*, 2010, **29**, 2176–2179.

49 M. Gerisch, J. R. Krumper, R. G. Bergman and T. D. Tilley, *Organometallics*, 2003, **22**, 47–58.

50 C. M. Hartshorn and P. J. Steel, *Organometallics*, 1998, **17**, 3487–3496.

51 A. J. Wessel, J. W. Schultz, F. Tang, H. Duan and L. M. Mirica, *Org. Biomol. Chem.*, 2017, **15**, 9923–9931.

52 B. E. Love and E. G. Jones, *J. Org. Chem.*, 1999, **64**, 3755–3756.

53 K. Wang, M. E. Goldman, T. J. Emge and A. S. Goldman, *J. Organomet. Chem.*, 1996, **518**, 55–68.

54 B. W. Bangerter, R. P. Beatty, J. K. Kouba and S. S. Wreford, *J. Org. Chem.*, 1977, **42**, 3247–3251.

55 N. F. Wood, R. N. Haszeldine and R. Fields, *J. Chem. Soc.*, 1970, 1370–1375.

56 G. Wong, *Pers. Commun.*

Chapter 3. Coordination Chemistry of Methyl-Substituted Pincer Iridium Complexes

3.1 Introduction

Several investigations of hydrogenation and dehydrogenation chemistry have employed ^{R4}PCP (C_6H_4-1,3-[CH_2PR_2]$_2$) and ^{R4}POCOP (C_6H_4-1,3-[OPR_2]$_2$) iridium compounds (R = ^{t}Bu or ^{i}Pr).[1,2] However, there are a limited number of reports of pincer complexes with steric or electronic variation of the phosphine R-groups.[3–7] This shortcoming may result from the difficulty in synthesizing other ^{R4}PCP and ^{R4}POCOP ligands (where R ≠ ^{t}Bu or ^{i}Pr). We developed a convenient synthesis of ^{Me4}PCP (**5**) and ^{Me4}POCOP (**19**) (see Chapter 2 for more information), which has allowed us to explore the coordination chemistry of ^{Me4}PCP (**5**) and ^{Me4}POCOP (**19**) with focus on the corresponding iridium complexes.[8]

Ligands **5** and **19** have been previously synthesized and metallated, but only limited examples exist. The Kaska and Goldman groups reported the synthesis of organometallic ^{Me4}PCP complexes (Scheme 3.1).[9,10] Kaska and Creaser synthesized (^{Me4}PCP)Fe(H)(DMPE) by reducing an oligomeric material [(^{Me4}PCP)$FeCl_2$]$_n$ (prepared by treating ^{Me4}PCP with $FeCl_2$) with Na/Hg in the presence of DMPE (DMPE = 1,3-bis(dimethylphosphino)ethane); however they did not report a yield or extensive characterization of the complex. Like Kaska and Creaser, others have reported oligomer formation during metallation of sterically-undemanding pincer ligands.[11] Goldman and coworkers synthesized (^{Me4}PCP)Rh(CO) via the reaction of [Rh(COE)$_2$Cl]$_2$, ^{Me4}PCP, and Li(HMDS) under a CO atmosphere (HMDS = hexamethyl-disilylamine).[10] However, (^{Me4}PCP)Rh(CO) was not fully characterized, and a yield was not reported.[10] Guan and coworkers

reported the synthesis of (^{Me4}POCOP)NiCl by forming ^{Me4}POCOP *in situ*, then adding $NiCl_2$ (Scheme 3.2).[12]

Scheme 3.1 (a) Synthesis of (^{Me4}PCP)Fe(H)(DMPE). [9] (b) Synthesis of (^{Me4}PCP)Rh(CO).[10]

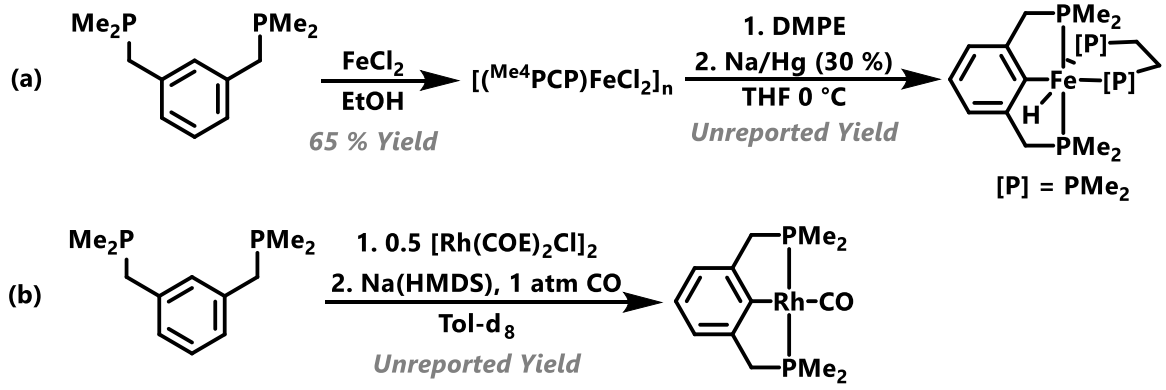

Scheme 3.2 Synthesis of (^{Me4}POCOP)NiCl. [12]

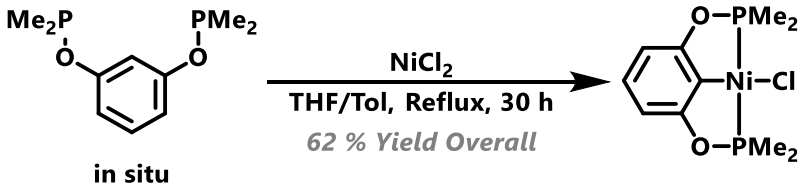

Because these examples are limited and do not involve iridium, we turned to adapting metallation techniques for other ^{R4}PCP and ^{R4}POCOP ligands to the metallation of ^{Me4}PCP and ^{Me4}POCOP. As shown in Scheme 3.3, Roddick and coworkers reported a sterically-similar but electronically quite different ^{R4}PCP derivative, $^{(CF3)4}$PCP, which they metallated with iridium through the reaction of 0.5 equiv. $[Ir(COE)_2Cl]_2$ or $[Ir(COD)Cl]_2$, $^{(CF3)4}$PCP, and an L-type ligand (e.g. CO, MeCN, or ethylene). Roddick and coworkers found that commonly-used iridium precursors, especially those that react with pincer ligands to form a 5-coordinate species, react with $^{(CF3)4}$PCP to afford oligomeric complexes in the absence of added L-type ligands.[3,5] Our group has previously reported the metallation of sterically-undemanding ^{R4}POCOP ligand (R = OMe) with $Ir(CO)_2Cl$(*p*-toluidine) to afford stable 6-coordinate iridium complexes (Scheme 3.4).[13]

Scheme 3.3 Synthesis of ($^{(CF3)4}$PCP)Ir(HCl)L.

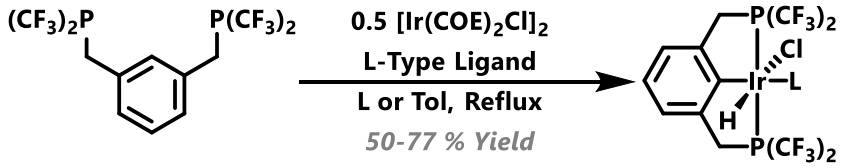

Scheme 3.4 Synthesis of ($^{(OMe)4}$PCP)Ir(HCl)CO.

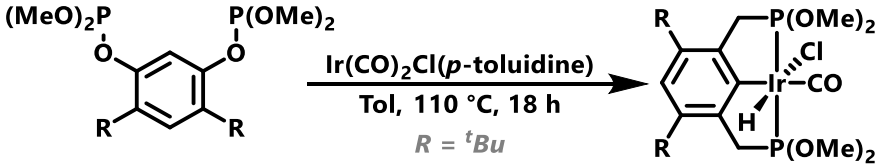

Here, we describe the synthesis of (^{Me4}PCP)Ir, (^{Me4}PCP)Rh, and (^{Me4}POCOP)Ir derived complexes through the adaptations of the aforementioned syntheses. Initially, we hypothesized that functional groups on the aryl moiety of the ^{Me4}PCP or ^{Me4}POCOP ligands would be necessary to prevent oligomerization described by previous reports, however we found that these modifications were not necessary in certain cases. Additionally, we compare the steric and electronic properties of these compounds with previously reported ^{R4}PCP and ^{R4}POCOP iridium complexes.

3.2 Results and Discussion

3.2.1 Synthesis and Coordination Chemistry of (^{Me4}PCP)Ir Complexes

3.2.1.1 Synthesis of (^{Me4}PCP$_{R2}$)Ir(HCl)CO (23^{Me} and 23'^{Me})

Scheme 3.5 Synthesis of (^{Me4}PCP$_{Me2}$)Ir(HCl)CO (**23'^{Me}**).

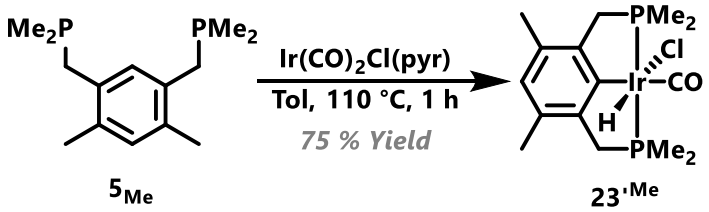

Previously reported metallations of ^{R}PCP generally proceed through a 5-coordinate iridium species, (^{R4}PCP)Ir(HCl).[2,14,15] However, attempts to synthesize analogs of these 5-coordinate species with $^{Me4}PCP_{Me4}$ gave intractable products. Thus, we focused on adapting the previously reported synthesis of (^{iPr4}POCOP)Ir(HCl)CO to prepare ($^{Me4}PCP_{Me2}$)Ir(HCl)CO (**23'^{Me}**). As shown in Scheme 3.5, $Ir(CO)_2$(pyridine)Cl reacts with $^{Me4}PCP_{Me2}$ (**5$_{Me}$**) at 110 °C over 1 h to afford ($^{Me4}PCP_{Me2}$)Ir(HCl)CO (**23'^{Me}**). The ^{1}H NMR spectrum of **23'^{Me}** exhibits two doublets of virtual triplets at 3.55 ppm and 3.20 ppm for the inequivalent methylene protons; two overlapping virtual triplets centered at 1.75 ppm for the methyl protons (-P(CH_3)$_2$); and a triplet at -18.8 ppm ($^2J_{HP}$ = 13.8 Hz) for the iridium-bound hydride.

Scheme 3.6 Synthesis of (^{Me4}PCP)Ir(HCl)CO (**23^{Me}**).

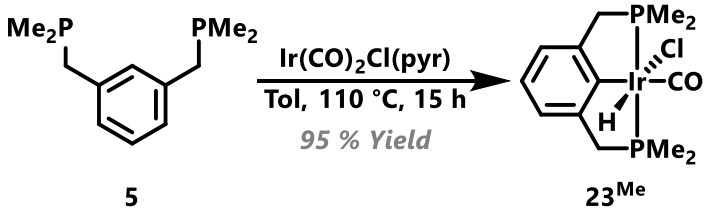

Due to previous reports, we were operating under the hypothesis that metallating ^{Me4}PCP (**5**) required steric bulk to prevent organometallic oligomers;[13,16,14] however, steric bulk is not necessary with ^{Me4}PCP (**5**) and specific metal precursors. As shown in Scheme 3.6, **5** reacts with $Ir(CO)_2Cl$(pyridine) at 110 °C to afford (^{Me4}PCP)Ir(HCl)CO, (**23^{Me}**; Scheme 3.06). The ^{1}H NMR spectrum of **23^{Me}** exhibits two doublets of virtual triplets at 3.75 ppm and 3.36 ppm for the inequivalent methylene protons; two overlapping virtual triplets centered at 1.84 ppm for the methyl protons; and a triplet at -18.8 ppm ($^2J_{HP}$ = 13.9 Hz) for the hydride. Attempts to metallate **5** with other precursors such as $[Ir(COE)_2Cl]_2$ and $[Ir(COD)_2Cl]_2$ resulted in products insoluble in common organic solvents even when CO, H_2 or MeCN was present.[2,5] These presumably

polymeric materials may form because smaller pincer ligands tend to form oligomers with metal precursors and/or the methyl groups may become activated by coordinately unsaturated iridium species.[13,16,14]

3.2.1.2 Synthesis of (^{Me4}PCP$_{R2}$)Ir(CO) (24^{Me} and 24$'^{Me}$)

Scheme 3.7 Synthesis of (^{Me4}PCP$_{Me2}$)Ir(CO) (**24**$'^{Me}$).

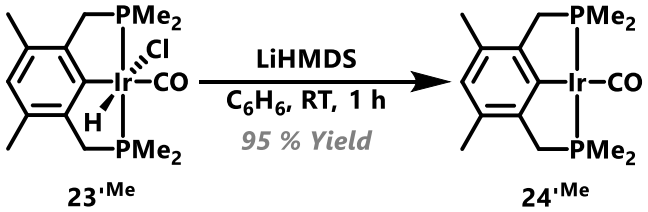

23'Me 24'Me

LiHMDS (Li[N(SiMe$_3$)$_2$]) dehydrohalogenates **23'^{Me}** to afford (^{Me4}PCP$_{Me2}$)Ir(CO) (**24'^{Me}**; Scheme 3.7). The ^{1}H NMR spectrum of **24'^{Me}** is as expected with symmetrical signals for the methylene protons at 3.12 ppm and methyl protons (-P(C*H*$_3$)$_2$) at 1.36 ppm. The ^{31}P{^{1}H} NMR spectrum of **24'^{Me}** shows a singlet at 16.6 ppm.

Scheme 3.8 Synthesis of (^{Me4}PCP)Ir(HCl)(CO) (**24**^{Me}).

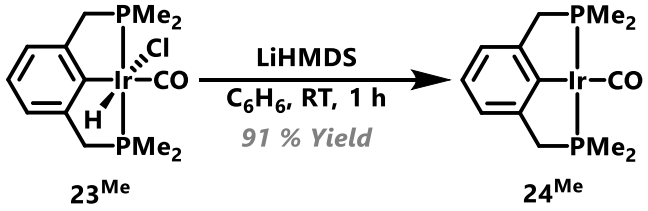

23Me 24Me

KHMDS (K[N(SiMe$_3$)$_2$]) dehydrohalogenates **23^{Me}** to afford (^{Me4}PCP)Ir(CO) (**24^{Me}**; Scheme 3.8). The ^{1}H NMR spectrum of **24^{Me}** shows a virtual triplet at 3.07 ppm for the methylene protons, and a virtual triplet at 1.23 ppm for the methyl protons. The ^{31}P{^{1}H} NMR spectrum of **24^{Me}** shows a singlet at 17.1 ppm. Figure 3.1 shows the solid-state structure of **2^{Me}**. The bond lengths of **24^{Me}**

are similar to other (^{R4}PCP)Ir(CO) complexes, however the C_2 twist (e.g. C(3)-C(1)-Ir(1)-P(1) torsion angle) is larger than other (^{R4}PCP)Ir(CO) (R = ^{i}Pr, ^{t}Bu) species. Roddick and coworkers have attributed a larger C_2 twist in ($^{(CF3)4}$PCP)Ir(CO) to its reduced steric bulk; **24^{Me}** likely shows a relatively large C_2 twist for the same reason. The C_2 twist originates from spatial configuration, and is generally more pronounced for the ^{R4}PCP systems because the C_{aryl} - C_{benzyl} - P length is larger than the C_{aryl} - O - P length.[6]

Figure 3.1 (Left) ORTEP of (^{Me4}PCP)Ir(CO) (**24^{Me}**) shown with thermal ellipsoids at 50% probability. (Right) A table of selected angles and bond-distances for **24^{Me}**.

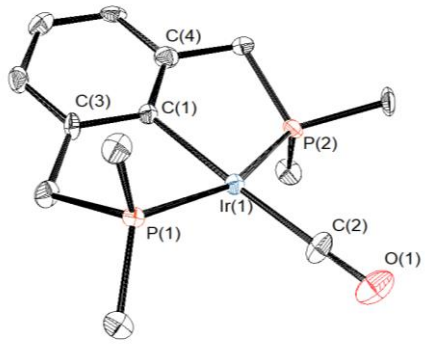

Bond (Å) or Angle (°)	Value
Ir(1)-C(1)	2.109 (4) Å
Ir(1)-C(2)	1.883 (10) Å
Ir(I)-O(1)	3.023 (8) Å
P(1)-Ir(1)-P(2)	160.61 (9) °
C(1)-Ir(1)-C(2)	177.7 (4) °
C(3)-C(1)-Ir(1)-P(1)	16.2 (5) °
C(4)-C(1)-Ir(1)-P(2)	17.7 (5) °

3.2.1.3 Synthesis of trans-(^{Me4}PCP$_{R2}$)Ir(H)$_2$(CO) (trans-25^{Me} and trans-25'^{Me})

Scheme 3.9 Synthesis of trans-(^{Me4}PCP$_{Me2}$)Ir(H)$_2$(CO) (**trans-25'^{Me}**).

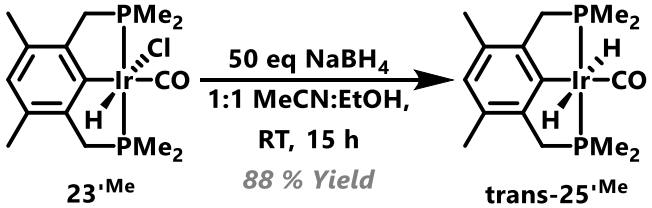

Compound **23'^{Me}** undergoes transmetalation with $NaBH_4$ in a 1:1 mixture of EtOH:MeCN to afford trans-(^{Me4}PCP$_{Me2}$)Ir(H)$_2$CO (**trans-25'^{Me}**; Scheme 3.9). The ^{1}H NMR spectrum of **trans-**

25′^{Me} shows a virtual triplet at 3.14 ppm for the methylene protons, a virtual triplet at 1.49 ppm for the methyl protons (-P(CH_3)$_2$), and a triplet at -9.45 ($^2J_{HP}$ = 16.4 Hz) for the hydrides. Like other trans-dihydride metal complexes, **trans-25′^{Me}** reacts with DCM to afford the HCl complex, **23′^{Me}**.[17]

Scheme 3.10 Synthesis of trans-(^{Me4}PCP)Ir(H)$_2$(CO) (**trans-25^{Me}**).

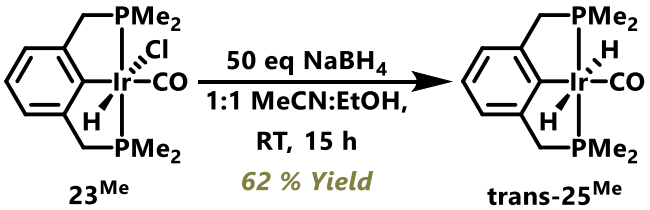

Compound **23^{Me}** undergoes transmetalation with $NaBH_4$ in a 1:1 mixture of EtOH:MeCN to afford trans-(^{Me4}PCP)Ir(H)$_2$CO, (**trans-25^{Me}**; Scheme 3.10). The ^{1}H NMR spectrum of the dihydride complex shows a virtual triplet at 3.21 ppm for the methylene protons, a virtual triplet at 1.49 ppm for the methyl protons, and a triplet at -9.16 ($^2J_{HP}$ = 16.4 Hz) for the hydrides. Like **trans-25′^{Me}**, **trans-25^{Me}** reacts with DCM to afford the HCl complex, **23^{Me}**. Figure 3.2 shows the solid-state structure of **trans-25^{Me}**. The bond lengths of **trans-25^{Me}** are similar to other (^{R4}PCP)Ir complexes, and like **trans-25′^{Me}**, the C_2-twist torsion angles are larger than analogous (^{R4}PCP)Ir complexes (R = ^{i}Pr, ^{t}Bu).

Figure 3.2 (Left) ORTEP of trans-(^{Me4}PCP)Ir(H)$_2$(CO) (**trans-25^{Me}**) shown with thermal ellipsoids at 50% probability. (Right) A table of selected angles and bond-distances for **trans-25^{Me}**. The hydrogen atoms, except for the hydrides, are omitted for clarity.

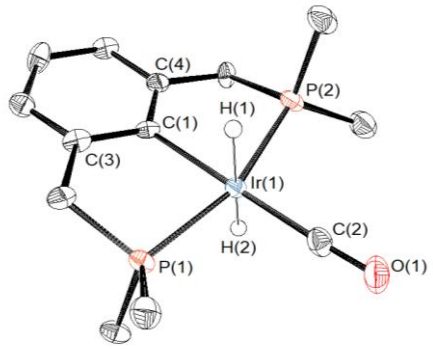

Bond (Å) or Angle (°)	Value
Ir(1)-C(1)	1.877 (10) Å
Ir(1)-C(2)	1.877 (10) Å
Ir(I)-O(1)	3.046 (2) Å
P(1)-Ir(1)-P(2)	161.19 (9) °
C(1)-Ir(1)-C(2)	178.1 (3) °
C(3)-C(1)-Ir(1)-P(1)	15.2 (6) °
C(4)-C(1)-Ir(1)-P(2)	14.2 (6) °

3.2.1.4 Synthesis of [(^{Me4}PCP)Ir(H)(pyr)CO][OTf] (26^{Me})

Scheme 3.11 Synthesis of [(^{Me4}PCP)Ir(H)(pyr)CO][OTf] (**26^{Me}**).

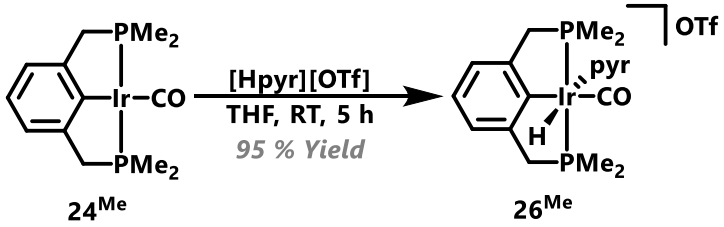

24^{Me} 26^{Me}

One equivalent of pyridinium triflate [Hpyr][OTf] protonates **24^{Me}** to afford [(^{Me4}PCP)Ir(H)(pyr)CO][OTf] (**26^{Me}**; Scheme 3.11). The ^{1}H NMR spectrum of **26^{Me}** shows three sharp signals for bound pyridine (8.16(d), 7.97(t), 7.39(t) ppm), two doublets of virtual triplets at 3.57 ppm and 3.44 ppm for the diastereotopic methylene protons, two virtual triplets at 1.97 ppm and 1.39 ppm for the methyl protons, and a triplet at -19.35 ppm ($^{2}J_{HP}$ = 16.4 Hz**)** for the hydride. One equivalent of acid with weakly-coordinating conjugate bases such as H[BF$_4$], H[Bar$^{F}_4$], and lutidinium protonate **24^{Me}** to afford new species [(^{Me4}PCP)Ir(H)(L)CO][X] (L is the conjugate base or solvent, and X may be the conjugate base). [(^{Me4}PCP)Ir(H)CO]$^{+}$ coordinates adventitious ligands because of its reduced steric bulk.

3.2.1.5 Synthesis of (^{Me4}PCP)Ir(OAc)$_2$(CO) (27^{Me}).

Scheme 3.12 Synthesis of (^{Me4}PCP)Ir(OAc)$_2$(CO) (**27^{Me}**).

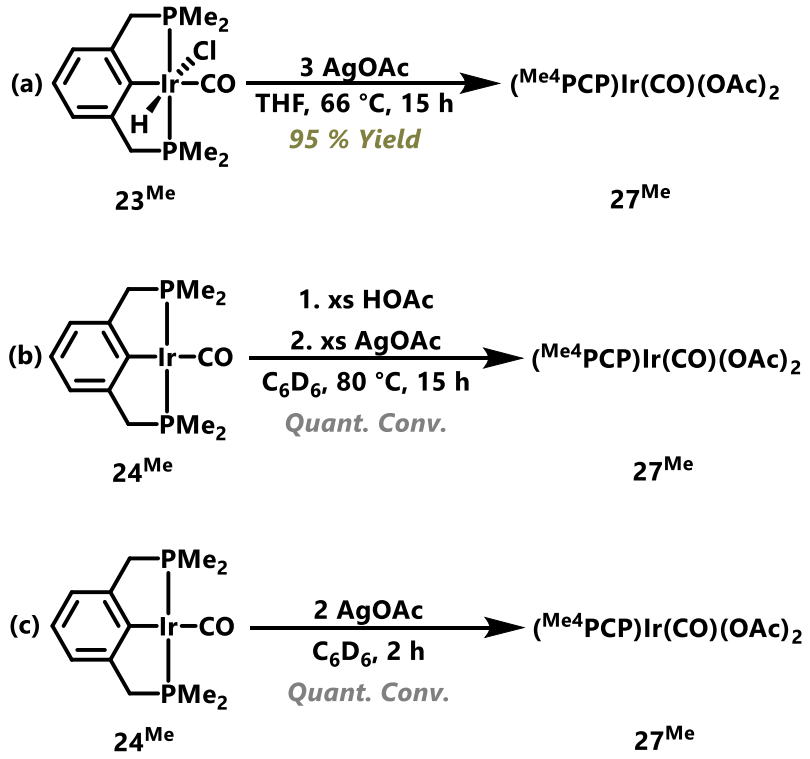

Compounds **23^{Me}** and **24^{Me}** show interesting reactivity with silver acetate. Three equivalents of silver acetate react with **23^{Me}** to afford a species with spectroscopic features consistent with assignment to (^{Me4}PCP)Ir(OAc)$_2$(CO) (**27**; Scheme 3.12a). During this reaction in Scheme 3.12a, a gray precipitate forms and acetic acid is observed by ^{1}H NMR spectroscopy. The ^{1}H NMR spectrum of **27^{Me}** shows two doublets of virtual triplets at 3.35 ppm and 2.66 ppm for the diastereotopic benzyl protons, two virtual triplets at 1.44 ppm and 1.39 ppm for the methyl protons, and two singlets at 2.27 and 1.76 for the acetate ligands. The ^{13}C{^{1}H} NMR spectra shows three distinct C=O functional groups, and an HMBC experiment shows that two of these three C=O functional groups are related to the acetate methyl protons. The IR spectrum shows a single CO stretch at 2035 cm^{-1}. Thus, the iridium center has two chemically inequivalent acetates, a CO, and

the ^{Me4}PCP ligand bound. Similarly, compound **24^{Me}** reacts with excess acetic acid to form a hydride acetate intermediate, then that intermediate reacts with excess silver acetate to afford a species with identical spectroscopic features as **27^{Me}** (Scheme 3.12b)**.** Compound **27^{Me}** can also be synthesized directly from **24^{Me}** through the reaction of **24^{Me}** and two equivalents of silver acetate at RT. This reaction to afford **27^{Me}** is interesting in that redox chemistry must be taking place between the iridium center and silver acetate. Figure 3.3 shows a proposed mechanism for this reaction based upon the syntheses in Scheme 3.12. Starting from **23^{Me}**, one equivalent of silver acetate undergoes transmetalation with **23^{Me}** to afford the hydrido acetate complex, **23a^{Me}**. Alternatively, **24^{Me}** reacts with acetic acid to afford **23a^{Me}**. Then, **23a^{Me}** could reductively eliminate acetic acid at elevated temperatures to afford **24^{Me}** (Figure 3.3, top pathway); or, **23a^{Me}** could undergo a redox reaction with another equivalent of silver acetate to afford a 20-electron, Ir(IV) complex (Figure 3.3, bottom pathway). Then, the Ir(IV) could reductively eliminate acetic acid to afford the proposed Ir(II) complex (Figure 3.3, bottom pathway); or **24^{Me}** could undergo a redox reaction with silver acetate to afford the proposed Ir(II) complex (Figure 3.3, bottom pathway). Finally, this proposed Ir(II) complex could undergo a redox reaction with the final equivalent of silver acetate to afford **27^{Me}.** The heat required to form the acetate complex from the protonated species, **23^{Me}** and **23a^{Me}** is likely needed to eliminate the acid or form the Ir(IV) intermediate. Van Koten and coworkers observed similar reactivity between silver acetate and a sterically-unencumbered rhodium complex.[18] They found that their rhodium(I) complex quickly reacts with two equivalents of silver acetate to form the corresponding bis-acetate complex.[18] They hypothesized the high-availability of the metal center allowed for an Ag-Rh, followed by an electron transfer event.[18] This explanation is plausible for the reactivity we observe with our system.

Figure 3.3 Proposed mechanism for the synthesis of **27^{Me}**.

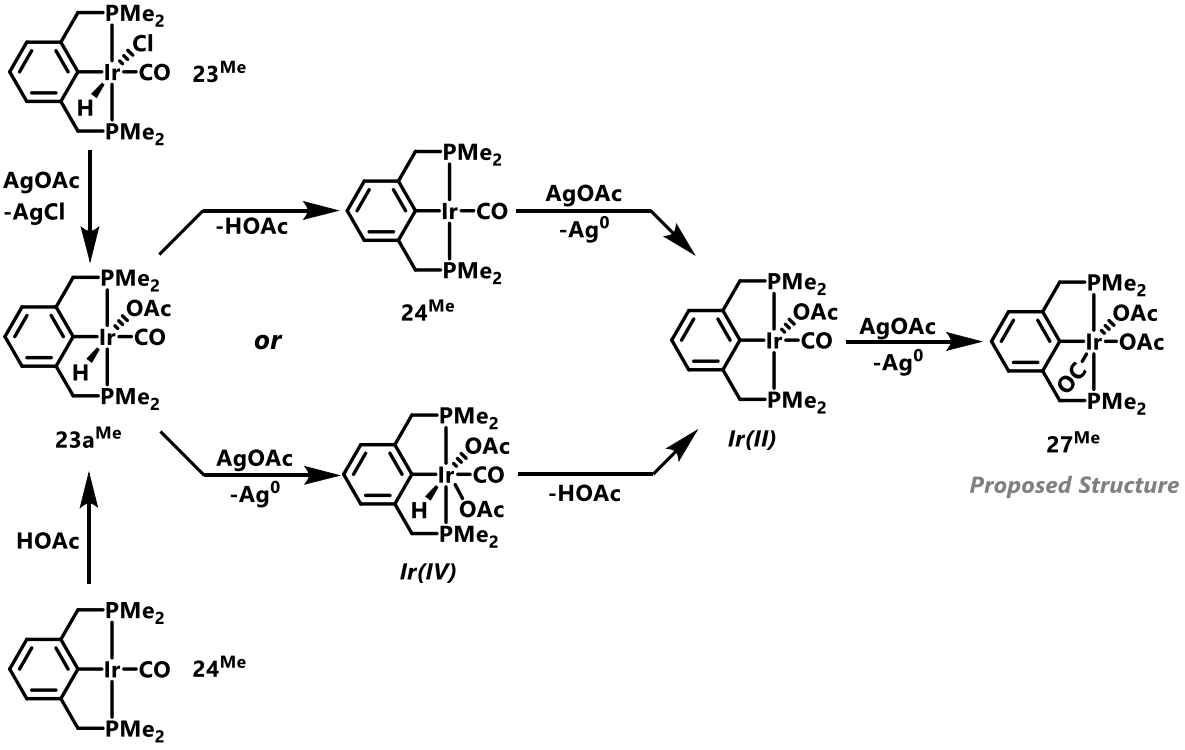

3.2.1.6 Coordination of L-type ligands to (^{Me4}PCP)Ir(CO)

Scheme 3.13 Coordination of CO (a; **28^{Me}**) or PMe_3 (b; **29^{Me}**) to (^{Me4}PCP)Ir(CO) (**24^{Me}**).

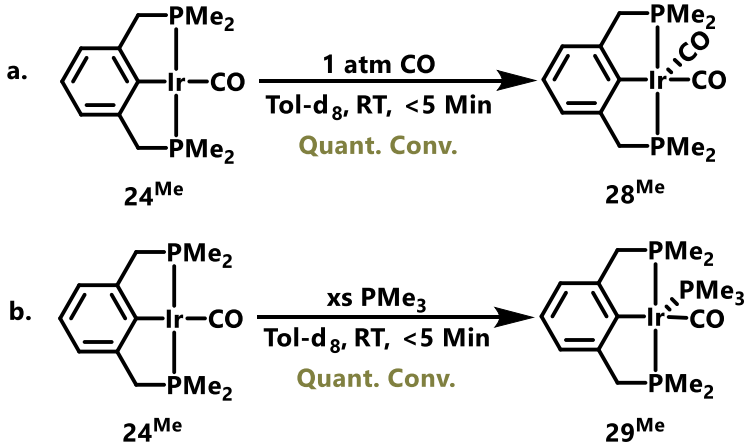

Compound **24^{Me}** coordinates CO under 1 atm CO at room temperature to afford (^{Me4}PCP)Ir(CO)2 (**28^{Me}**; Scheme 3.13a). The ^{1}H and ^{31}P{^{1}H} NMR spectra of **28^{Me}** are shifted relative to **24^{Me}**, and the IR spectrum of **28^{Me}** shows two CO stretches at 2010 and 1930 cm^{-}.

Compound **24^{Me}** also coordinates PMe_3 to give (^{Me4}PCP)Ir(PMe_3)(CO) (**29^{Me}**; Scheme 3.13b). The $^{31}P\{^1H\}$ NMR spectrum of **29^{Me}** shows a doublet at -1.79 ppm and triplet at -56.5 ppm ($^2J_{PP}$ = 112 Hz). Heating **29^{Me}** at 80 °C in toluene-d_8 does not result in conversion to a new species. ^1H and $^{31}P\{^1H\}$ NMR spectroscopy shows no evidence for interaction of weakly coordinating ligands, such as pyridine or triethylamine, with **24^{Me}**. Attempts to crystallize **28^{Me}** or **29^{Me}** were unsuccessful.

3.2.1.7 Electronic Comparison of (^{R4}PCP)Ir Complexes (R = ^{t}Bu, ^{i}Pr, Me, CF_3)

Table 3.5 (see section 3.4) shows the Ir-CO and Ir-H stretching frequencies for compounds (**23**-**26**, and **28)**. The ν(CO) of the ^{Me4}PCP iridium complexes are slightly higher in energy than the ^{iPr4}PCP and ^{tBu4}PCP analogs because methyl groups are less electron rich than *tert*-butyl and *iso*-propyl groups. Though, the electronic differences between the aliphatic-substituted complexes are not very pronounced, so one should not expect large electronic differences between the methyl, *tert*-butyl and *iso*-propyl substituted complexes. The CF_3 substituted complexes are electron deficient compared to the aliphatic series, and one should expect significant electronic differences between the methyl and CF_3-substituted complexes.

3.2.1.8 Steric Comparison of (^{R4}PCP)Ir Complexes (R = ^{t}Bu, ^{i}Pr, Me, CF_3).

Table 3.1 shows the space-filling models and Table 3.2 shows select structural values of compounds **24^{Me}**, **24^{iPr}**, **24^{tBu}**, **24^{CF3}**. As expected, **24^{Me}** has the lowest $\%V_{bur}$ out of the set of complexes. The metric $\%V_{bur}$ is the volume percentage that specified ligand takes up in a given sphere originating at the metal center.[19] Like **24^{CF3}**, **24^{Me}** has a large C_2 twist (measured by the dihedral angle between the CH_2-C_{Ar}-CH_2 and P-Ir-P planes).[6] This C_2 twist is more pronounced for sterically small PCP ligands on square planar iridium complexes because of the reduced steric

clash between phosphine groups.[6] Compound **24^{Me}** also has a relatively small P-M-P angle, which is also congruent with a lower %V_{bur} and larger C_2 twist.[6]

Table 8 Space-filling models of **24^{Me}**, **24^{iPr}**, **24^{tBu}**, and **24^{CF3}**.

Me (24^{Me})	**^{i}Pr (24^{iPr})**[20]	**^{t}Bu (24^{tBu})**[21]	**CF_3 (24^{CF3})**[4]
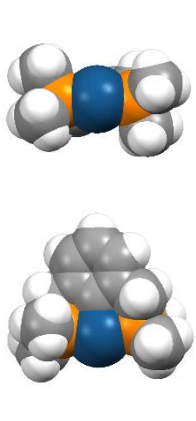	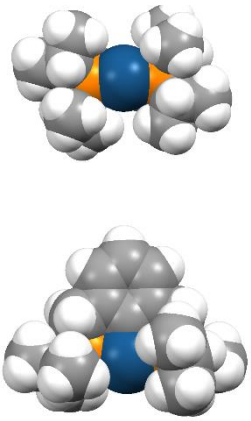	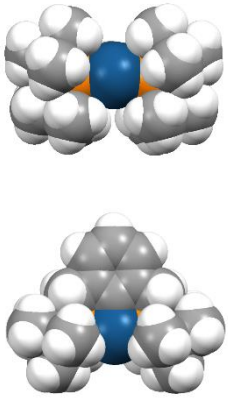	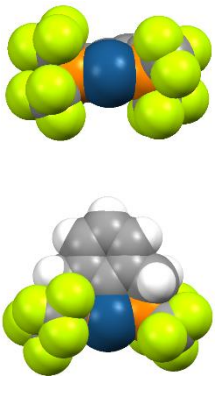

Table 9 Select Structural Data for (^{R4}PCP)Ir(CO) (**24^{R}**). a Calculated by the SambVca 2.0 program.[19] [b] The torsion angle between the benzyl carbon, ipso carbon, iridium and respective phosphorus.

2^{R}	%V_{bur}[a]	Twist[b] (°)	P-M-P (°)
2^{Me}	55.7	16.2(5), 17.2(5)	160.61(9)
2^{iPr}	67.6	8.0(3), 10.4(3)	163.71(4)
2^{tBu}	72.2	5.1(7), 1.0(7)	164.11(12)
2^{CF3}	61.4	12.5(14)	159.86 (2)

The fluxionality of pyridine on the NMR time scale in compounds **26^{Me}**, **26^{iPr}**, **26^{tBu}** can be used as proxy for understanding the steric environment in the cis-void space. The ^{1}H NMR spectrum of **26^{Me}** shows three sharp resonances for bound pyridine. In contrast, the ^{1}H NMR spectrum of **26^{tBu}** shows five sharp signals for bound pyridine, and the ^{1}H NMR spectrum of **26^{iPr}** shows three broad signals for bound pyridine.[2] The spectral differences suggest that the pyridine ligand of compound **26^{M}** freely rotates, the pyridine ligand of **26^{iPr}** undergoes hindered rotation,

and the pyridine ligand of **26^{tBu}** is static on the NMR time-scale. The differences in the rotation of the pyridine is most likely due to its steric interactions with the respective PCP ligand.

3.2.2 Attempts to Metallate ^{Me4}PCP (5) with Rhodium Complexes

Table 3.3 summarizes the attempts to metallate ^{Me4}PCP (**5**) with rhodium. Like iridium derivatives, rhodium precursors that usually lead to a 5-coordinate ^{R4}PCP species (R = ^{i}Pr or ^{t}Bu) form oligomeric materials in non-coordinating solvents. Rhodium precursors, $Rh(CO)Cl(PPh_3)_2$, $Rh(CO)H(PPh_3)_3$, and $Rh(CO)_2Cl$(pyridine) react with **5** to form multiple intractable species or oligomeric materials.

Scheme 3.14 Synthesis of (^{Me4}PCP)$(Rh(COD)Cl)_2$ (**30**).

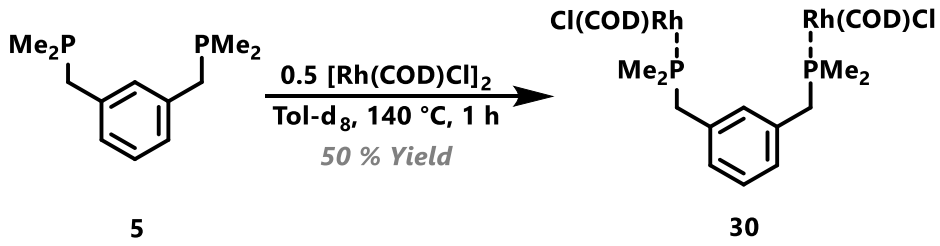

However, as shown in Scheme 3.14, 0.5 equiv. $[Rh(COD)Cl]_2$ reacts with **5** in toluene at 140 °C to afford a single species which we hypothesize is **30**, based upon NMR spectroscopy. The ^{1}H NMR spectrum of **30** shows three aryl signals, four broad signals for a COD ligand(s), a doublet for the benzylic protons, and a doublet for the methyl protons (-P(CH_3)$_2$). The three aryl signals show that C-H activation did not occur. The four broad signals for COD signify that the COD ligands are in an unsymmetrical environment, and the doublets for the benzyl and methyl protons signify that one rhodium is not bonded to both phosphine arms. Further heating did not result in conversion to a new species, nor did addition of excess NEt_3.

Scheme 3.15 Synthesis of (^{Me4}PCP)Rh(MeCN)(HCl) (**31**).

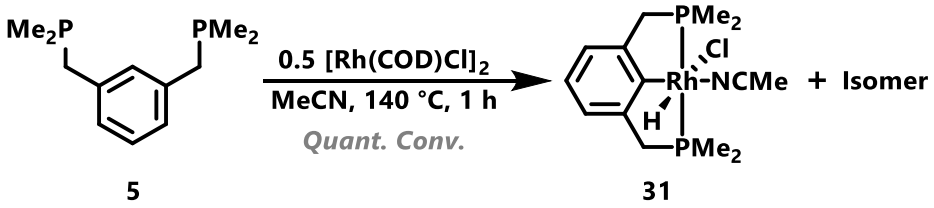

Heating 0.5 equiv. $[Rh(COD)Cl]_2$ with **5** in MeCN at 80 °C results in two similar species (Scheme 3.15) by ^{1}H NMR spectroscopy (hydride region) and $^{31}P\{^1H\}$ NMR spectroscopy. We hypothesize that these two species are isomers of (^{Me4}PCP)Rh(H)(Cl)(MeCN), **31**. The hydride region of the ^{1}H NMR spectrum of **31** shows two doublets of triplets at -17.6 and -18.1 in a 40:60 ratio. The $^{31}P\{^1H\}$ spectrum of **31** shows two overlapping doublets at 5.40 and 5.42 in a similar ratio. The hydrides signify that C-H activation did occur and that the rhodium is coordinated to both phosphorus arms. Further heating did not change the ratio of the two isomers.

Table 10 Attempts to metallate ^{Me4}PCP with rhodium.

Entry	Rh Precursor	Conditions (Adapted From)	Result
1	0.5 $[Rh(CO)_2Cl]_2$	Tol-d_8, 110 °C, 15 h	Intractable
2	0.5 $[Rh(CO)_2Cl]_2$	Tol-d_8, 110 °C, 15 h, xs $K(N(SiMe_3)_3)$	Intractable
3	0.5 $[Rh(COE)_2Cl]_2$	Tol-d_8, 110 °C, 1 h	**30**
4	0.5 $[Rh(COE)_2Cl]_2$	Tol-d_8, 110 °C, 1 h, 1 atm CO	Intractable
5	0.5 $[Rh(COE)_2Cl]_2$	THF, 66 °C, 4 h, xs PMe_3	Intractable
6	0.5 $[Rh(COE)_2Cl]_2$	THF, RT, KO^tBu, CO	Intractable
7	0.5 $[Rh(COD)Cl]_2$	Tol-d_8, 140 °C, 3 h	Intractable
8	0.5 $[Rh(COD)Cl]_2$	MeCN, 80 °C, 15 h	**31**
9	$Rh(CO)_2$(pyridine)Cl	Tol-d_8, 110 °C, 4 h	Intractable
10	$RhH(CO)(PPh_3)$	Tol-d_8, 110 °C, 4 h	2-3 species
11	$RhH(CO)(PPh_3)$	Tol-d_8, 110 °C, 4 h, xs $K(N(SiMe_3)_3)$	Intractable
12	$RhCl(CO)(PPh_3)$	Tol-d_8, 110 °C, 4 h	Intractable

3.2.3 Synthesis and Coordination Chemistry of (^{Me4}POCOP)Ir Complexes

3.2.3.1 Synthesis of (^{Me4}POCOP$_{R2}$)Ir(HCl)CO (32^{Me} and 32′^{Me})

Scheme 3.16 Synthesis of (^{Me4}POCOP$_{R2}$)Ir(HCl)CO (**32^{Me}**).

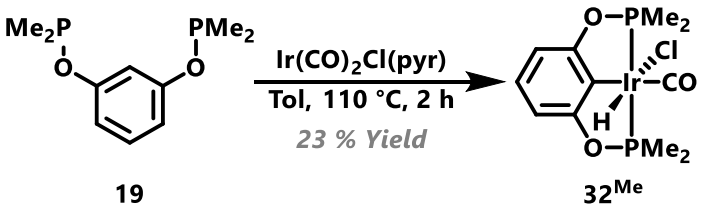

19 **32^{Me}**

As shown in Scheme 3.16, ^{Me4}POCOP (**5**) reacts with Ir(CO)$_2$Cl(pyridine) at 110 °C to afford (^{Me4}POCOP)Ir(HCl)CO (**32^{Me}**). The ^{1}H NMR spectrum of **32^{Me}** exhibits two overlapping virtual triplets at 2.18 and 2.15 ppm for the methyl protons; and a triplet at -18.3 ppm ($^2J_{HP}$ = 15.3 Hz) for the hydride. Attempts to metallate **5** with other precursors such as [Ir(COE)$_2$Cl]$_2$ and [Ir(COD)$_2$Cl]$_2$ resulted in products insoluble in common organic solvents even when CO, H$_2$ or MeCN was present.[2,5] In contrast to the ^{Me4}PCP system, metallations of ^{Me4}POCOP with Ir(CO)$_2$Cl(pyridine) or Ir(CO)$_2$Cl(*p*-toluidine) resulted in abundant precipitates which do not dissolve in common organic solvents. This apparent oligomerization affects the yield and consistency of this metallation reaction. We observed better yields with more dilute reactions, however oligomerization was always an issue. Moreover, (^{Me4}POCOP)Ir(HCl)CO (**32^{Me}**) is stable as a solid in air, however it may decompose similarly to (^{Me4}PCP)Ir(HCl)CO (**23^{Me}**) when in solution on the benchtop.

Figure 3.4 (Left) ORTEP of (^{Me4}POCOP)Ir(HCl)CO (**32^{Me}**) shown with thermal ellipsoids at 50% probability. (Right) Table of selected bond lengths.

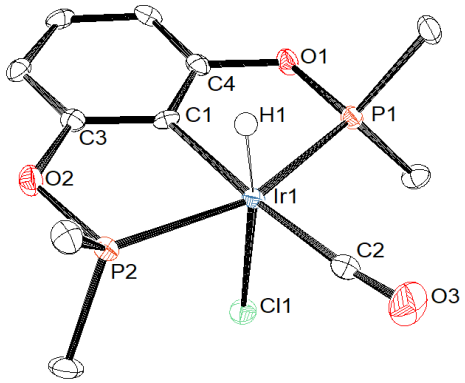

Bond (Å) or Angle (°)	Value
Ir(1)-C(1)	2.046 (5) Å
Ir(1)-C(2)	1.899 (6) Å
Ir(I)-O(1)	3.041 (4) Å
P(1)-Ir(1)-P(2)	158.85 (5) °
C(1)-Ir(1)-C(2)	173.1 (4) °
C(3)-C(1)-Ir(1)-P(1)	2.6 (4) °
C(4)-C(1)-Ir(1)-P(2)	1.4 (4) °

Scheme 3.17 Synthesis of (^{Me4}POCOP$_{tBu2}$)Ir(HCl)CO (**32'^{Me}**).

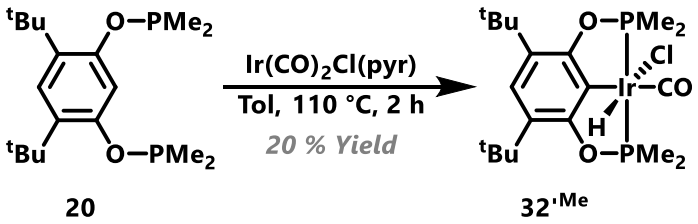

20 **32'^{Me}**

Similarly, ^{Me4}POCOP$_{tBu2}$ reacts with Ir(CO)$_2$Cl(*p*-toluidine) at 110 °C to afford (^{Me4}POCOP$_{tBu2}$)Ir(HCl)CO (**32'^{Me}**). The ^{1}H NMR spectrum of **32'^{Me}** exhibits two overlapping virtual triplets at 2.20 and 2.16 ppm for the methyl protons; a singlet at 1.32 for the *tert*-butyl groups; and, a triplet at -18.3 ppm ($^2J_{HP}$ = 15.3 Hz) for the hydride. The metallation of ^{Me4}POCOP$_{tBu2}$ with Ir(CO)$_2$Cl(*p*-toluidine) suffers from the same oligomerization and purification issues as ^{Me4}POCOP. Unpublished work from Dr. Gene Wong shows similar results.[22] He reported the crystal structure of **32'^{Me}** (Figure 3.5), which shows that bond lengths and angles are congruent with other (^{R4}POCOP)Ir(HCl)(CO) complexes.[13]

Figure 3.5 (Left) ORTEP of (^{Me4}POCOP$_{tBu2}$)Ir(HCl)CO (**32'^{Me}**) shown with thermal ellipsoids at 50% probability. (Right) Table of selected bond lengths for **32'^{Me}**.[22]

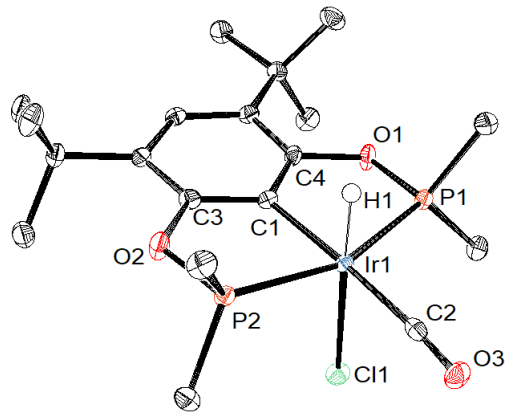

Bond (Å) or Angle (°)	Value
Ir(1)-C(1)	2.072(3) Å
Ir(1)-C(2)	1.917(3) Å
Ir(I)-O(1)	3.050(2) Å
P(1)-Ir(1)-P(2)	157.67(3) °
C(1)-Ir(1)-C(2)	176.27(12) °
C(3)-C(1)-Ir(1)-P(1)	1.2(2) °
C(4)-C(1)-Ir(1)-P(2)	1.0(2) °

3.2.3.2 Synthesis of (^{Me4}POCOP)Ir(CO) (33^{Me})

Scheme 3.18 Synthesis of (^{Me4}POCOP)Ir(CO) (**33^{Me}**).

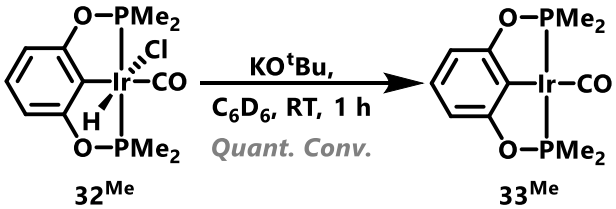

Potassium *tert*-butoxide (KO^{t}Bu) dehydrohalogenates **33^{Me}** to afford (^{Me4}POCOP)Ir(CO) (**33^{Me}**; Scheme 3.18**)**. The ^{1}H NMR spectrum of **33^{Me}** shows a virtual triplet at 3.07 ppm for the benzyl protons, and a virtual triplet at 1.23 ppm for the methyl protons. The ^{31}P{^{1}H} NMR spectrum of **33^{Me}** shows a singlet at 17.1 ppm. Compound **33^{Me}** is highly sensitive to oxygen and moisture.

3.2.3.3 Electronic Comparison of (^{R4}POCOP)Ir (R = ^{t}Bu, ^{i}Pr, Me) Complexes

Table 3.7 (see section 3.4) shows the Ir-CO stretching frequencies for ^{R4}POCOP (R = Me, ^{i}Pr, ^{t}Bu) iridium complexes. The ν(CO) of the ^{Me4}POCOP iridium complexes are slightly higher in energy than the ^{iPr4}POCOP and ^{tBu4}POCOP analogs because methyl groups are less electron rich than *tert*-butyl and *iso*-propyl groups.

3.2.3.4 Steric Comparison of (^{R4}POCOP)Ir (R = ^{t}Bu, ^{i}Pr, Me) Complexes

Table 3.4 shows select structural values and Table 3.5 shows the space-filling models of compounds **32^{Me}**, **32^{iPr}**, **32^{tBu}**. As expected, **32^{Me}** has the lowest %V_{bur} out of the set of complexes. Additionally, **32^{Me}** has a smaller %V_{bur} than **23^{Me}**. ^{R4}POCOP ligands are generally sterically-smaller than the respective ^{R4}PCP ligand.[6] Compared to the analogous (^{R4}PCP)Ir complexes, the P-M-P angles are closer to linear and the C_2 twist angles are smaller for complexes **32^{Me}**, **32^{iPr}**, and **32^{tBu}**. In general, when ligated, ^{R4}POCOP ligands are less distorted from the plane than the ^{R4}PCP analog.[6]

Table 11 Selected structural data for (^{R4}POCOP)Ir(HCl)CO (**32^{R}**). a Calculated by the SambVca 2.0 program.[19] [b]The torsion angle between the oxygen, ipso carbon, iridium and respective phosphorus.

2^{R}	**%V_{bur}[a]**	**Twist[b] (°)**	**P-M-P (°)**
32^{Me}	54.4	1.4 (4)	158.85 (5)
32^{iPr}	64.9	3.1 (5)	157.36 (7)
32^{tBu}	72.3	0.2 (4)	157.57 (5)

Table 12 Space-filling models of **32^{Me}**, **32^{iPr}**, **32^{tBu}**. The H, Cl, and CO ligands have been removed for clarity.

Me (32^{Me})	**^{i}Pr (32^{iPr})**[13]	**^{t}Bu (32^{tBu})**[23]
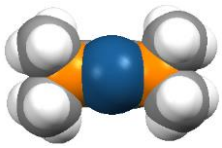	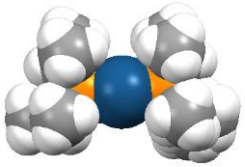	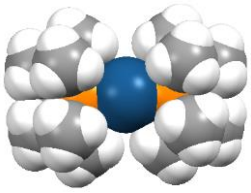
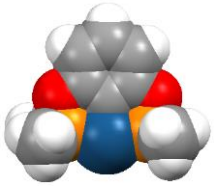	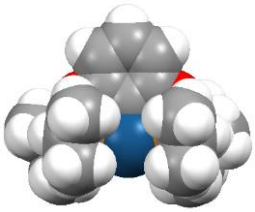	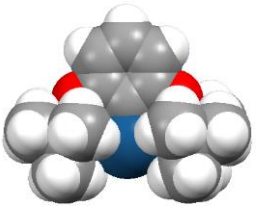

3.3 Conclusions

Depending on the metal, metal precursor, and ligand, the metallation of ^{Me4}PCP or ^{Me4}POCOP may result in oligomeric material. This oligomeric material likely results from the small steric profile of these ligands. Careful choice of the reaction conditions and metal precursor allow for successful metallation of unsubstituted ^{Me4}PCP and ^{Me4}POCOP ligands. $Ir(CO)_2Cl$(amine) is an effective precursor for metallating both ^{Me4}PCP and ^{Me4}POCOP. The resulting iridium complexes show electronically similar but sterically different properties to other ^{R4}PCP and ^{R4}POCOP (R = ^{t}Bu, ^{i}Pr) iridium complexes.

3.4 Tables of Selected Spectroscopic Data?

Table 13 Selected spectroscopic data for compounds **23-26** and **28**.

Compound	^{1}H Ir-*H* *(ppm)*	$^{2}J_{HP}$ *(Hz)*	^{31}P {^{1}H} *(ppm)*	ν(*CO*) (*cm*$^{-}$)	ν(Ir-*H*) (*cm*$^{-}$)	Ref
23^{R}: (^{R4}PCP)Ir(HCl)(CO)						
23^{Me}	-18.7[a]	13.8[a]	-2.68[a]	2020[c]	2171[c]	-
23^{iPr}	-18.3[e]	11.6[e]	50.8[e]	2010[d]	2197[d]	17
23^{tBu}	-7.60[g]	15.0[g]	56.1[g]	1994[f]	2165[f]	24
23^{CF3}	-16.5[a]	14.4[a]	56.7[a]	2091[c]	N/A	5
2^{R}: (^{R4}PCP)Ir(CO)						
24^{Me}	-	-	17.1[a]	1933[a]	-	-
24^{iPr}	-	-	66.2[a]	1920[c]	-	17
24^{tBu}	-	-	82.9	1913[d]	-	13
24^{CF3}	-	-	69.7[a]	2018[c]	-	4
trans-3^{R}: *trans*-(^{R4}PCP)Ir(H)$_2$(CO)						
trans-25^{Me}	-9.16[a]	16.4[a]	-6.08[a]	1992[c]	1722[c]	-
trans-25^{iPr}	-9.69[e]	15.0[e]	57.8[e]	1978[d]	1746[d]	17
trans-25^{CF3}	-9.10[a]	19.2[a]	59.7[a]	2068[c]	2090[c]	4
cis-3^{R}: *cis*-(^{R4}PCP)Ir(H)$_2$(CO)						
cis-25^{Me}	-9.85[a]	19.4[a]	-15.6[a]	[a]	2055[a]	-
	-11.1[a]	12.6[a]			1950[a]	
cis-25^{iPr}	-10.9[a]	16.9[a]	51.7[e]	1950[d]	2066[d]	17
	-11.9[a]	11.9[a]			1965[d]	
4^{R}: [(^{R4}PCP)Ir(H)(Pyridine)(CO)]$^{+}$						
26^{Me}	-19.4[c]	16.4[c]	1.07[c]	2032[c]	2182[c]	-
26^{iPr}	-19.1[a]	12.0[a]	47.8[a]	2023[c]	N/A	2
26^{tBu}	-19.7[a]	14.0[a]	60.8[a]	2018[c]	N/A	2
5^{Me}: (^{R4}PCP)Ir(CO)$_2$						
28^{Me}	-	-	-	2010[a], 1920[a]	-	-
28^{CF3}	-	-	-	2068[c], 2020[c]	-	4

Table 14 Selected spectroscopic values for compounds 1-4.

Compound	^{1}H Ir-*H (ppm)*	$^{2}J_{HP}$ *(Hz)*	^{31}P {^{1}H} *(ppm)*	ν(*CO*) (*cm*$^{-}$)	Ref
32: (^{R4}POCOP)Ir(HCl)(CO)					
32^{Me}	-18.3[a]	15.3[a]	128.3[a]	2043[a]	-
32^{iPr}	-18.5[a]	12.0[a]	166.5[b]	2035[b]	13
32^{tBu}	-17.6[d]	13.3[c]	170.6[d]	2031[b]	13
33: (R4POCOP)Ir(CO)					
33^{Me}	-	-	151.1[c]	1951[c]	-
33^{iPr}	-	-	191.2[a]	1944[b]	13
33^{tBu}	-	-	199.0[c]	1937[b]	13, 25

[a]In CD_2Cl_2. [b]In CH_2Cl_2. [c]In C_6D_6. [e]In toluene-d_8.

3.5 Experimental

General Considerations

All manipulations and reactions used standard Schlenk techniques under an argon atmosphere unless otherwise stated. Glassware, diatomaceous earth, and sodium sulfate were stored in an oven maintained at 140 °C for at least 24 h prior to use. All protio solvents were passed through activated alumina and activated 3Å molecular sieves prior to use. Deuterated solvents were dried over calcium hydride (CD_2Cl_2) or sodium (C_6D_6, Tol-d_8, THF-d_8) and stored over molecular sieves. ^{1}H, ^{31}P{^{1}H}, and ^{13}C{^{1}H} NMR spectra were recorded on a Bruker DRX-700, AV-500, DRX-499, or AV-300 instrument. ^{1}H NMR and ^{13}C{^{1}H} NMR spectra were referenced to residual solvent signals.[26] ^{31}P{^{1}H} NMR spectra were referenced to an 85% H_3PO_4 standard. All NMR spectra were recorded at ambient temperature unless otherwise stated. ^{Me4}PCP,[27] $[Ir(COE)_2Cl]_2$,[28] $Ir(CO)_2Cl$(pyridine),[29] $[Rh(CO)_2Cl]_2$,[30] $[Rh(COE)_2Cl]_2$,[28] $[Rh(COD)Cl]_2$,[31] $RhH(CO)(PPh_3)_3$,[32] $RhCl(CO)(PPh_3)_2$,[33] and $Rh(CO)_2Cl$(pyridine)[34] were synthesized as previously described. Reagents KHMDS, [Hpyr][OTf], AgOAc, and PMe_3 were purchased from Sigma Aldrich. PMe_3 was vacuum transferred prior to use. Elemental analysis was performed at the CENTC facility at the University of Rochester (funded by NSF CHE-0650456) and at Atlantic Microlab, GA.

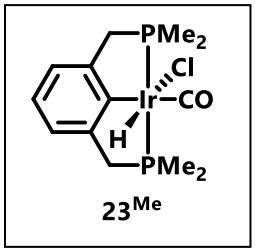

23^{Me}: (^{Me4}PCP)Ir(HCl)CO. $Ir(CO)_2Cl$(pyridine) (0.505g, 1.54 mmol) was added to a solution of ^{Me4}PCP (0.350 g, 1.54 mmol) in toluene (15 mL). The addition was accompanied by effervescence, and an abundant precipitate. The mixture was heated at 110 °C for 15 h, resulting in a yellow solution. The solution was filtered through diatomaceous earth to remove trace particulates. The volatiles were removed under vacuum to afford a white powder. The white powder was triturated with pentane (3 x 1 mL), and then dried under vacuum to afford **23^{Me}** (0.704 g, 1.46 mmol, 95 % yield). X-ray quality crystals of (^{Me4}PCP)Ir(HCl)CO were grown from a concentrated solution of (^{Me4}PCP)Ir(HCl)CO in benzene (1 part) layered with pentane (9 parts) at -35 °C after 1 day. ^{1}H NMR (300 MHz, CD_2Cl_2): δ 7.07 (d; $^3J_{HH}$ = 7.5 Hz; 2H; Ar-*H*), 6.93 (t; $^3J_{HH}$ = 7.5 Hz; 1H; Ar-*H*), 3.80-3.30 (m; 4H, Ar(-C*H*$_2$-)), 1.84 (m; 12H, -P(C*H*$_3$)), -18.8 (t; $^2J_{HP}$ = 13.8 Hz; 1H; Ir-*H*). ^{31}P{^{1}H} NMR (121.5MHz, CD_2Cl_2): δ -2.68. ^{13}C{^{1}H} NMR (126 MHz, C_6D_6): δ 178.4 (s; Ir-*C*O), 147.3 (s; C_{Ar}), 125.1 (s; C_{Ar}), 122.7 (s; C_{Ar}), 46.0 (vt; -(*C*H$_2$)-), 17.7 (vt; P(*C*H$_3$)), 11.8 (vt; P(*C*H$_3$)). IR (solution, CH_2Cl_2, cm$^-$) ν(CO) 2020, ν(*Ir-H*) 2171. Calc: C 32.40; H 4.18, Found: C 33.57; H 4.12.

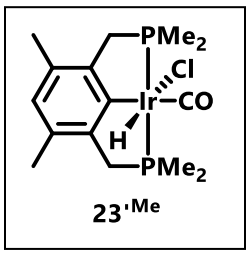

23′^{Me}: (^{Me4}PCP$_{Me2}$)Ir(HCl)CO. A Kontes flask with a Teflon pin stopper was charged with $Ir(CO)_2Cl$(pyridine) (0.300 g, 0.827 mmol), ^{Me4}PCP$_{Me2}$ (0.215 g, 0.845 mmol) and toluene (3 mL). The mixture was heated to 110 °C for 1 h. The solvent was removed under vacuum to afford a light-orange solid. The solid was dissolved in DCM and eluted through neutral alumina. The volatiles were removed to afford a light-orange solid **23′^{Me}** (0.315 g, 0.618 mmol, 75 % yield). ^{1}H NMR (300 MHz, CD_2Cl_2): δ 6.55 (s; Ar-*H*), 3.60-3.15 (m; 4H; Ar(-C*H*$_2$-)),2.15 (s; 6H; Ar(C*H*$_3$)), 1.75 (m; 12H; -P(C*H*$_3$)), -18.8 (t; $^2J_{HP}$ = 13.8 Hz; 1H; Ir-*H*). ^{31}P{^{1}H} NMR (121.5 MHz, CD_2Cl_2): δ 1.28.

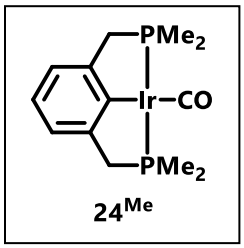

24^{Me}

24^{Me} : (^{Me4}PCP)Ir(CO). (^{Me4}PCP)Ir(HCl)(CO) (**1^{Me}**) (0.22 g, 0.46 mmol) and KHMDS (0.092 g, 0.46 mmol) were stirred in C_6H_6 for 1 hour at room temperature. The mixture was filtered through diatomaceous earth, and then the solvent was removed under vacuum to afford **24^{Me}** (0.188 g, 0.42 mmol, 91 % yield). X-ray diffraction quality crystals of **24^{Me}** were grown by slow evaporation of a concentrated solution of **24^{Me}** in pentane at -35 °C over 7 days. ^{1}H NMR (300 MHz, C_6D_6): δ 7.17 (d; $^3J_{HH}$ = 7.3 Hz; 2H; Ar-*H*), 7.09 (t; $^3J_{HH}$ = 7.3 Hz; 1H; Ar-*H*), 3.07 (vt; 4H; Ar(-C*H*$_2$-)), 1.84 (vt; 12H; -P(C*H*$_3$)). ^{31}P{^{1}H} NMR (121.5 MHz, C_6D_6): δ 17.1. ^{13}C{^{1}H} NMR (126 MHz, C_6D_6): δ 196.8 (m; Ir-*C*O), 180.8 (m; *C*$_{Ar}$), 152.9 (m; *C*$_{Ar}$), 126.3 (m; *C*$_{Ar}$), 121.3 (m; C$_{Ar}$), 47.7 (vt, -(*C*H$_2$)-), 16.9 (vt, -P(*C*H$_3$). IR (solution, C_6D_6, cm$^-$). Calc: C 35.05; H 4.03; Found C 34.67; H 4.04.

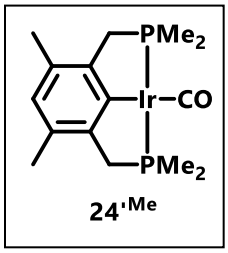

24′^{Me}

24′^{Me}: (^{Me4}PCP$_{Me2}$)Ir(CO). A J-Young NMR tube was charged with **23′^{Me}** (0.008 g, 0.01 mmol), LiHMDS (0.002 g, 0.01 mmol), and C_6D_6 (350 µL). The solution immediately turned from light yellow to dark orange. The solvent was removed, then the remaining orange solid was extracted pentane (2 mL) and filtered. The volatiles were removed under vacuum to afford an orange solid, **24′^{Me}** (0.006 g, 0.01 mmol, 97 %). ^{1}H NMR (500 MHz, C_6D_6): δ 6.79 (s; 1H; Ar-*H*), 3.12 (vt; 4H; Ar(-C*H*$_2$-)), 1.35 (vt; 12H; -P(C*H*$_3$)). ^{31}P{^{1}H} NMR (202 MHz, C_6D_6): δ 16.5.

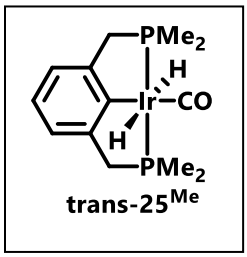

trans-25^{Me}

trans-25^{Me}: trans-(^{Me4}PCP)Ir(H)$_2$(CO). $NaBH_4$ (0.416 g, 11.0 mmol) and **23^{Me}** (0.106 g, 0.220 mmol) were stirred in 1:1 ethanol (10 mL): acetonitrile (10 mL) in a 50 mL Schlenk tube. The solvent was removed under vacuum, resulting in a white solid. The solid was extracted with benzene and the mixture was filtered through diatomaceous earth. The solvent was removed under vacuum to give a white solid, which was washed with cold (-35 °C) pentane to afford **trans-25^{Me}** (0.061g, 0.136 mmol, 62 % yield). ^{1}H NMR (300 MHz, C_6D_6): δ 7.09 (m; 3H; Ar-*H*), 3.14 (vt; 4H; Ar(-C*H*$_2$-)), 1.42 (vt; 12H, -P(C*H*$_3$)), -9.23 (t; $^2J_{HP}$ = 16.4; 2H; Ir-*H*). ^{31}P{^{1}H} NMR (121.5 MHz, C_6D_6): δ -6.08. ^{13}C{^{1}H} NMR (126 MHz, C_6D_6): δ 179.8 (s; Ir-*C*O), 153.6 (s; *C*$_{Ar}$), 146.2 (s; *C*$_{Ar}$), 123.1 (s; *C*$_{Ar}$), 122.0 (s; *C*$_{Ar}$), 50.3 (vt; -(*C*H$_2$)-), 20.9 (vt; P(*C*H$_3$)). IR (solution, C_6D_6, cm^{-1}) ν(CO) 1992, ν(Ir-H) 1722. Calcd: C 34.89; H 4.73 Found C 35.78; H 4.77.

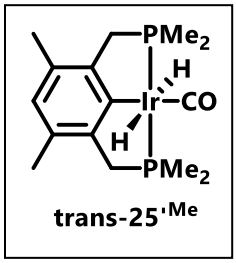

trans-25′^{Me}

trans-25′^{Me}: trans-(^{Me4}PCP$_{Me2}$)Ir(H)$_2$(CO). $NaBH_4$ (0.046 g, 1.20 mmol) and **23′^{Me}** (0.012 g, 0.002 mmol) were stirred in 1:1 ethanol (2 mL): acetonitrile (2 mL) in a 50 mL Schlenk tube. The solvent was removed under vacuum, resulting in a white solid. The solid was extracted with benzene and the mixture was filtered through diatomaceous earth. The solvent was removed under vacuum to give a white solid, which was washed with cold (-30 °C) pentane (2 mL) to afford **trans-25′^{Me}** (0.010 g, 0.002 mmol, 88% yield). ^{1}H NMR (300 MHz, C_6D_6): δ 6.97 (s; 1H; Ar-*H*), 3.85 (vt; 4H; Ar(-C*H*$_2$-)), 2.67 (s; 6H; Ar(C*H*$_3$)), 2.35 (vt; 12H, -P(C*H*$_3$)), -9.45 (t; $^2J_{HP}$ = 16.4; 2H; Ir-*H*). ^{31}P{^{1}H} NMR (121.5 MHz, C_6D_6): δ -6.74.

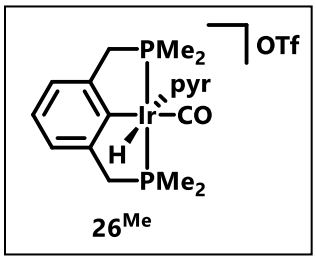

26^{Me}

26^{Me}: [(^{Me4}PCP)Ir(H)(pyr)CO][OTf]. Compound **24^{Me}** (42 mg, 0.09 mmol) and [HPyr][OTf] (15 mg, 0.09 mmol) were stirred in THF (1 mL) in a scintillation vial for 5 h. The precipitate was removed by filtration through diatomaceous earth, then the volatiles were removed under vacuum. The resulting off-white solid was washed with benzene, then the volatiles were removed under vacuum to afford **26^{Me}** (54 mg, 0.08 mmol, 95 % yield). ^{1}H NMR (300 MHz, CD_2Cl_2): δ 8.09 (d; $^{3}J_{HH}$ = 5.2 Hz; 2H; C_5H_5N), 7.89 (t; $^{3}J_{HH}$ = 7.45 Hz; 1H; C_5H_5N), 7.32 (app t; 2H; C_5H_5N), 7.17 (m; 2H; Ar-*H*), 7.09 (m; 1H; Ar-*H)*, 3.55-3.32 (m; 4H; Ar(-CH_2-)), 1.89 (vt; 6H; -P(CH_3)$_2$), 1.31 (vt; 6H; -P(CH_3)$_2$), -19.4 (t; $^{3}J_{HH}$ = 14.2 Hz 1H; Ir-*H*). ^{31}P{^{1}H} NMR (121.5 MHz, CD_2Cl_2): δ 1.07. ^{13}C{^{1}H} NMR (176 MHz, CD_2Cl_2): δ 177.3 (s; Ir-*C*O), 157.9 (s; C_{Ar}), 154.1 (s; C_{Ar}), 147.9 (t; $^{3}J_{CP}$ = 7.5 Hz; C_{Ar}), 140.1 (s; C_{Ar}), 128.0 (s; C_{Ar}), 127.3 (s; C_{Ar}), 124.6 (t; $^{3}J_{CP}$ = 8.6 Hz; C_{Ar}), 45.5 (vt; -(*C*H$_2$)-), 19.0 (vt; P(*C*H$_3$)), 16.1 (vt; P(*C*H$_3$)). IR (solution, CD_2Cl_2, cm^{-1}) ν(CO) 2032, ν(Ir-H) 2183. Calcd: C 33.83; N 2.08; H 3.74, Found: C 33.82; N 2.11; H 3.57.

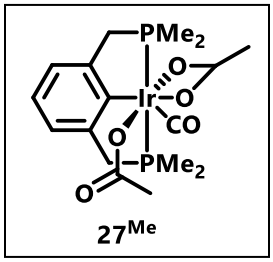

27^{Me}

27^{Me}: (^{Me4}PCP)Ir(OAc)$_2$(CO). A 100 mL Schlenk flask equipped with a glass stopper was charged with **23^{Me}** (87 mg, 0.18 mmol), AgOAc (100 mg, 0.60 mmol), and THF (8 mL). The brown mixture was heated to 66 °C overnight (ca. 15 h). The volatiles were removed to give a gray solid. The gray solid was washed with benzene (ca. 5 x 3 mL) and the gray precipitate was removed by filtration through diatomaceous Earth. The volatiles were removed under vacuum, and the sticky, off-white solid was recrystallized in toluene and pentane (1:9) at -35 °C to afford an off-white solid, **27^{Me}** (96 mg, 0.17 mmol, 96 % yield). ^{1}H NMR (300 MHz, C_6D_6): δ 6.88-6.78 (m; 3H; Ar-*H*), 3.35 (dvt; 2H; Ar(-CH_2-)), 2.66 (dvt; 2H; Ar(-CH_2-)), 2.27 (s; 3H; Ir-OC(O)CH_3), 1.76 (s; 3H;

Ir-OC(O)CH_3), 1.44 (vt; 6H; -P(CH_3)), 1.39 (vt; 6H; -P(CH_3)). $^{31}P\{^1H\}$ NMR (121.5 MHz, C_6D_6): δ 4.71 (s) $^{13}C\{^1H\}$ NMR (176 MHz, C_6D_6): 177.3 (s; Ir-O*C*(O)CH_3), 173.9 (s; Ir-O*C*(O)CH_3), 164.6 (t; $^3J_{HH}$ = 9.1 Hz; Ir-*C*O), 146.8 (vt; C_{Ar}), 135.5 (s; C_{Ar}), 125.6 (s; C_{Ar}), 123.6 (vt; C_{Ar}), 42.7 (vt, -(*C*H_2)-), 23.0 (s; Ir-OC(O)*C*H_3), 22.2 (s; Ir-OC(O)*C*H_3), 14.6 (vt, -P(*C*H_3), 10.9 (vt, -P(*C*H_3). IR (solution, C_6D_6, cm^{-1}): ν(CO): 2035.

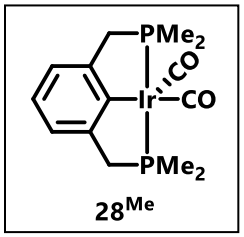

28^{Me}

28^{Me}: (^{Me4}PCP)Ir(CO)$_2$. A solution of (^{Me4}PCP)Ir(CO) (**2^{Me}**) (ca. 5 mg, 0.01 mmol) in toluene-d$_8$ (0.350 mL) was pressurized with 1 atm of CO. The solution was vigorously shaken and turned from yellow to colorless. The spectral features are consistent with assignment to **28^{Me}**. Upon removal of the solvent under vacuum, **28^{Me}** loses CO to afford **24^{Me}**.Compound **28^{Me}** does not immediately lose CO when just the CO atmosphere is removed. ^1H NMR (300 MHz, Tol-d$_8$): δ 7.10 – 6.98 (m; 3H; Ar-*H*), 3.07 (vt; 4H, Ar(-CH_2-)), 1.34 (vt; 12H, -P(CH_3)). $^{31}P\{^1H\}$ NMR (121.5 MHz, Tol-d$_8$): δ -5.77. $^{13}C\{^1H\}$ NMR (126 MHz, Tol-d$_8$): δ 186.6 (s; Ir-*C*O), 147.1 (t; $^2J_{CP}$ = 7.9 Hz; C_{Ar}), 122.9 (s; C_{Ar}), 121.0 (s; C_{Ar}), 51.2 (vt; -(*C*H_2)-), 18.8 (vt; P(*C*H_3)). IR (solution, C_6D_6, cm^{-1}) ν(CO) 2010, 1930.

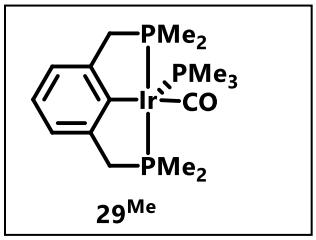

29^{Me}

29^{Me}: (^{Me4}PCP)Ir(CO)(PMe$_3$). A J-Young NMR tube was charged with **24^{Me}** (ca. 5 mg, 0.01 mmol) in toluene-d$_8$ (0.350 mL) and PMe_3 (0.05 mL). The volatiles were removed to afford a white solid with spectroscopic features consistent with **29^{Me}**. ^1H NMR (300 MHz, C_6D_6): δ 7.09 (d; $^3J_{HP}$ = 7.3 Hz; 2H; Ar-*H*), 6.98 (d; $^3J_{HP}$ = 7.3 Hz ;1H; Ar-*H*), 3.25-2.73 (br m; 4H; Ar(-CH_2-)), 1.60-1.37 (br m; 12H; -P(CH_3)$_2$), 1.08 (d; 9H; -P(CH_3)$_3$). $^{31}P\{^1H\}$ NMR (121.5 MHz,

C_6D_6): δ -0.92 (d; $^2J_{PP}$ = 112.4 Hz; 2P; -P(CH_2)(CH_3)$_2$), -55.9 (d; $^2J_{PP}$ = 112.4 Hz; 1P; -P(CH_3)$_3$). $^{13}C\{^1H\}$ NMR (176 MHz, C_6D_6): δ 192.3 (m; Ir-*C*O), 146.8 (m; C_{Ar}), 128.5 (s; C_{Ar}), 121.7 (s; C_{Ar}), 121.4 (m; C_{Ar}), 52.7 (m; -(*C*H_2)-), 25.7 (m; P(*C*H_3)$_2$), 24.4 (d; $^1J_{PC}$ = 20.0 Hz P(*C*H_3)$_3$), 21.5 (m; P(*C*H_3)$_2$). IR (solution, C_6D_6, cm^{-1}) ν(CO) 1923.

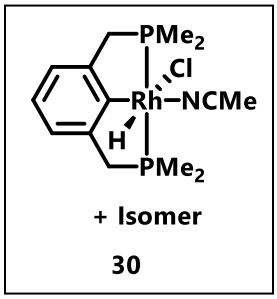

30

30: (^{Me4}PCP)Rh(HCl)(MeCN). A J-Young tube was charged with [Rh(COD)$_2$Cl]$_2$ (0.010 g, 0.020 mmol), ^{Me4}PCP (0.009 g, 0.040 mmol) and MeCN (350 µL). NMR Spectra were recorded after heating the solution at 80 °C for 15 h. ^{1}H NMR (300 MHz, CH_3CN, Hydride Region): δ -17.59 (dt; $^1J_{RhH}$ = 43.6 Hz; $^2J_{HP}$ = 15.7 Hz; 1H; Rh-*H*), -18.06 (dt; $^1J_{RhH}$ = 38.5 Hz; $^2J_{HP}$ = 14.0 Hz; 1H; Rh-*H*). $^{31}P\{^1H\}$ NMR (121.5 MHz, CH_3CN): δ 5.40 (d; $^3J_{RhP}$ = 151.8 Hz), 5.42 (d; $^3J_{RhP}$ = 151.8 Hz).

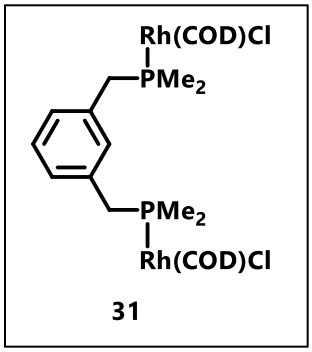

31

31: (^{Me4}PCPH)Rh$_2$(COD)$_2$Cl$_2$. A J-Young NMR tube was charged with [Rh(COD)$_2$Cl]$_2$ (0.011 g, 0.022 mmol), ^{Me4}PCP (0.010 g, 0.044 mmol) and Tol-d_8 (0.350 mL). The mixture was heated at 140 °C for 5 minutes. The solution was decanted and filtered through diatomaceous Earth. The volatiles were removed to afford a yellow solid **31** (0.009 g, 0.011 mmol, 50 % yield). ^{1}H NMR (300 MHz, CD_2Cl_2): δ 7.57 (t; $^4J_{HP}$ = 1.6 Hz; 1H; Ar-*H*), 7.05 (d; $^3J_{HH}$ = 7.7 Hz; 1H; Ar-*H*), 6.77 (t; $^3J_{HH}$ = 7.7 Hz; 1H; Ar-*H*), 5.34 (s; 4H; -C*H*$_2$=C*H*$_2$-), 2.82 (d; $^2J_{HP}$ = 11.2 Hz; 4H; Ar-C*H*$_2$-), 2.61 (s; 4H; -C*H*=C*H*-), 1.70 (m; 8H; -C*H*$_2$C*H*$_2$-), 0.50 (d; $^2J_{HP}$ = 8.4 Hz; 12H; P-(C*H*$_3$)$_2$). $^{31}P\{^1H\}$ NMR (121.5 MHz, C_6D_6): δ 1.58 (d; $^3J_{RhP}$ = 151.0 Hz).

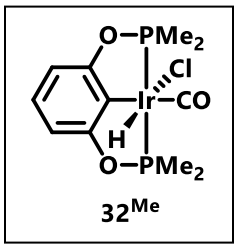

32^{Me}: (^{Me4}POCOP)Ir(HCl)CO. A solution of ^{Me4}POCOP (**19**) (40 mg, 0.17 mmol) and Ir(CO)$_2$Cl(pyridine) (63 mg, 0.17 mmol) in toluene was heated at 110°C for two hours. The brown precipitate was removed by filtration to afford a yellow solution. The solvent was removed to afford an orange solid. The solid was dissolved in DCM and eluted through an alumina plug. The volatiles were removed, and the off-white solid was washed with pentane to afford **32^{Me}** (19 mg, 0.04 mmol, 23% yield). ^{1}H NMR (300 MHz, CD_2Cl_2): δ 6.90 (t; $^3J_{HH}$ = 8.0 Hz; 1H; Ar-*H*), 6.54 (d; $^3J_{HH}$ = 8.0 Hz; 2H; Ar-*H*), 2.18 (vt; 6H; P-(C*H*$_3$)$_2$), 2.15 (vt; 6H; P-(C*H*$_3$)$_2$), -18.3 (t; $^2J_{HP}$ = 15.3 Hz; 1H; Ir-*H*). ^{31}P{^{1}H} NMR (121.5 MHz, CD_2Cl_2): δ 128.3 (s). IR (solution, CH_2Cl_2, cm^{-1}) ν(CO) 2043.

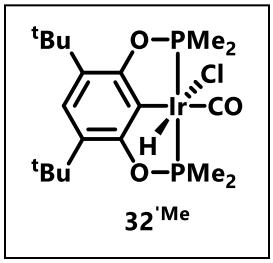

32′^{Me}: (^{Me4}POCOP$_{tBu}$)Ir(CO). A J-Young NMR tube was charged with Ir(CO)$_2$Cl(*p*-toluidine) (0.070 g, 0.179 mmol), ^{Me4}POCOP$_{tBu2}$ (**20**) (0.061 g, 0.179 mmol), and Tol-d$_8$ (0.5 mL). The mixture was heated to 110 °C for 15 h. The solvent was decanted and the remaining solid was extracted with toluene. The volatiles were removed, then the remaining solid was dissolved in DCM and eluted through neutral alumina. The volatiles were removed to afford **32′^{Me}** (0.021 g, 0.035 mmol, 20 % yield). ^{1}H NMR (300 MHz, CD_2Cl_2): δ 6.90 (t; $^3J_{HH}$ = 8.0 Hz; 1H; Ar-*H*), 2.20 (vt; 6H; P-(C*H*$_3$)$_2$), 2.16 (vt; 6H; P-(C*H*$_3$)$_2$), 1.32 (s; 18H; Ar-(C*H*$_3$)), -18.2 (t; $^3J_{HH}$ = 15.2 Hz; 1H; Ir-*H*). ^{31}P{^{1}H} NMR (121.5 MHz, CD_2Cl_2): δ 124.5 (s).

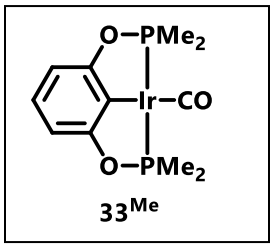

33Me

33^{Me}: (^{Me4}POCOP)Ir(CO). A J-Young NMR tube was charged with (^{Me4}POCOP)Ir(HCl)CO (40 mg, 0.08 mmol), KO^{t}Bu (9 mg, 0.08 mmol) and 400 μL of C_6D_6. The reaction was tracked by ^{1}H and ^{31}P{^{1}H} NMR spectroscopy. After 1 hour at room temperature, the reaction converged to one major species with NMR signals congruent with **33^{Me}**. The white precipitate was removed by filtration. The volatiles were removed to afford an orange solid. Multiple species form upon exposure to DCM. NEt_3 does not dehydrohalogenate **32^{Me}**. ^{1}H NMR (300 MHz, C_6D_6): δ 6.96 (t; $^{3}J_{HH}$ = 7.6 Hz; 1H; Ar-*H*), 6.85 (d; $^{3}J_{HH}$ = 7.6 Hz; 2H; Ar-*H*), 1.53 (vt; 6H; P-(C*H*$_3$)$_2$). ^{31}P{^{1}H} NMR (121.5 MHz, C_6D_6): δ 151.1 (s). IR (solution, C_6D_6, cm^{-1}) ν(CO) 1951.

3.6 References

1 J. Choi, A. H. R. Macarthur, M. Brookhart and A. S. Goldman, *Chem. Rev.*, 2011, **111**, 1761–1779.

2 J. M. Goldberg, S. D. T. Cherry, L. M. Guard, W. Kaminsky, K. I. Goldberg and D. M. Heinekey, *Organometallics*, 2016, **35**, 3546–3556.

3 J. J. Adams, N. Arulsamy and D. M. Roddick, *Dalt. Trans.*, 2011, **40**, 10014–10019.

4 J. J. Adams, N. Arulsamy and D. M. Roddick, *Organometallics*, 2011, **30**, 697–711.

5 J. J. Adams, A. Lau, N. Arulsamy and D. M. Roddick, *Organometallics*, 2011, **30**, 689–696.

6 D. M. Roddick, in *Organometallic Pincer Chemistry*, Springer, 2012, pp. 49–88.

7 J. J. Adams, N. Arulsamy and D. M. Roddick, *Organometallics*, 2012, **31**, 1439–1447.

8 T. T. Lekich, P. G. Askelson, R. K. Burdick and D. M. Heinekey, *Organometallics*, 2018, **37**, 211−213.

9 C. S. Creaser and W. C. Kaska, *Inorg. Chim. Acta.*, 1978, **30**, 325–326.

10 K. Wang, M. E. Goldman, T. J. Emge and A. S. Goldman, *J. Organomet. Chem.*, 1996, **518**, 55–68.

11 R. B. Bedford, Y.-N. Chang, M. F. Haddow and C. L. McMullin, *Dalt. Trans.*, 2011, **40**,

9034.

12 J. Zhang, C. M. Medley, J. A. Krause and H. Guan, *Organometallics*, 2010, **29**, 6393–6401.

13 J. M. Goldberg, G. W. Wong, K. E. Brastow, W. Kaminsky, K. I. Goldberg and D. M. Heinekey, *Organometallics*, 2015, **34**, 753–762.

14 S. Kundu, Y. Choliy, G. Zhuo, R. Ahuja, T. J. Emge, R. Warmuth, M. Brookhart, K. Krogh-Jespersen and A. S. Goldman, *Organometallics*, 2009, **28**, 5432–5444.

15 I. Göttker-Schnetmann, P. S. White and M. Brookhart, *Organometallics*, 2004, **23**, 1766–1776.

16 C. Creaser and W. Kaska, *Inorg. Chim. Acta.*, 1978, **30**, 325–326.

17 B. Rybtchinski, Y. Ben-David and D. Milstein, *Organometallics*, 1997, **16**, 3786–3793.

18 A. A. H. Van der Zeijden, G. Van Koten, R. A. Nordemann, B. Kojic-Prodic and A. L. Spek, *Organometallics*, 1988, **7**, 1957–1966.

19 L. Falivene, R. Credendino, A. Poater, A. Petta, L. Serra, R. Oliva, V. Scarano and L. Cavallo, *Organometallics*, 2016, **35**, 2286–2293.

20 L. M. Guard, *Pers. Commun.*

21 R. Ghosh, X. Zhang, P. Achord, T. J. Emge, K. Krogh-Jespersen and A. S. Goldman, *J. Am. Chem. Soc.*, 2007, **129**, 853–866.

22 G. Wong, *Pers. Commun.*

23 J. A. F. Takiya, *Pers. Commun.*

24 B. C. J. Moulton and B. L. Shaw, *J.C.S. Dalt.*, 1975, **0**, 1020–1024.

25 I. Göttker-Schnetmann, P. White and M. Brookhart, *J. Am. Chem. Soc.*, 2004, **126**, 1804–1811.

26 G. R. Fulmer, A. J. M. Miller, N. H. Sherden, H. E. Gottlieb, A. Nudelman, B. M. Stoltz, J. E. Bercaw and K. I. Goldberg, *Organometallics*, 2010, **29**, 2176–2179.

27 T. T. Lekich, P. G. Askelson, R. K. Burdick and D. M. Heinekey, *Organometallics*, 2018, **37**, 211−213.

28 A. van der Ent, A. L. Onderdelinden and R. Schunn, *Inorg. Synth.*, 1990, **28**, 90–92.

29 D. Roberto, E. Cariati, R. Psaro and R. Ugo, *Organometallics*, 1994, **13**, 4227–4231.

30 F. Bonati and G. Wilkinson, *J. Chem. Soc.*, 1964, 3156–3160.

31 G. Giordano and H. Crabtree, R, *Inorg. Synth.*, 1990, **28**, 88–90.

32 N. Ahmad, J. J. Levison, S. D. Robinson, M. F. Uttley, E. R. Wonchoba and G. W. Parshall, *Inorg. Synth.*, 1990, **28**, 81–83.

33 J. A. McCleverty and G. Wilkinson, *Inorg. Synth.*, 1966, **8**, 214–217.

34 D. N. Lawson and G. Wilkinson, *J. Chem. Soc.*, 1965, 1900–1907.

Chapter 4. Activation of H_2 and C-X Bonds by (^{Me4}PCP)Ir(CO)

4.1 Part 1 - H_2 Addition to (^{Me4}PCP)Ir(CO)

4.1.1 Introduction

Hydrogen addition to square planar iridium complexes is well-studied: H_2 coordinates as a sigma complex, then undergoes oxidative addition to afford a cis-dihydride species.[1] This reaction has been studied for various (^{R}PCP)Ir(CO) systems (R = ^{t}Bu, ^{i}Pr, CF_3). Milstein and coworkers found that (^{iPr}PCP)Ir(CO) (**24^{iPr}**) reacts with H_2 to initially form cis-(^{iPr}PCP)Ir(H)$_2$(CO) (**cis-25^{iPr}**), but then isomerizes to trans-(^{iPr}PCP)Ir(H)$_2$(CO) (**trans-25^{iPr}**; Scheme 4.1a).[2] This isomerization was surprising because one would expect that the hydrides would have an energetically unfavorable trans-influence on one another. Through calculations, Hall and coworkers explained that this thermodynamic preference could be due to a favorable π interaction between the aryl backbone and CO ligand.[3]

Scheme 4.1 Reactivity of H_2 with (^{iPr4}PCP)Ir(CO) and ($^{(CF3)4}$PCP)Ir(CO).[2,4]

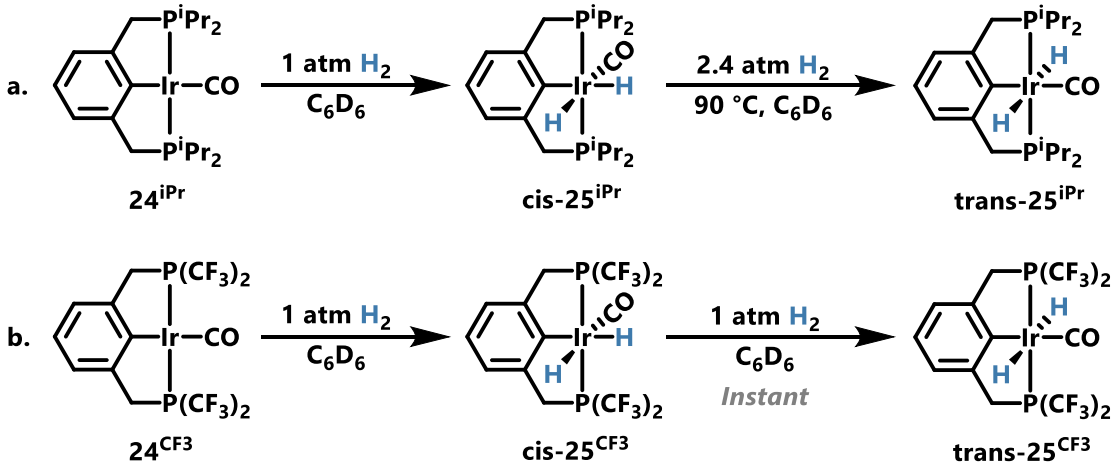

Our group has previously reported that H_2 addition and isomerization also occurs with (^{iPr}POCOP)Ir(H)$_2$(CO).[5] However, similar complexes with bulkier ligands, (^{tBu}PCP)Ir(CO) and (^{tBu}POCOP)Ir(CO), do not oxidatively add H_2 through this mechanism.[5] Roddick and coworkers showed that (^{CF3}PCP)Ir(CO) (**24^{CF3}**) adds H_2 to initially form cis-(^{CF3}PCP)Ir(H)$_2$(CO) (**cis-25^{CF3}**) which rapidly isomerizes to trans-(^{CF3}PCP)Ir(H)$_2$(CO) (**trans-25^{CF3}**; Scheme 4.01b).[4] The rate of cis to trans-dihydride isomerization was observed to be much faster at room temperature when R = CF_3 than R = ^{i}Pr.[2,4] Additionally, cis-(^{CF3}PCP)Ir(H)$_2$(CO) was observed to be in equilibrium with its facially-coordinated PCP isomer. This isomer was determined to likely be off the isomerization mechanism pathway.[4]

This hydrogen addition and isomerization reaction is also reversible under specific conditions. Roddick and coworkers showed that trans-(^{CF3}PCP)Ir(H)$_2$(CO) (**trans-25^{CF3}**) quickly loses H_2 when not under an H_2 atmosphere (Scheme 4.2b).[4] This H_2 loss likely proceeds through the isomerization back to cis-(^{CF3}PCP)Ir(H)$_2$(CO) (**cis-25^{CF3}**) then reductive elimination of H_2 to afford (^{CF3}PCP)Ir(CO) (**24^{CF3}**).[4] In contrast, Milstein and coworkers showed that trans-(^{iPr}PCP)Ir(H)$_2$(CO) is stable without an H_2 atmosphere (Scheme 4.2a).[6]

Scheme 4.2 (^{R4}PCP)Ir(CO) (R = ^{i}Pr, CF_3) under a non-H_2 atmosphere.[4,6]

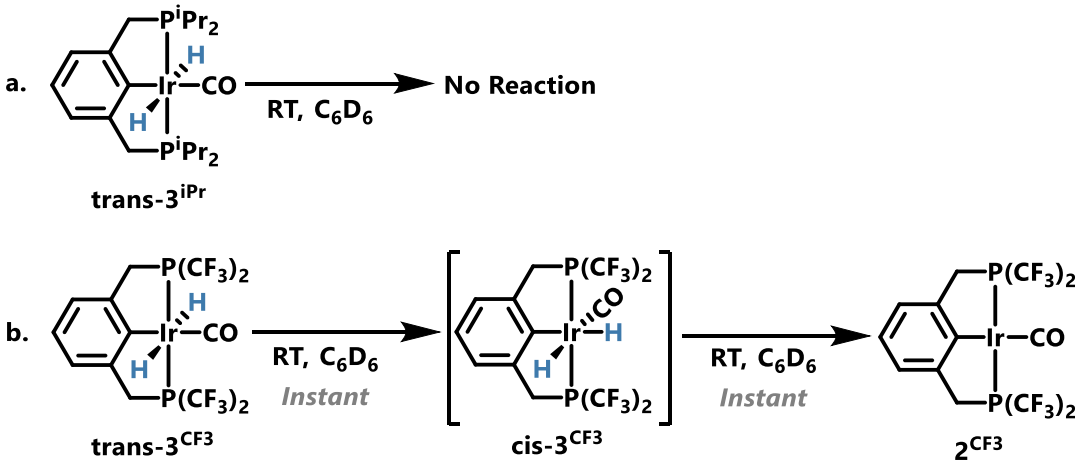

Because the nature of hydrogen addition and elimination is important in understanding aspects of (de)hydrogenation chemistry for which these ^{R}PCP iridium complexes are commonly used, we compare the reactivity of H_2 with (^{Me4}PCP)Ir(CO) (**24^{Me}**) and previously reported (^{R4}PCP)Ir(CO) (R = ^{t}Bu, ^{i}Pr, CF_3) complexes to elucidate differences in reactivity that result from the reduced steric profile of ^{Me4}PCP.[7]

4.1.2 Results and Discussion

4.1.2.1 Hydrogen Addition to 24^{Me}

Compound **24^{Me}** oxidatively adds H_2 at room temperature in toluene-d_8 to initially form cis-(^{Me4}PCP)Ir(H)$_2$(CO) (**cis-25^{Me}**), then isomerizes to **trans-25^{Me}** (Scheme 4.03). The isomerization reaches equilibrium after about 1 day at room temperature and under 1 atm H_2 (ΔG_{298} = -2.5 kcal/mol). Kinetic analysis, conducted under 1 atm H_2, suggests that this isomerization is first order in **24^{Me}.**

Scheme 4.3 H_2 Addition to **24^{Me}** gives **cis-25^{Me}**, which isomerizes to **trans-25^{Me}**.

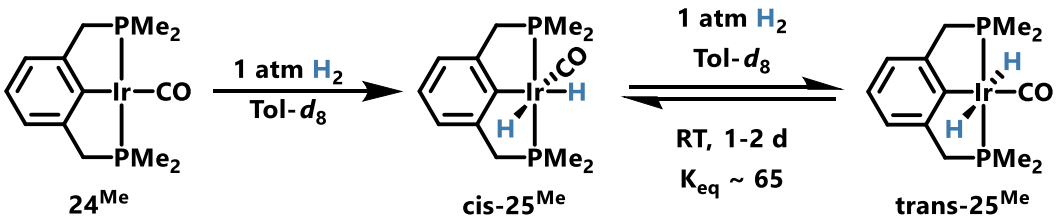

Figure 4.1 shows the Eyring plot and extracted thermodynamic values for the highest-energy transition state in the **cis/trans-25^{Me}** isomerization**.**

Figure 4.1 Eyring plot and thermodynamic values for the isomerization of **cis-25^{Me}** to **trans-25^{Me}** under 1 atm H_2.

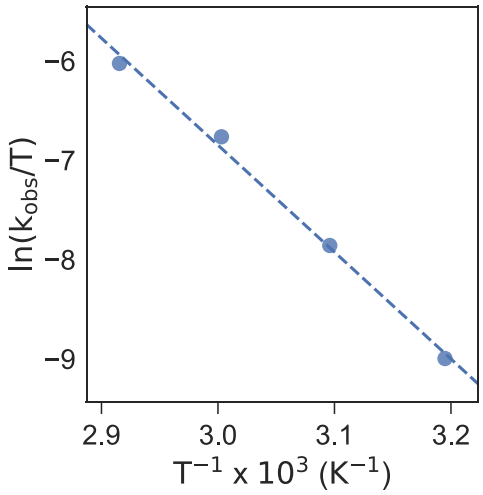

$\Delta H^{\ddagger}$ = 21.2 ± 1.3 (kcal • mol^{-1})

$\Delta S^{\ddagger}$ = -8.84 ± 3.9 (cal • mol^{-1})

$\Delta G^{\ddagger}_2$ = 23.6 ± 2.2 (kcal • mol^{-1})

Unlike previous H_2 addition studies involving **24^{tBu}**, **24^{iPr}**, and **24^{CF3}** which all use C_6D_6 as the solvent, we found that heating **cis-25^{Me}** under 1 atm H_2 in C_6D_6 at 80 °C to equilibrium affords a mixture of **trans-25^{Me}** and **trans-25$^{Me\text{-}d}$** (25 % of **trans-25^{Me}**; Scheme 4.04).[4–6] Similar reactivity is also observed when heating **trans-25^{Me}** under 1 atm H_2 in C_6D_6 at 80 °C to equilibrium. Compound **trans-25$^{Me\text{-}d}$** was characterized by a new ^{1}H NMR hydride signal at -9.06 ppm (t; $^2J_{HP}$ = 16.4 Hz) in C_6D_6 and an increase in the concentration of residual protio-solvent signal due to C_6D_5H. All other NMR signals are identical between **trans-25$^{Me\text{-}d}$** and **trans-25^{Me}**. Furthermore, the presence of **trans-25$^{Me\text{-}d}$** was confirmed by comparison with an independently synthesized mixture of **trans-25$^{Me\text{-}d}$** and **trans-25^{Me}**. A mixture of **trans-25$^{Me\text{-}d}$** and **trans-25^{Me}** can be synthesized by treating **23^{Me}** with $NaBD_4$ in an analogous preparation to the synthesis of **trans-25^{Me}**. No further H/D exchange occurs after the isomerization reaches equilibrium, and thus the exchange must occur with an intermediate iridium species. This reactivity suggests that this intermediate species interacts with C_6D_6 at elevated temperatures in either a sigma-bond or oxidative-addition fashion. For this type of reactivity to occur, this intermediate species must contain on open coordination site or expand to a 7 or 8 coordinate 20-electron species. We did not

observe any H/D exchange between **cis-25^{Me}** or **trans-25^{Me}** in toluene-d_8 up to 80 °C, or in the presence of pyridine or $NaBF_4$ in C_6D_6.

Scheme 4.4 H/D exchange with C_6D_6 during the isomerization of **cis-25^{Me}** to **trans-25^{Me}**.

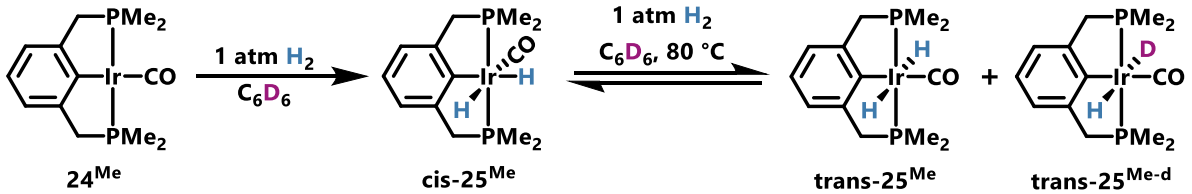

The rates of H_2 addition or isomerization were not measured for other (^{R4}PCP)Ir(CO) systems, however we can find insights into these systems by comparing their the reactivity with H_2 qualitatively. Qualitatively, **24^{iPr}**, **24^{CF3}**, and **24^{Me}** oxidatively add H_2 at a similar rate to form **cis-25^{R}** under 1 atm H_2 (see Schemes 4.1 and 4.2).[2,4] However, the qualitative rate of isomerization from **cis-25^{R}** to **trans-25^{R}** differs for different R groups.[2,4] Compound **cis-25^{CF3}** is only observable at low temperatures under 1 atm H_2, whereas **cis-25^{iPr}** can only be converted to **trans-25^{iPr}** at 100 °C and under 2.4 atm H_2.[2,4] Sterically, methyl groups are smaller than isopropyl groups, but similar in size to CF_3 groups. Thus, the qualitative rate of isomerization from **cis-25^{R}** to **trans-25^{R}** must be due to coupled steric and electronic factors imposed upon these systems by the respective PCP ligand.

Compound **cis-25^{Me}** slowly converts to both **24^{Me}** (ca. 5 %) and **trans-25^{Me}** (ca. 94 %) upon removal of the H_2 atmosphere at room temperature. This suggests that the rate of H_2 elimination from **cis-25^{Me}** and the isomerization of **cis-25^{Me}** to **trans-25^{Me}** is competitive, and that **cis-25^{Me}** is in equilibrium with **24^{Me}** and H_2. Compound **trans-25^{Me}** is stable at room temperature when not under an H_2 atmosphere, though it loses H_2 when heated to 80 °C under vacuum in solution.

To further elucidate a possible mechanism for this isomerization, we introduced additives to the isomerization under 1 atm H_2. Figure 4.2 compares the isomerization rates at 40 °C with an added L-type ligand (pyridine) and Lewis acid ($NaBF_4$). Both the pyridine and $NaBF_4$ accelerate the isomerization. Because an L-type ligand increases the rate of reaction, we hypothesize that the dissociation of a phosphine arm or CO is unlikely during isomerization. As well, a previously proposed Bailar Twist mechanism would be unaffected by added ligands or Lewis acids.[2,3] A reductive elimination (followed by an inversion) may be facilitated by an L-type ligand, however a Lewis Acid should not affect this mechanism. The only mechanistic pathway that would be accelerated by a L-type ligand and Lewis Acid is a CO-migratory insertion pathway.

Figure 4.2 The effect of additives on the isomerization rate of **24^{Me}** to **trans-25^{Me}** at 40 °C under 1 atm H_2.

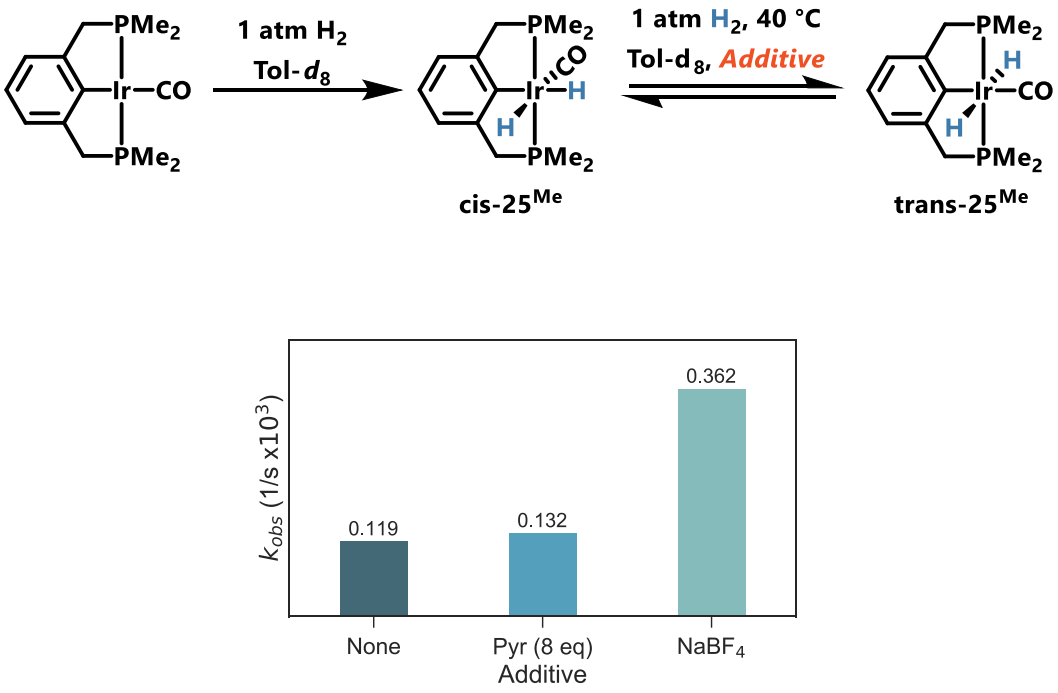

We hypothesized that a strongly coordinating ligand may trap an intermediate iridium species with an open coordination site if one is formed during the isomerization from **cis-25^{Me}** to **trans-**

3^{Me}. Table 4.1 summarizes the reactivity of **cis-25^{Me}** and **trans-25^{Me}** with strong ligands (PMe_3, or *tert*-butyl isonitrile) under 1 atm H_2.

Table 15 Summary of attempts to trap an intermediate during the isomerization of **cis/trans-25^{Me}**. All experiments were conducted under 1 atm H_2 in C_6D_6. [a]At 80°C. See Schemes 4.5 and 4.6 for a graphical representation.

Exp #	Staring	Reactant	Result
1	**cis-25^{Me}**	Excess PMe_3	H_2 Loss; **29^{Me}**
2	**cis-25^{Me}**	$^{t\text{Bu}}$isonitrile	Intractable
3[a]	**trans-25^{Me}**	Excess PMe_3	**34^{Me}**
4[a]	**trans-25^{Me}**	$^{t\text{Bu}}$isonitrile	Intractable
5[a]	**28^{Me}**	-	**trans-25^{Me}**
6[a]	**29^{Me}**	-	**34^{Me}**

These reactions were unsuccessful at trapping an intermediate species. The attempts with *tert*-butyl isonitrile led to intractable products which likely came about through exchange with the original CO ligand and possibly hydrogenation of the C-N bond. Reactions involving PMe_3 lead to exchange between the CO and PMe_3 or H_2 elimination (Scheme 4.5). Adding PMe_3 to **24^{Me}** results in the formation of (^{Me4}PCP)Ir(CO)(PMe_3) **29^{Me}**. Compound **29^{Me}** does not react with hydrogen at room temperature. However, **29^{Me}** converts to **34^{Me}** at 110 °C in toluene under 1 atm H_2. Compound **trans-25^{Me}** reacts with PMe_3 at 110 °C to afford **34^{Me}** (Scheme 4.5c). However, **cis-24^{Me}** reacts with PMe_3 to afford **29^{Me}**. These results suggest that H_2 competes with PMe_3 as a ligand to **24^{Me}**, and H_2 eventually coordinates and is activated at elevated temperatures. The elevated temperature likely speeds the cis/trans isomerization such that the isomerization is faster than H_2 dissociation in the presence of PMe_3. Figure 4.3 shows the crystal structure of **34^{Me}.** The Ir-P(3) bond (2.2866(9) Å), trans to the aryl ligand, is noticeably elongated compared to the Ir-P bonds of the ^{Me4}PCP ligand, Ir-P(1) (2.2633 (18) Å) and Ir-P(2) (2.2664 (8) Å). The C(1)-Ir-P(3) angle is similar to that of the C(1)-Ir-CO angle reported for **24^{Me}** and **trans-25^{Me}**.

Scheme 4.5 Attempts to trap an intermediate species during the **cis/trans-25^{Me}** isomerization with PMe_3.

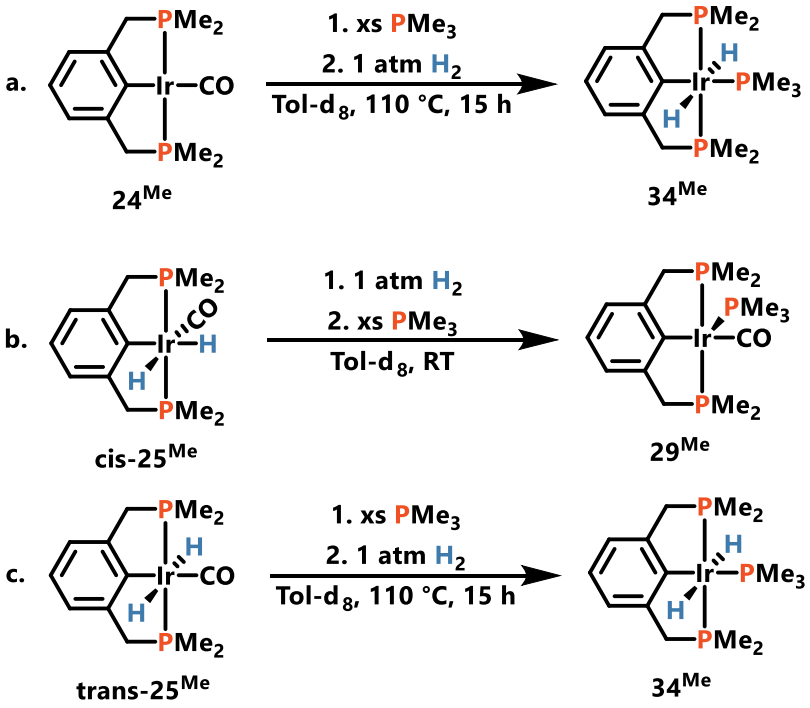

Figure 4.3 (Left) ORTEP of trans-(^{Me4}PCP)Ir(H)$_2$(PMe$_3$) (**34^{Me}**) shown with thermal ellipsoids at 50% probability; the hydrogen atoms except the hydrides are omitted for clarity. (Right) A table of selected angles and bond-distances for **34^{Me}**.

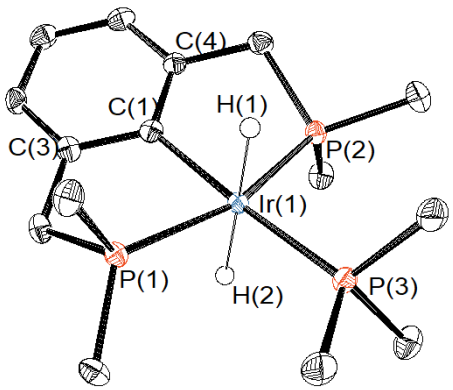

Bond (Å) or Angle (°)	Value
Ir(1)-C(1)	2.101(3) Å
Ir(1)-P(3)	2.2866(9) Å
Ir(I)-P(1)	2.2633 (18) Å
Ir(I)-P(2)	2.2664 (8) Å
P(1)-Ir(1)-P(2)	159.70(3) °
C(3)-C(1)-Ir(1)-P(1)	176.17(9) °
C(4)-C(1)-Ir(1)-P(2)	13.6(3) °
C(4)-C(1)-Ir(1)-P(2)	19.5(2) °

Reactions involving added CO either resulted in loss of H_2 (with excess CO) or rapid isomerization (ca. 1 equiv. of CO; Scheme 4.6). These experiments with added strong ligands only suggest that the original CO ligand will exchange with a strongly electron donating ligand during the **cis/trans-25^{Me}** isomerization.

Scheme 4.6 Attempts to trap an intermediate with CO.

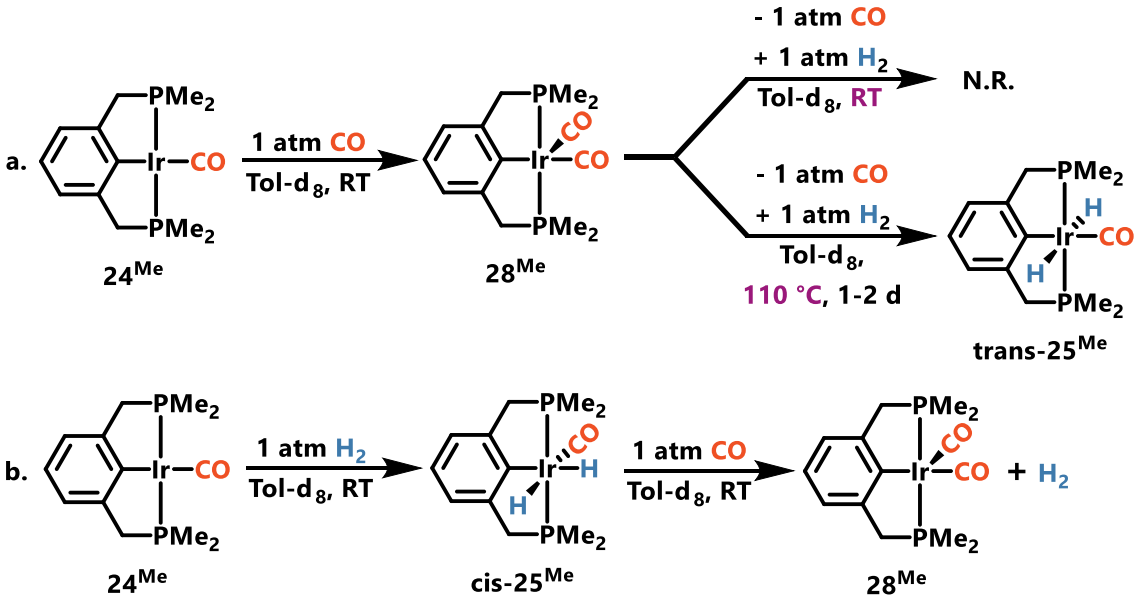

4.1.3 Conclusions

Reducing the steric bulk of the PCP ligand has a significant effect on the reactivity with H_2 of (^{R4}PCP)Ir(CO) complexes and their derivatives. In the series where R is ^{t}Bu, ^{i}Pr, or Me, decreasing the size of the R group allows species to interact with the metal center under more facile conditions, which promotes previously unobserved reactivity. The kinetic data with additives suggest that the **cis/trans-25^{Me}** isomerization proceeds through a CO insertion pathway. Attempts to trap this proposed intermediate were unsuccessful.

4.2 Part 2 - DCM Activation by (^{Me4}PCP)Ir(CO)

4.2.1 Introduction

The oxidative addition of alkyl halides to transition metals is important to many transformations, most notably to acetic acid formation which uses a rhodium catalyst.[8] Thus, many groups have studied the oxidative addition of alkyl halides to rhodium complexes.[9–16] Others have studied similar reactions with other transitions metals, including: palladium, platinum, and iridium. Previous investigations of alkyl halide addition to iridium showed that multiple reaction mechanisms could take place depending on the reaction conditions and alkyl halide.[11] However, there is a consensus that more electron-rich metal centers will show increased reactivity with alkyl halide reagents.[11] More electrophilic alkyl halides such as benzyl halides or alkyl halides with better leaving groups such as methyl iodide are more reactive with nucleophilic metal centers.[11] Thus, only a few reports have studied the activation of carbon-chlorine bonds as many metal complexes are inert to carbon-chlorine bonds and are commonly handled in solvents such as DCM and chloroform.[9–16] For example, previous studies involving (^{R}PCP)Ir(CO) (R = ^{t}Bu or ^{i}Pr) complexes use DCM as a solvent for various transformations.[5,6,17] By contrast, here we report the activation of DCM by (^{Me4}PCP)Ir(CO).

4.2.2 Results and Discussion

Scheme 4.7 Synthesis of **35^{Me}** (a) and **35$^{Me\text{-}d}$** (b).

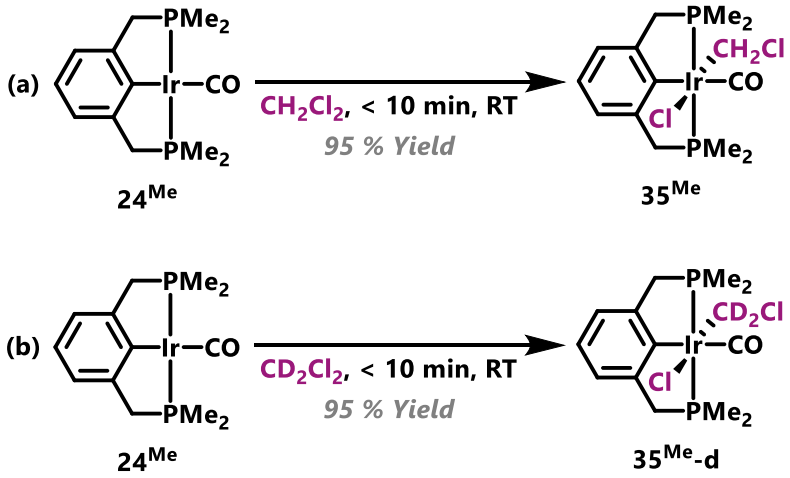

Compound **24^{Me}** reacts instantly with CH_2Cl_2 or CD_2Cl_2 at room temperature to afford trans-(^{Me4}PCP)Ir(Cl)(CH_2Cl)(CO) (**35^{Me}**; Scheme 4.07a) or trans-(^{Me4}PCP)Ir(Cl)(CD_2Cl)(CO) (**35^{Me}-d**; Scheme 4.07b), respectively. The ^{1}H NMR spectrum of **35^{Me}** shows two doublets of virtual triplets at 3.66 ppm and 3.50 ppm for the inequivalent methylene protons; a triplet at 3.47 ppm for the methylene chloride ligand ($^3J_{HP}$ = 6.3 Hz) and two virtual triplets at 1.88 pm and 1.82 ppm for the methyl protons. The ^{1}H NMR spectrum of **35^{Me}-d** is identical to the ^{1}H NMR spectrum of **35^{Me}** except for the absence of the signal from the methylene chloride ligand. The ^{31}P{^{1}H} NMR spectra of **35^{Me}** and **35^{Me}-d** show a singlet at 2.30. The signal for the carbon of the methylene chloride ligand shows as a triplet ($^2J_{CP}$ = 5.0 Hz) in the ^{13}C{^{1}H} NMR spectrum. Figure 4.4 shows the crystal structure of **35^{Me}**.

Figure 4.4 (Left) ORTEP of (^{Me4}PCP)Ir(Cl)(CH_2Cl)(CO) (**35^{Me}**) shown with thermal ellipsoids at 50% probability. (Right) A table of selected angles and bond-distances for **35^{Me}**.

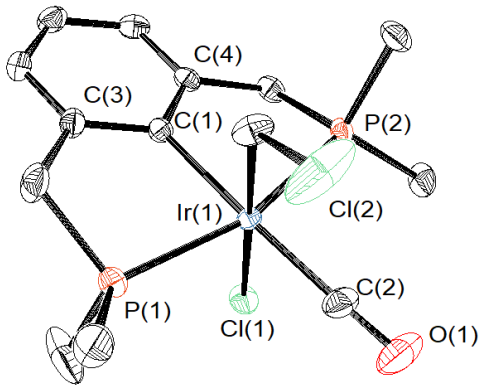

Bond (Å) or Angle (°)	Value
Ir(1)-C(1)	2.097(3) Å
Ir(1)-C(2)	1.927 (3) Å
Ir(I)-O(1)	3.066 (2) Å
P(1)-Ir(1)-P(2)	160.92 (3) °
C(1)-Ir(1)-C(2)	177.96 (10) °
C(3)-C(1)-Ir(1)-P(1)	16.96 (18) °
C(4)-C(1)-Ir(1)-P(2)	14.18 (18) °

This reaction is intriguing because many previous examples of DCM activation involve concerted oxidative addition, activation across multiple metal centers, or radical-initiated additions. Moreover, this reaction is facilitated by the reduced steric profile of the ^{Me4}PCP ligand, because the electronic differences between the series (^{R4}PCP)Ir(CO) (R = ^{t}Bu, ^{i}Pr, Me) are not nearly as significant as the steric differences. We hypothesize that **35^{Me}** forms as the result of an S_N2 reaction between **24^{Me}** and DCM. We have not observed any intermediate species while tracking this reaction by ^{1}H or ^{31}P{^{1}H} NMR spectroscopy under dilute conditions. We also observed that the rate of this reaction is reproducible with the exclusion of ambient light, therefore suggesting a radical pathway is not operative. Ongoing experiments are being conducted to further determine the mechanism of this reaction. These experiments include: measuring the reaction rate in polar and non-polar solvents, comparing the activation of alkyl chlorides and alkyl tosylates, and using chiral substrates to determine if there is an inversion of stereochemistry, a hallmark of S_N2 reactions.

4.2.3 Conclusion

Compound **24^{Me}** is highly nucleophilic as demonstrated by facile reaction with chlorocarbons, which are usually slow to undergo nucleophilic attack. The sterically encumbered analogs of **24^{Me}**, **24^{iPr}** and **24^{tBu}**, are presumably at least as nucleophilic as **24^{Me}**, but the steric profile of the larger PCP ligand inhibits reactivity with DCM.

4.3 Experimental

General Considerations

All manipulations and reactions used standard Schlenk techniques under an argon atmosphere unless otherwise stated. Glassware, diatomaceous earth, and sodium sulfate were stored in an oven maintained at 140 °C for at least 24 h prior to use. All protio solvents were passed through activated alumina and activated 3Å molecular sieves prior to use. Deuterated solvents were dried over calcium hydride (CD_2Cl_2, *o*-$C_6D_4Cl_2$) or sodium (C_6D_6, Tol-d_8, THF-d_8) and stored over molecular sieves. ^{1}H, ^{31}P{^{1}H}, and ^{13}C{^{1}H} NMR spectra were recorded on a Bruker DRX-700, AV-500, DRX-499, or AV-300 instrument. ^{1}H NMR and ^{13}C{^{1}H} NMR spectra were referenced to residual solvent signals.[18] ^{31}P{^{1}H} NMR spectra were referenced to an 85% H_3PO_4 standard. All NMR spectra were recorded at ambient temperature unless otherwise stated. Reagents PMe_3, $NaBF_4$ were purchased from Sigma Aldrich. PMe_3 was vacuum transferred prior to use. Elemental analysis was performed at the CENTC facility at the University of Rochester (funded by NSF CHE-0650456) and at Atlantic Microlab, GA.

Kinetics General Experimental. A J-young NMR tube was charged with (^{Me4}PCP)Ir(CO) **24^{Me}**, 1,3,5-Trimethoxybenzne, an optional additive and toluene-d_8. The solution was degassed, then

filled with 1 atm of H_2 at room temperature. The reaction was monitored by ^1H spectroscopy while the instrument was heated at the given temperature. The order of the reaction was determined by residual analysis of the linear regression fits of the zeroth, first, and second order plots using the concentration of cis-(^{Me4}PCP)Ir(H)$_2$(CO) **cis-25^{Me}**. The reation rates were determined by the slope of the linear regression fit of the first order plot of the concentration of cis-(^{Me4}PCP)Ir(H)$_2$(CO) **cis-25^{Me}**.

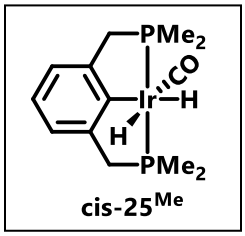

cis-25^{Me}

cis-25^{Me}: cis-(^{Me4}PCP)Ir(H)$_2$(CO). A J-Young NMR tube was charged with (^{Me4}PCP)Ir(CO) (**24^{Me}**) (ca. 5 mg, 0.01 mmol) and C_6D_6. The solution was degassed, then introduced to 1 atm H_2. The J-Young NMR tube was vigorously shaken for 20 seconds. ^1H and $^{31}P\{^1H\}$ NMR spectra were recorded ca. 5 minutes after H_2 addition. ^1H NMR (300 MHz, C_6D_6): δ 7.16 (m; 3H; *Ar*), 3.18 (vt; 4H; -C*H*$_2$-), 1.40 (vt; 6H; P(C*H*$_3$)$_2$), 1.36 (vt; 6H; P(C*H*$_3$)$_2$), -9.85 (t; $^2J_{HP}$ = 19.2 Hz; 1H), -11.0 (t; $^2J_{HP}$ = 12.4 Hz; $^2J_{HH}$ = 3.0 Hz 1H). $^{31}P\{^1H\}$ NMR (121.5 MHz, C_6D_6): δ -12.3. IR (solution, C_6D_6, cm$^-$) ν(*CO*) 2010, ν(*Ir-H*) 2055, 1950.

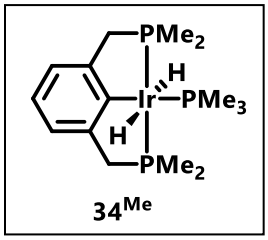

34^{Me}

34^{Me}: **trans-(^{Me4}PCP)Ir(H)$_2$(PMe$_3$). Method A.** A J-Young NMR tube was charged with (^{Me4}PCP)Ir(CO) (**24^{Me}**) (5.2 mg, 0.01 mmol), toluene-d$_8$, PMe$_3$ (0.01 mL, 0.1 mmol). The solution was degassed, pressurized with 1 atm H_2, then vigorously shaken for 20 seconds. The solution was heated at 110 °C overnight.

Method B. A J-Young NMR tube was charged with trans-(^{Me4}PCP)Ir(H)$_2$(CO) (**trans-25^{Me}**) (4.5 mg, 0.01 mmol), toluene-d$_8$, and PMe_3 (0.01 mL, 0.1 mmol). The solution was degassed, pressurized with 1 atm H_2, then vigorously shaken for 20 seconds. The solution was heated at 110 °C overnight. Crystals suitable for X-ray diffraction were grown from an impure solution of **34^{Me}** and minor side-products in benzene (1 part) layered with pentane (9 parts) at -35 °C. Spectroscopic features of the major species besides PMe_3 produced by methods A and B are congruent with the structure of **34^{Me}**. ^{1}H NMR (300 MHz, Tol-d$_8$): δ 7.16 (m; 1H; Ar-H),7.05 (m; 2H; Ar-H),3.41 (vt; 4H; Ar(-C*H*$_2$-)), 1.56-1.51 (m; 21H; -P(C*H*$_3$)), -10.8 (q; $^2J_{HP}$ = 17.1 Hz 2H; Ir-*H*), ^{31}P{^{1}H} NMR (121.5 MHz, Tol-d$_8$): δ 1.54 (d; $^2J_{PP}$ = 20.5 Hz), -44.7 (t; $^2J_{PP}$ = 20.5 Hz).

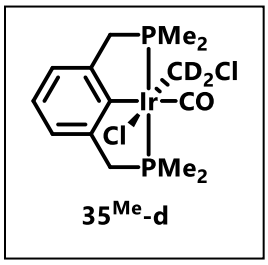

35^{Me}-d

35^{Me}-d: (^{Me4}PCP)Ir(Cl)(CD$_2$Cl)(CO). (^{Me4}PCP)Ir(CO) (ca. 5 mg, 0.01 mmol) was dissolved in DCM-d$_2$ (350 µL). The solution was kept at room temperature overnight (ca. 15 h). The resulting ^{1}H and ^{31}P{^{1}H} NMR spectroscopy data was consistent with quantitative conversion to (^{Me4}PCP)Ir(Cl)(CD$_2$Cl)(CO) **35^{Me}-d** . ^{1}H NMR (300 MHz, CD_2Cl_2): δ 7.07 (d; $^3J_{HH}$ = 7.4 Hz; 2H; Ar-H), 6.94 (t; $^3J_{HH}$ = 7.3 Hz; 1H; Ar-H) 3.63 (dvt; 2H; Ar(-C*H*$_2$-)), 3.46 (dvt; 2H; Ar(-C*H*$_2$-)), 1.88 (vt; 6H; -P(C*H*$_3$)), 1.81 (vt; 6H; -P(C*H*$_3$)). ^{31}P{^{1}H} NMR (121.5 MHz, CD_2Cl_2): δ 2.23 (s).

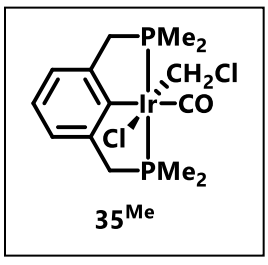

35^{Me}

35^{Me}: (^{Me4}PCP)Ir(Cl)(CH$_2$Cl)(CO). (^{Me4}PCP)Ir(CO) (80 mg, 0.18 mmol) was dissolved in DCM (5 mL). The solution was kept at room temperature overnight (ca. 15 h), then the volatiles were removed under vacuum. The resulting solid was washed with pentane, and dried under vacuum to afford (^{Me4}PCP)Ir(Cl)(CH$_2$Cl)(CO) **35^{Me}** (89 mg, 0.17 mmol; 95 % yield). Crystals suitable for x-ray

diffraction were grown from a concentrated solution of **35^{Me}** in benzene (1 part) layered with pentane (9 parts) at -35 °C. ^{1}H NMR (300 MHz, CD_2Cl_2): δ 7.07 (d; $^{3}J_{HH}$ = 7.3 Hz; 2H; Ar-*H*), 6.95 (t; $^{3}J_{HH}$ = 7.3 Hz; 1H; Ar-*H*), 3.66-3.60 (dvt; 2H; Ar(-C*H*$_2$-)), 3.50-3.45 (m; 2H; Ar(-C*H*$_2$-)), 3.50-3.45 (m; 2H; Ir-C*H*$_2$Cl), 1.88 (vt; 6H; -P(C*H*$_3$)), 1.82 (vt; 6H; -P(C*H*$_3$)). ^{31}P{^{1}H} NMR (283.4 MHz, CD_2Cl_2): δ 2.3 (s). ^{13}C{^{1}H} NMR (126 MHz, CD_2Cl_2): δ 176.4 (t; $^{3}J_{CP}$ = 6.2 Hz; Ir-*C*O), 159.5 (s; *C*$_{Ar}$), 147.0 (vt; *C*$_{Ar}$), 125.8 (vt; *C*$_{Ar}$), 123.5 (vt; *C*$_{Ar}$), 43.6 (vt; -(*C*H$_2$)-), 12.4 (vt; -P(*C*H$_3$)), 12.4 (vt; -P(*C*H$_3$)), 7.0 (t; $^{3}J_{CP}$ = 5.0 Hz; Ir-*C*H$_2$Cl). IR (solution, DCM, cm^{-1}) ν(CO) 2037. EA: ($C_{14}H_{21}Cl_2IrOP_2$) Calc: C 31.70; H 3.99; Found C 31.34; H 3.88.

4.4 References

1 P. G. Jessop and R. H. Morris, *Coord. Chem. Rev.*, 1992, **121**, 155–284.

2 B. Rybtchinski, Y. Ben-David and D. Milstein, *Organometallics*, 1997, **16**, 3786–3793.

3 Sh. Li and M. B. Hall, *Organometallics*, 1999, **18**, 5682–5687.

4 J. J. Adams, N. Arulsamy and D. M. Roddick, *Organometallics*, 2011, **30**, 697–711.

5 J. M. Goldberg, S. D. T. Cherry, L. M. Guard, W. Kaminsky, K. I. Goldberg and D. M. Heinekey, *Organometallics*, 2016, **35**, 3546–3556.

6 B. Rybtchinski, Y. Ben-David and D. Milstein, *Organometallics*, 1997, **16**, 3786–3793.

7 A. Kumar, T. M. Bhatti and A. S. Goldman, *Chem. Rev.*, 2017, **117**, 12357–12384.

8 D. Forster and T. C. Singleton, *J. Mol. Catal.*, 1982, **27**, 299–314.

9 J. K. Stille and K. S. Y. Lau, *Acc. Chem. Res.*, 1977, **10**, 434–442.

10 J. A. Labinger, J. A. Osborn and N. J. Coville, *Inorg. Chem.*, 1980, **19**, 3236–3243.

11 M. Huser, M. T. Youinou and J. A. Osborn, *Angew. Chemie Int. Ed. English*, 1989, **28**, 1386–1388.

12 J. A. Labinger, R. J. Braus, D. Dolphin and J. A. Osborn, *J. Chem. Soc. D*, 1970, **0**, 612b–613.

13 J. Halpern, *Acc. Chem. Res.*, 1970, **3**, 386–392.

14 P. R. Ellis, J. M. Pearson, A. Haynes, H. Adams, N. A. Bailey and P. M. Maitlis, *Organometallics*, 1994, **13**, 3215–3226.

15 B. Blank, G. Glatz and R. Kempe, *Chem. Asian J.*, 2009, **4**, 321–327.

16 J. P. Collman and R. Boulatov, *Inorg. Chem.*, 2001, **40**, 560–563.

17 J. M. Goldberg, G. W. Wong, K. E. Brastow, W. Kaminsky, K. I. Goldberg and D. M. Heinekey, *Organometallics*, 2015, **34**, 753–762.

18 G. R. Fulmer, A. J. M. Miller, N. H. Sherden, H. E. Gottlieb, A. Nudelman, B. M. Stoltz, J. E. Bercaw and K. I. Goldberg, *Organometallics*, 2010, **29**, 2176–2179.

Appendix A. Crystallographic Tables

Table A1. Crystallographic data for compounds **22**, **24^{Me}**, **trans-25^{Me}**, and **26^{Me}/35^{Me}**.

Parameter	22	24^{Me}	trans-25^{Me}	Cocrystal 26^{Me}/35^{Me}
Empirical formula	$C_4H_{12}OP_2$	$C_{13}H_{19}IrOP_2$	$C_{13}H_{21}IrOP_2$	$C_{32}H_{46}BCl_2F_4Ir_2NO_2P_4$
Formula weight	138.08	445.42	447.44	1142.69
Temperature	100(2) K	100(2) K	100(2) K	100(2) K
Wavelength	0.71073 Å	0.71073 Å	0.71073 Å	0.71073 Å
Crystal system	Monoclinic	Monoclinic	Orthorhombic	Monoclinic
Space group	C 2/m	P 21/c	P b c a	P 21/n
a	5.4291(7) Å	13.5827(9) Å	10.0756(12) Å	10.603(4) Å
b	11.1977(17) Å	10.6830(7) Å	12.0992(17) Å	30.146(10) Å
c	12.2707(18) Å	20.4334(13) Å	25.280(4) Å	12.288(5) Å
α	90 °	90 °	90 °	90 °
β	99.213(8) °	96.186(3) °	90 °	91.41(2) °
γ	90 °	90 °	90 °	90 °
Volume	736.35(18) Å^3	2947.7(3) Å^3	3081.9(7) Å^3	3926(2) Å^3
Z	4	8	8	4
Density (calculated)	1.245 Mg/m^3	2.007 Mg/m^3	1.929 Mg/m^3	1.933 Mg/m^3
Absorption coefficient	0.492 mm$^-$	9.258 mm^{-1}	8.856 mm^{-1}	7.120 mm^{-1}
F(000)	296	1696	1712	2200
Crystal size	0.470 x 0.320 x 0.150 mm^3	0.360 x 0.280 x 0.100 mm^3	0.150 x 0.080 x 0.050 mm^3	0.100 x 0.050 x 0.050 mm^3
Theta range for data collection	1.681 to 28.284°.	2.005 to 25.350°.	1.611 to 25.348°.	1.790 to 26.448°.
Index ranges	-7<=h<=7, -14<=k<=14, -16<=l<=16	-16<=h<=16, -12<=k<=12, -24<=l<=24	-12<=h<=12, -14<=k<=14, -30<=l<=30	-13<=h<=13, 0<=k<=37, 0<=l<=15
Reflections collected	9292	20213	5174	12694
Independent reflections	962 [R(int) = 0.0296]	5344 [R(int) = 0.0274]	2772 [R(int) = 0.0356]	12694 [R(int) = 0.3343]
Completeness to theta = 25.000°	99.1 %	99.0 %	98.1 %	96.1 %
Refinement method	Full-matrix least-squares on F^2	Full-matrix least-squares on F^2	Full-matrix least-squares on F^2	Full-matrix least-squares on F^2
Data / restraints / parameters	962 / 0 / 39	5344 / 0 / 279	2772 / 0 / 158	12694 / 266 / 395
Goodness-of-fit on F^2	1.104	1.096	1.077	1.030
Final R indices [I>2sigma(I)]	R1 = 0.0192, wR2 = 0.0515	R1 = 0.0485, wR2 = 0.1225	R1 = 0.0329, wR2 = 0.0571	R1 = 0.1495, wR2 = 0.3174
R indices (all data)	R1 = 0.0208, wR2 = 0.0526	R1 = 0.0547, wR2 = 0.1281	R1 = 0.0727, wR2 = 0.0721	R1 = 0.2878, wR2 = 0.3895
Largest diff. peak and hole	0.406 and -0.245 e.Å^{-3}	10.722 and -1.833 e.Å^{-3}	1.754 and -1.129 e.Å^{-3}	3.821 and -3.357 e.Å^{-3}

Table A2. Crystallographic data for compounds **32^{Me}**, **32'^{Me}**, **34^{Me}**, and **35^{Me}**.

Parameter	32^{Me}	32'^{Me}	34^{Me}	35^{Me}
Empirical formula	$C_{11}H_{16}ClIrO_3P_2$	$C_{19}H_{32}ClIrO_3P_2$	$C_{15}H_{30}IrP_3$	$C_{14}H_{21}Cl_2IrOP_2$
Formula weight	485.83	598.04	495.50	530.35
Temperature	100(2) K	100(2) K	100(2) K	100(2) K
Wavelength	0.71073 Å	0.71073 Å	0.71073 Å	0.71073 Å
Crystal system	Monoclinic	Monoclinic	Monoclinic	Monoclinic
Space group	P 2_1/n	P 2_1/n	P 21/c	P 2_1/n
a	10.1632(5) Å	12.1567(9) Å	22.1041(10) Å	8.4198(14) Å
b	13.6053(7) Å	9.9013(7) Å	9.3471(5) Å	11.526(2) Å
c	10.7430(5) Å	38.365(3) Å	18.9388(9) Å	18.374(3) Å
α	90 °	90 °	90 °	90 °
β	93.510(3) °	92.341(3) °	109.749(2) °	94.044(7) °
γ	90 °	90 °	90 °	90 °
Volume	1482.68(13) Å^3	4614.0(6) Å^3	3682.8(3) Å^3	1778.7(5) Å^3
Z	4	8	8	4
Density (calculated)	2.176 Mg/m^3	1.722 Mg/m^3	1.787 Mg/m^3	1.981 Mg/m^3
Absorption coefficient	9.397 mm^{-1}	6.057 mm^{-1}	7.499 mm^{-1}	7.980 mm^{-1}
F(000)	920	2352	1936	1016
Crystal size	0.150 x 0.100 x 0.010 mm^3	0.45 x 0.15 x 0.10 mm^3	0.140 x 0.130 x 0.060 mm^3	0.300 x 0.150 x 0.120 mm^3
Theta range for data collection	2.418 to 28.353°.	2.13 to 26.37°.	1.958 to 28.445°.	2.087 to 28.491°.
Index ranges	-13<=h<=13, 0<=k<=18, 0<=l<=14	-15<=h<=15, -12<=k<=12, -47<=l<=47	-29<=h<=29, -12<=k<=12, -25<=l<=25	-11<=h<=11, -15<=k<=15, -24<=l<=24
Reflections collected	84438	170455	17903	17251
Independent reflections	3701 [R(int) = 0.0773]	9373 [R(int) = 0.0330]	9253 [R(int) = 0.0162]	4469 [R(int) = 0.0279]
Completeness to theta = 25.000°	99.8 %	99.3 %	99.9 %	100.0 %
Refinement method	Full-matrix least-squares on F^2	Full-matrix least-squares on F^2	Full-matrix least-squares on F^2	Full-matrix least-squares on F^2
Data / restraints / parameters	3701 / 0 / 172	9373 / 0 / 495	9253 / 6 / 369	4469 / 0 / 185
Goodness-of-fit on F^2	1.156	1.169	1.008	1.054
Final R indices [I>2sigma(I)]	R1 = 0.0302, wR2 = 0.0603	R1 = 0.0194, wR2 = 0.0365	R1 = 0.0194, wR2 = 0.0434	R1 = 0.0186, wR2 = 0.0417
R indices (all data)	R1 = 0.0371, wR2 = 0.0626	R1 = 0.0264, wR2 = 0.0400	R1 = 0.0254, wR2 = 0.0458	R1 = 0.0215, wR2 = 0.0432
Largest diff. peak and hole	1.642 and -2.157 e.Å^{-3}	1.451 and -1.952 e.Å^{-3}	1.949 and -1.337 e.Å^{-3}	1.030 and -1.366 e.Å^{-3}

Appendix B. Compound Numbering Scheme

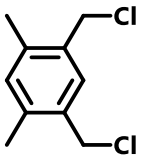

1^{Cl}

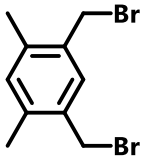

1^{Br}

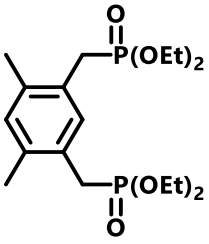

2^{Et}

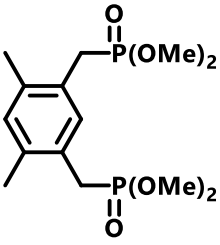

2^{Me}

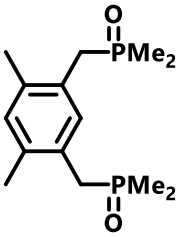

3_{Me}

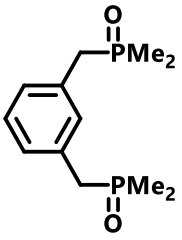

3

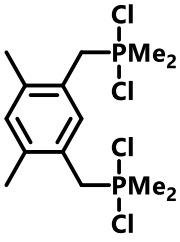

4_{Me}

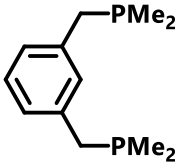

5

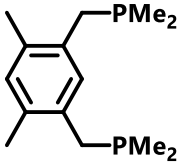

5_{Me}

Et_2NPMe_2

6^{Et}

$^{i}Pr_2NPMe_2$

6^{iPr}

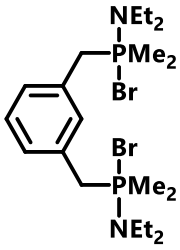

7

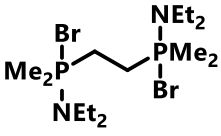

8

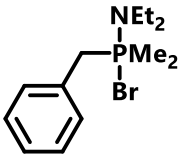

9^{Et}

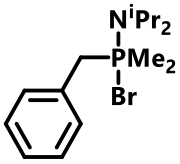

9^{iPr}

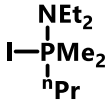

10

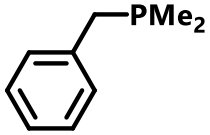

11

$^{n}PrPMe_2$

12

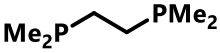

13

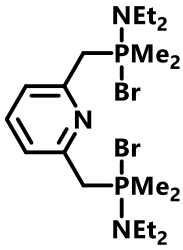

14

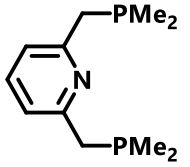

15

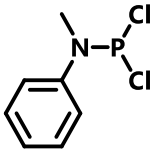

17a

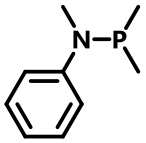

17

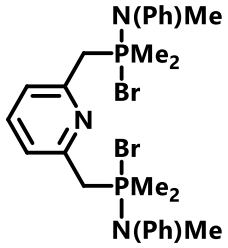

18

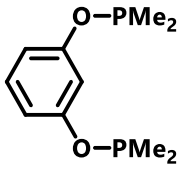

19

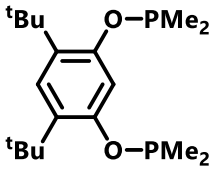

20

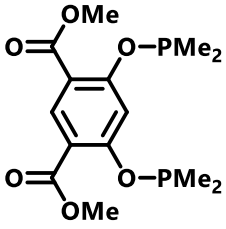

21

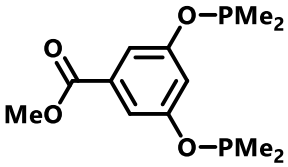

21a

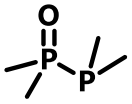

22

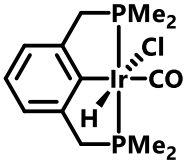

23Me

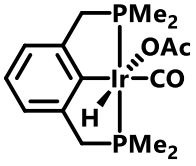

23aMe

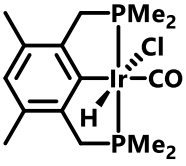

23'Me

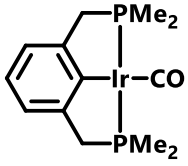

24Me

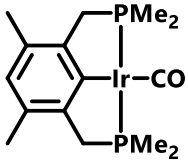

24'Me

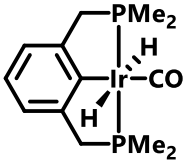

trans-25Me

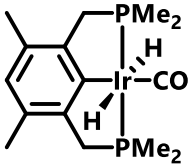

trans-25'Me

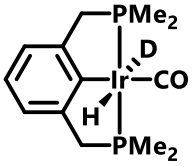

trans-25Me-d

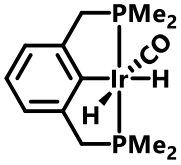

cis-25Me

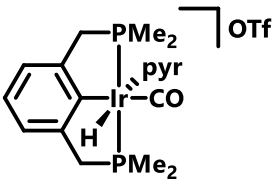

26Me

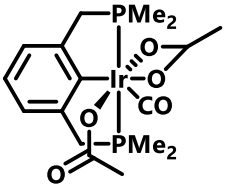

27Me

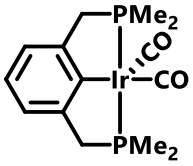

28Me

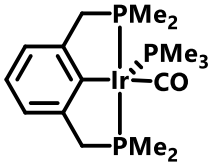

29Me

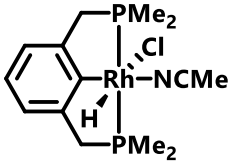

+ Isomer

30

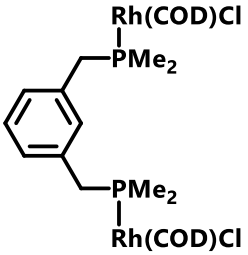

31

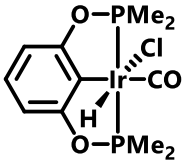

32Me

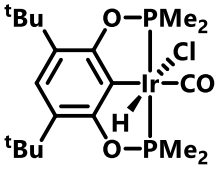

32'Me

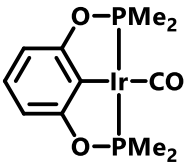

33Me

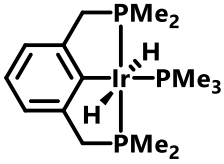

34Me

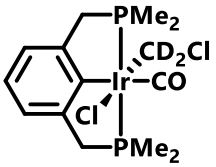

35Me-d

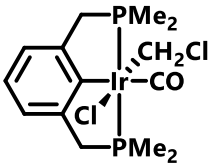

35Me